ISBN 978-82-471-1631-9 (printed ver.)
ISBN 978-82-471-1632-6 (electronic ver.)
ISSN 1503-8181

Doctoral theses at NTNU, 2009:123

Roger A. Khalil

Thermal conversion of biomass with emphasis on product distribution, reaction kinetics and sulfur abatement.

Doctoral Thesis

Roger A. Khalil

NTNU
Norwegian University of
Science and Technology

NTNU
Norwegian University of
Science and Technology
Thesis for the degree of
philosophiae doctor
Faculty of Engineering Science and Technology
Department of Energy and Process Technology

Doctoral theses at NTNU, 2009:123

NTNU

NTNU
Norwegian University of
Science and Technology

Roger A. Khalil

Thermal conversion of biomass with emphasis on product distribution, reaction kinetics and sulfur abatement.

Thesis for the degree of philosophiae doctor

Trondheim, May 2009

Norwegian University of
Science and Technology
Faculty of Engineering Science and Technology
Department of Energy and Process Technology

NTNU
Norwegian University of
Science and Technology

NTNU
Norwegian University of Science and Technology

Thesis for the degree of philosophiae doctor

Faculty of Engineering Science and Technology
Department of Energy and Process Technology

ISBN 978-82-471-1631-9 (printed ver.)
ISBN 978-82-471-1632-6 (electronic ver.)
ISSN 1503-8181

Doctoral Theses at NTNU, 2009:123

Printed by Tapir Uttrykk

The Norwegian University of Science and Technology
Norges Teknisk-Naturvitenskapelige Universitet

Report no:

Classification:
Open

ADDRESS:
NTNU
DEPARTMENT OF ENERGY AND PROCESS Engineering
Kolbjørn Hejes vei 1A
N-7491 Trondheim - NTNU

TELEPHONE
Switchboard NTNU: 73 59 40 00
Department office: 73 59 27 00
Hydropower section: 73 59 38 57

TELEFAX
Department office: 73 59 83 90
Hydropower section: 73 59 38 54

Title of report Thermal conversion of biomass with emphasis on product distribution, reaction kinetics and sulfur abatement.	Date May 2009 No. Of pages/appendixes 124/58
Author Roger A. Khalil	Project manager Johan E. Hustad
Division Faculty of Engineering Science and technology Department of Energy and Process Engineering	Project no.
ISBN no. 978-82-471-1631-9	Price group

Client/sponsor of Project The Research Council of Norway	Client's ref.

Abstract
Most of the work performed in this study has concentrated on the thermal decomposition of biomass. This was done because to the simple fact that biomass is mainly composed of volatiles that evaporates prior to the gasification stage.

The characteristics of the devolatilized products during pyrolysis are reported in Paper I for several fuels types that have been considered as sources for energy production due to their fast growing abilities. Paper I also reports results for the same biomass types in oxidative atmosphere. An oxidative atmosphere is also important from the gasification point of view because partial combustion is normally used in a gasification process in order to produce the necessary energy for the endothermic gasification reactions. For these studies and the rest of the pyrolysis experiments (papers II and III), the macro-TGA was used which allows the use of large biomass samples (80 g. for most of the experiments).

Another goal of this study was to condition the devolatilized products in order to generate an upgraded gas product with reduced pollutants. Paper II gives a detailed study on the effect of non-thermal plasma on the devolatilized products from pyrolysis of straw pellets, while paper III concentrate on reducing the sulfuric compounds from the gas phase. Two different methods for reducing sulfur emission in pyrolysis of straw were looked upon. The first is an active method that involves hindering the sulfur release with the producer gas through chemical reactions in the char matrix. This was done by introducing calcium based additives to the straw prior to pelletization. The second method was gas product treatment with non-thermal plasma.

Finally the gasification kinetics of two types of wood chars, pine and birch were reported in paper IV. This work was aimed at finding the reaction rates for these types of wood chars.

	Indexing Terms: English	Norwegian
Group 1	Biomass thermal treatment	Termisk behandling av biomasse
Gruup 2	Calcium additives for retention of sulfur	Kalsium baserte additiver for binding av svovel
Selected by author	Non thermal plasma for removal of sulfur	Ikke termisk plasma for fjerning av svovel
	CO_2 gasification kinetics	CO_2 gassifisering kinetikk
	Straw pellets	Halm pellets

Preface

Let there be no scales to weigh your unknown treasure;

And seek not the depths of your knowledge with staff or sounding line.

For self is a sea boundless and measureless.

Say not, "I have found the truth," but rather, "I have found a truth."

Say not, “I have found the path of the soul.” Say rather, “I have met the soul walking upon my path.”

The prophet (Gibran Khalil Gibran, 1883 – 1931)

This work has been carried out at the Norwegian University of Science and Technology (NTNU), the Department of Energy and Process Engineering with Professor Johan E. Hustad as main supervisor and Dr. Morten Grønli as second supervisor.

This work is dedicated to the two women in my life. The first my mother, I thank for bringing me to life. The second Isabelle, for stealing my time and delaying my PhD but in return gave my life a meaning.

Acknowledgments

Fulfilling a PhD degree is a quite challenging and almost impossible without the guidance of the people who were directly involved in the completion of this work and others who simply exist in my life. First, my gratitude goes to my supervisor Johan E. Hustad who through the PhD period has been a lighthouse in his guidance. His patience and understanding of the difficulties that has stood in the way, both privately and work related is very much appreciated. My gratitude goes also to my co-authors Gabor Várhegyi and Erika Mészáros, the fruitful collaboration has resulted in the publication of two papers and a nice visit to Hungary where I was welcomed in a manner it made me feel home. I also would like to thank Morten Grønli for his constant interest in our work and his help in facilitating the laboratory experiments. Jens Holm is to be thanked for taking care of me and helping me during my stay in Denmark for the pellets production. I also thank the students who helped during the experimental work Susanne Haar, Monica Moen and Harris Utne. Also the help of Øyvind Skreiberg on his constructive feedback on the papers is appreciated. Finally I would like to thank my family and friends for being able to take my mind of troubles and the worries of the PhD work.

Table of contents

List of figures

List of tables

1 Introduction

1.1 Biomass as a renewable source of energy

In a modern society concerned with the impact of the release of greenhouse gases to the environment, alternative solutions have to be developed. Immerged technologies, although some have not attained a mature status, are able to convert the energy in the biomass not only to heat and power but also to liquid fuels that can be used in the transportation sector, chemicals with a high market value and hydrogen. The increased emission from the transport sector is contributing more and more not only to the greenhouse effect, but also to local problems since emissions from car exhaust causes smog and acid rain. Alternative solutions such as the establishment of "the hydrogen society" are still far from being an economical alternative that can be realized in a short term period. Biomass has the potential of playing the role of a transitional alternative because its energy conversion is feasible in our present time. Since biomass is a limited resource on our planet and cultivation of crops for energy purpose has to compete with food as well as feed production, it is important to find solutions where production relative to available land is maximized. Biomass has been used as a source of energy since the time humans discovered fire. At present time, more and more efforts have been put into extracting a "higher" form of energy from biomass. Some of theses technologies are quite new and cannot economically compete with more traditional energy sources like coal, oil or natural gas. In fact, fossil fuels are cheap to process and biomass might never be able to compete against such fuel types. Nevertheless, political decisions might put bio-energy on a better competitive ground. Countries tend to support biomass and make it an attractive energy source for several reasons. This is accomplished not only by financing research projects to accelerate technology development, but by also imposing restrictions on technologies that acquire fossil fuels or giving direct subsidies for energy production from biomass. Every country in Europe has included bio-energy in its energy and climate policies. The EU has set a target for increasing the share of renewable energy sources (RES) from 6 % to 12 % from year 1997 to 2010. In the same period the share of green electricity in the EU-region should increase from around 14 to 21 % of the gross electric consumption by 2010. In addition, EU has established a directive on cogeneration of heat and power, with a target of 18 % by 2010. A recent EC directive on biofuels for the transport sector sets targets for the use of biomass for transport fuels. Another way to make energy production from biomass more competitive compared to fossil fuels is to use a low-grade biomass types like waste

that are less expensive. However, The use of low-grade fuels impose serious challenges to overcome in terms of electrical efficiency loss due to corrosion, loss of reliability due to feeding and preparation of the fuel and fouling in boiler, and increased emissions due to the presence of more harmful species.

From an environmental point of view, biomass is attractive for two main reasons:

1. Bioenergy is a renewable resource that will not be depleted in time as long as the consumption equals the natural regeneration.

2. Bioenergy can be considered as a "none" contributor to the increase of CO_2 emission to the atmosphere. This is because CO_2 generated from biomass combustion or gasification is circulated back as a carbon source for plantation growth. This postulate is valid only when the biomass used for energy production is replaced by growing new plants or when utilizing the annual plantation growth of forests and such.

However, due to the heterogeneous nature of solid fuels, the energy conversion becomes a challenge in terms of process control. Because of the biomass heterogeneity, the air used for combustion will not be perfectly mixed with the fuel which will result in incomplete reactions and the release of pollutants. In addition, the ash content in the fuel might be the source of many other problems such as corrosion, sintering and fouling that will result in reduced boiler efficiency in several parts of the process. Emissions of sulfur, nitrous and heavy metal compounds should be reduced to acceptable levels prior to the flue gas release. All these challenges will result in a higher form of process complexity and added costs to energy conversion. In spite of this, the idea of having a sustainable energy source that has the potential of being used for heating purposes, electricity production and the production of transportation fuels evens out the mentioned disadvantages.

Norway has considerable amounts of biomass where the annual growth based on estimation of photosynthesis efficiency is 425 TWh (including the 100 TWh from aquatic resources). The share that is currently used (2003) as bio-energy is approximately 16 TWh/year [1]. It is also possible to increase the use of bio-energy by approximately 30 TWh/year. This increase takes into consideration plantation growth that is economically, ecologically and technically unexploited. Capacity reduction in the paper industry may further increase the available biomass.

1.2 Thermochemical conversion technologies

Biomass can be converted to energy by the use of biochemical or thermochemical processes. Biochemical processes are beyond the scope of this thesis. Briefly explained, these technologies include fermentation for the production of alcohol and anaerobic digestion processes for the production of gas rich in methane and carbon dioxide [2]. Thermochemical processes include pyrolysis, gasification, and combustion. They can be distinguished by their respective process parameters and by the types of products they produce. An overview of these technologies, their respective primary products and their end uses are shown in Figure 1-1 [3].

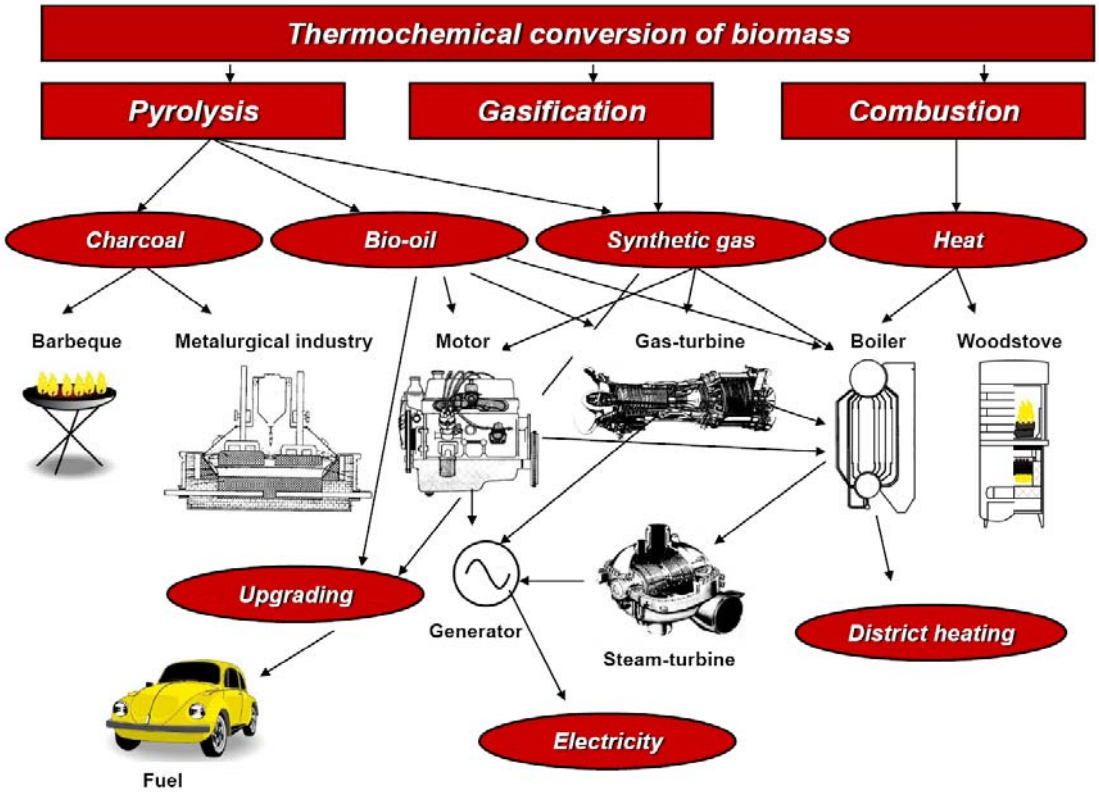

Figure 1-1: Products of thermochemical conversion technologies and there potential end uses

1.2.1 Pyrolysis

Pyrolysis is an endothermic process where the solid fuel in the absence of oxidant, degrades to form a mixture of liquid (tarry composition), gases and a highly reactive carbonaceous char of which the relative proportions depend very much on the method used. Conditions that will influence the distribution and the characteristics of the pyrolysis products are; temperature, pressure, heating rate and residence time of both the fuel and the

devolatilized products. In addition, the chemical and physical characteristics of the fuel type used can also have an influence on product distribution. For instance, low temperature and slow heating rate maximizes char formation, while high temperature promotes tar cracking which in return produce lighter hydrocarbons. Performing pyrolysis at high pressure will enhance the gas to solid reactions, which in return might result in higher yields of gas and liquid products. Pyrolysis conditions not only influences the distribution of the main products but also their chemical composition. For the char residue, the pyrolysis condition can affect its yield, physical characteristics and reactivity. For example, slow heating rate during pyrolysis will produce char which is less reactive compared to char produced at fast heating rate. This is mostly due to an increased specific area in the char produced at high heating rate and a more spread out distribution of the catalytic elements in the char matrix. The structure of the char matrix is therefore a key element in the determination of char reactivity. Char gasification reactivity is the topic of paper IV [4] in this thesis.

The gas pyrolysis products are mainly composed of CO, CO_2, H_2, CH_4, C_2H_2, C_2H_4, C_2H_6 and traces of other higher hydrocarbons. Gaseous compound from pyrolysis of biomass was studied in detail in this thesis (paper I [5] and paper II [6]). Paper I gives the detailed characteristics of the gaseous products released during the pyrolysis of some fast growing crops while Paper II deals with the major product release before and after treatment in a non-thermal plasma reactor. In addition to the gas release, saturated compounds such as water and alcohols will be present in the gas phase. Due to the nitrogen content in the fuel, trace elements of nitrous compounds such as NH_3 and HCN are also present [7]. These will react to form NO_x under the presence of an oxidizing agent for example during combustion. Other trace gas elements that are present due to the sulfur content in the raw fuel are H_2S and COS. These sulfur compounds are likely to be produced in gasification processes and are undesirable since they reduce process efficiency. As an example, one can mention the reduced efficiency or even the total destruction of solid oxide fuel cells when combined with a biomass gasification unit. The release of sulfur compounds during pyrolysis and means for their reduction is the focus of paper III of this thesis [8]. Other trace elements such as KCl, HCl and many more are quite normal to be found in the devolatilized products as well due to the alkali metals found in biomass.

The liquid phase is composed of polyaromatic hydrocarbons (PAH) and oxygenated aromatic compounds such as phenol and water. The liquid and gas fraction of the pyrolysis products can be used for heat and power generation or they can be processed further to produce chemicals, methanol and ammonia. The devolatilized products can be upgraded to produce hydrogen. The char residue can be upgraded to produce activated carbon where it can be used in the metallurgical industry. It can also be used for domestic cocking and barbecuing [3].

1.2.2 Gasification

Gasification is an endothermic process where solid fuels react with CO_2 and H_2O and form a combustible gas. Since gasification is an endothermic process, the energy needed to drive the chemical reactions forward are usually provided by feeding the reactor the necessary "under stoichiometric" amount of oxygen. Due to the existence of several reacting agents, biomass gasification is quite complex where a number steps occur simultaneously, regardless of the technology used. These steps include [9]:

- Drying of biomass
- Pyrolysis of biomass to condensable vapors (heavy hydrocarbons), gas and char fractions
- Subsequent thermal cracking of heavy hydrocarbons to gas and char
- Partial oxidation of combustible gases and char
- Gasification of char through reactions with CO_2 and H_2O.

As an example, we find in a fixed bed reactor several separate zones of combustion, volatile release, gasification of the char rest and drying of the raw fuel material. Contrary to pyrolysis, where the final products are many, a gasification process is designed to maximize gas production. In fact, rest products in form of char residues are avoided by process optimization. The liquid fractions (tars) are either cracked further and transformed into gaseous products or cleaned out. The gasification products are many and their relative distribution depends specifically on process parameters and the type of technology used. For instance, if air is chosen as a gasifying agent, the end product would be a low calorific gas (4 – 7 MJ/Nm^3) containing CO, CO_2, H_2, H_2O, CH_4 and a large fraction of nitrogen. It is possible to use pure oxygen instead of air in order to avoid dilution caused by the

nitrogen content in air. Although this yields a gas product with higher calorific value (10 – 18 MJ/Nm^3), it has not been a preferred method due to the increased energy and investments costs in connection to the addition of an oxygen/nitrogen separation unit to the gasification process. The process temperature of gasification is usually quite high (800 – 1100 ºC) compared to pyrolysis (400 – 800 ºC). The high temperature is needed to drive the main gasification reactions forward.

Depending on the gasification process and the processing of the produced gas, several end products can be generated:

- Syngas can be upgraded to produce methanol and other transport fuels
- By steam reforming of product gas hydrogen can be produced

Heat and electrical power can be produced by direct utilization of the syngas in boilers (hot water and steam production), combustion engines, gas turbines (heat and electricity) as well as Solid Oxide fuel cells (electricity and heat)

Several decades of reactor design has resulted in the existence of several reactor technologies. Theses are briefly described in the following section.

Fixed bed reactors

The differences between theses types of gasifiers lies in the direction of the gas flow relative to the reactor. The most popular fixed bed designs are:

Updraft gasifiers

Theses types represent the simplest reactor design where fuel is fed from the top and the air intake lies in the bottom. The producer gas is moving upward through the reactor and leaves at the top. Biomass moves downward a goes through different thermal stages consisting of a drying zone, followed by pyrolysis, reduction and char oxidation zone. Figure 1-2 (right) shows a schematic layout of the updraft design.

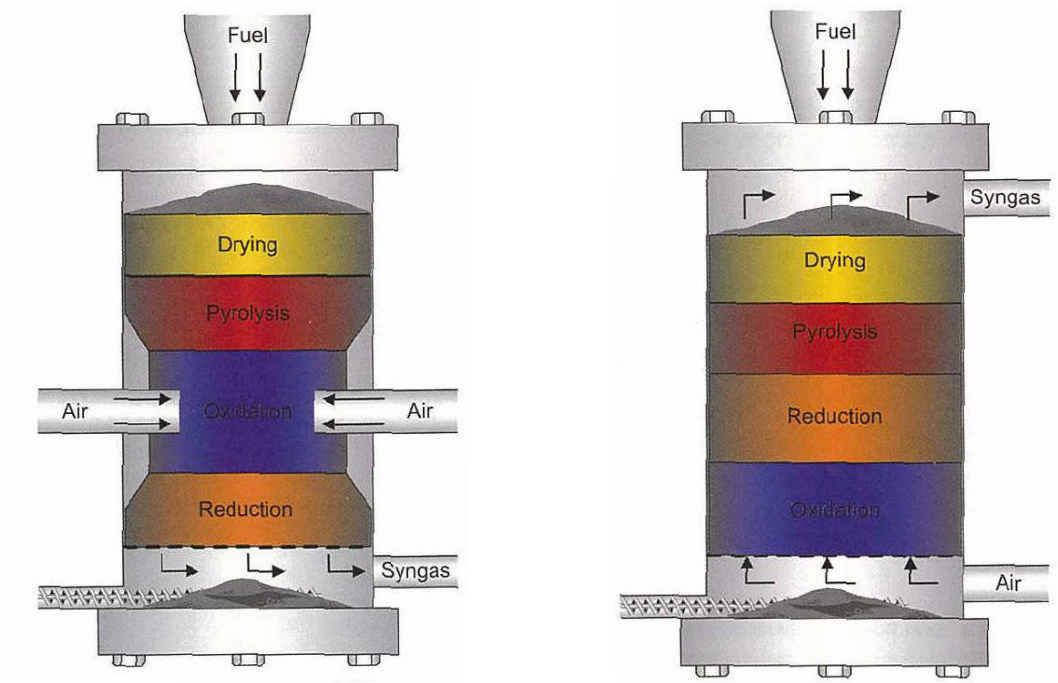

Figure 1-2: Fixed bed reactors downdraft (left) and updraft (right) [9]

Downdraft gasifiers

In the downdraft design, both the air and the fuel are fed from the top of the reactor where for the air intake can also be positioned on the side (Figure 1-2, left). The producer gas moves downward in the same direction as the biomass and leaves the reactor at the bottom. The downdraft design yields the same type of zones as the updraft design, although their placements relative to the updraft reactors are different (see Figure 1-2). Since air is added directly to the oxidation zone, the producer gas stays at high temperature and generates in this manner low amounts of tars (< 100 mg/Nm^3). Another derives of the downdraft reactors is the open-core design. These types are specially designed for fuels consisting of fine materials with low bulk density. Because of this low bulk density, the fuel feed can be hampered due to bridging and can stop completely in stratified type reactors. Due to its straight wall design, open-core gasifiers are more suitable for these fuel types where rotating grates can be easily applied to both stir the fuel and remove the high amount of ash these fuels usually produce.

Fluidized bed gasifiers

Fluidized bed gasifiers for biomass originate from the technology for coal gasification and are usually suitable for large scale operation. The reactors are built with a porous grate in the bottom where sand or other fluidization medium lies above. Air or other types of gasification agent such as steam, oxygen or a combination of theses pass through the

porous grate at an enough speed (μ_{mf}) so that the bed particles become suspended. The gas velocity through the grate is quite a critical parameter for the design and the optimization of the gasifier. Increasing μ_{mf} causes the bed particles to move more vigorously resembling a boiling liquid. Normally the inlet velocity of fluidized bed gasifiers is 5 – 30 times the fluidization velocity, but can be as high at 300 times μ_{mf}. When biomass is added to the bed, it gets also fluidized. The thermal degradation and the gasification reactions of the fuel take place at high speed in an environment that is well mixed due to turbulence. The bed material needs to attain high temperature, typically 700 – 900 ºC in order to drive the endothermic gasification reactions forward. The energy needed to keep the bed material at a suitable temperature can be transported to the bed in different methods. The most usual way is to burn some of the biomass, usually about 25 % of the incoming fuel [9]. Because of the intense mixing, the heat transport to the fuel happens at a high rate so that the different zones found in fixed bed reactors are not distinguished in fluidized beds. The fluidized bed reactors that are commonly used in gasification are; bubbling fluidized bed and circulating fluidized bed. Theses two types are shown in Figure 1-3 below.

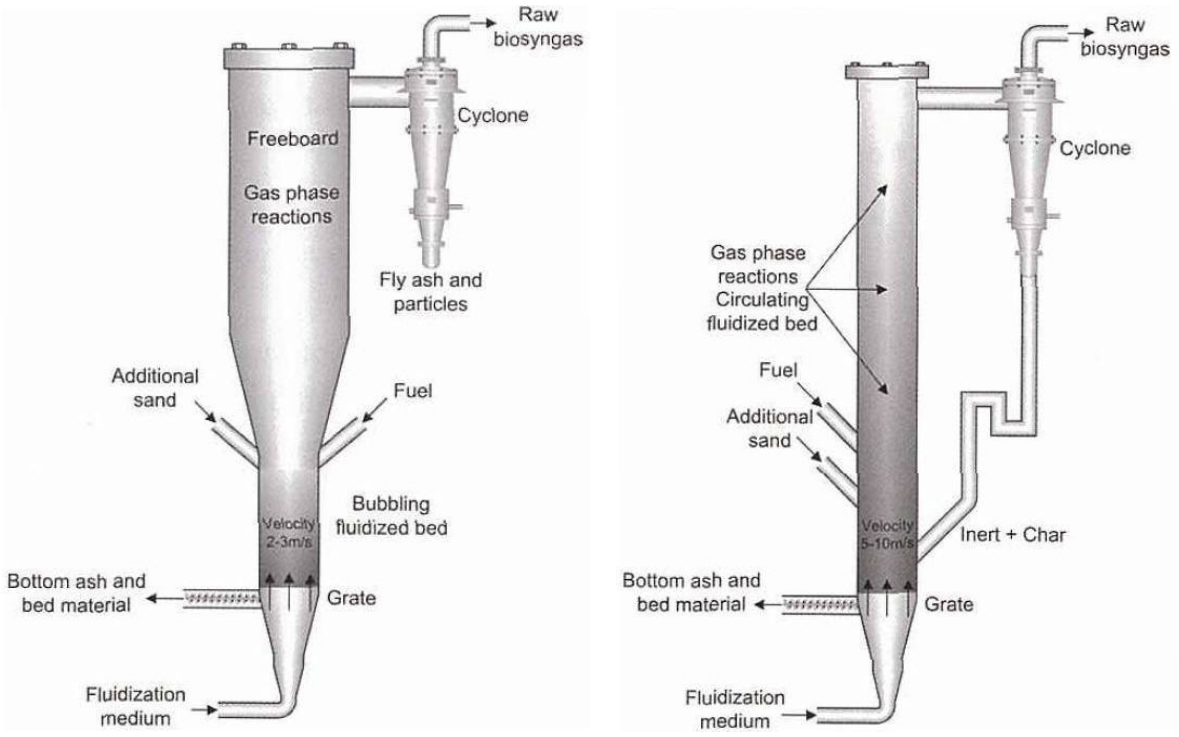

Figure 1-3: Fluidized bed reactors, bubbling (left) and circulating (right)

The difference in terms of advantages and drawbacks between fixed bed reactors and fluidized bed are highlighted in Table 1-1.

Table 1-1: Comparison between fixed bed and fluidized bed reactors

Advantage	Disadvantage
Updraft	
Simple design	High amounts of tars
High charcoal burnout	Extensive gas cleaning is required in cases where the gas is used for power production
High efficiency	
Can use fuel with high moisture (up to 60 % wet basis)	
Accepts variation in fuel size	
Downdraft	
Low tar content	Limited in terms of up scaling
Suitable for gas engines	Low load produces more tars
Low load produces low levels of particles	High amount of particles and ash in the gas
	Low efficiency
	Strict requirement to fuel moisture (<25 %)
	Requires uniform fuel particle size (4 – 10 cm)
Fluidized bed	
Compact design due to high heat exchange and intensive mixing	High tar and dust content in the producer gas
Uniform temperature profile (no hot spots)	Incomplete carbon conversion
Different feedstock can be used	Compression of gas streams generates a need for power consumption
Flexible to changes in fuel characteristics such as moisture-, ash content and bulk density	The need to control both the fuel supply and the air yields complex operation
Low and uniform bed temperature gives less problems related to ash melting	High producer gas temperature containing alkali metals in vapor state

Gussing plant

One of the few successful gasification plants so far, is the industrial plant erected in Gussing, Austria. This plant is specifically mentioned in this thesis due the successful operation of the plant and also due to collaboration of NTNU and the University of Vienna on hot gas filtration [10]. The plant at Gussing is able to produce a high calorific value gas rich in hydrogen. This has been possible not only due to the use of steam for the gasification but also due to reactor design that is able to separate the combustion from the gasification zone. It was mentioned earlier that a combustion zone is necessary in order to provide energy to the endothermic gasification reactions. The gasification reactor at the Gussing plant consists of a twin fluidized sections. The first reactor is a steam gasifier where biomass is fed and mixed with the bubbling hot sand. The unreacted char residues

that are not converted are transported along with the bed material to the combustion zone. This combustion zone uses air to combust the char residues which results in an increased temperature of the bed material. The hot sand is entrained due to the high velocity and is transported back to the gasification reactor where it acts as an energy source for the endothermic reactions. With this configuration the combusted products are separated from the gasification products resulting in a syngas containing lower amounts of CO_2 and almost no N_2. A sketch of the reactor configuration is shown in Figure 1-4.

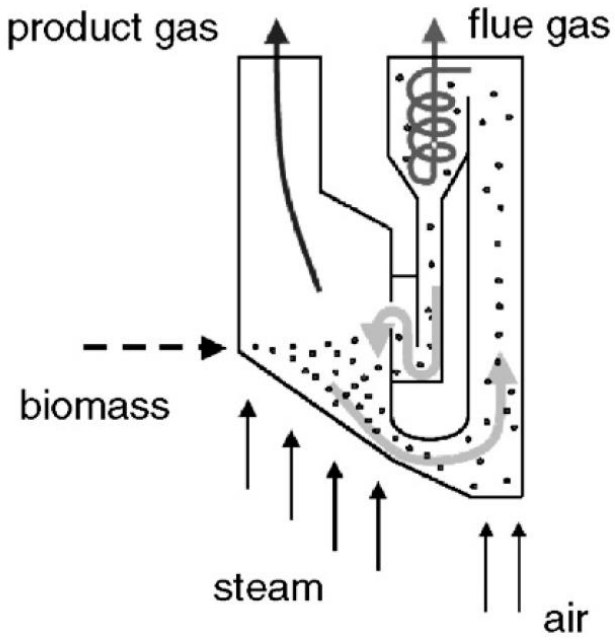

Figure 1-4: The principle behind the gasification process at the Gussing plant.

1.2.3 Combustion

The combustion process consists of a complete oxidation of the fuel by using excess air. For solid fuels, combustion is a complex process that consists of both homogenous and heterogeneous reactions (Figure 1-5). Similar to gasification, we find in a combustion process several different zones where drying, pyrolysis, oxidation of char and reactions in gas phase occur simultaneously. Several parameters in the combustion zone are quite crucial to the combustion process; among these are reactor technology, combustion temperature, size and moisture content of the fuel. Although combustion is quite conventional compared to other thermal processes, research and technological improvements are still an ongoing activity. For woodstoves, improvements on chamber design are of main concern. This includes combustion optimization by staged combustion. The main objectives are to reduce particle emissions. For larger installations, the main

concern is the reduction of pollutants such as sulfur, nitrous and heavy metal compounds. Such pollutants are not only hazardous to nature and the human life but they also create problems during the thermal conversion. For instance, understanding the behavior of fly ash in order to avoid slagging and corrosion in the boiler is still a hot topic that has drawn the attention of many research activities during the past decades and at present. Fly ash is usually caused by the content of alkali metals such as potassium (K) and chlorine (Cl). Such compounds react and form potassium chloride (KCl) which condensates at low temperature and create process and environmental related problems. The ash content in biomass differs depending on the fuel type. Woody biomass has very low ash content and nitrogen while straw and other agricultural biomass sources for instance have much higher ash content. During the selection of technology for biomass combustion it is very important to consider the type of fuel that will be used. Most of particle emissions from combustion of biomass are below 10 μm in size. The submicron and supermicron particles in a fluidized bed are mainly composed of K, Cl, S, Na and Ca while corrosive are composed mainly of Ca, Si, K, S, Na, Al, P and Fe. For combustion in fixed bed the particle load increases with increased reactor diameter. Particles usually coagulate and condensate in the lower temperature zone of the combustion chamber, usually close to the boiler.

Many primary and secondary measures for combating pollutions and optimizing the combustion process exist. One of the successful methods for combating nitrous compounds (NO_x) is staged combustion (Figure 1-5), which gives a better control over the temperature profile in the combustion chamber. The idea is to gain control over temperature gradients inside the combustion chamber and by that decreasing the formation of thermal NO_x. NO_x formation in combustion of biomass can originate from the nitrogen content in the fuel (fuel NO_x), or the oxidation of the nitrogen found in the air (thermal NO_x). NO_x reduction could also be achieved through secondary measure such as the direct injection of ammonia (NH_3) in the boiler. Staged combustions helps also to attain good mixture and turbulence conditions in all parts of the combustion chamber. When optimized conditions are met the level of unburned hydrocarbons are usually at a very low level (ex. CO < 50 mg/m3 and C_xH_y < 5 mg/m3). Optimized conditions are usually attainable by having a good control over three parameters, temperature, turbulence and time. While temperature and residence time are easily controlled (usually kept at respectively 850 ºC and 0.5 s), attaining acceptable level of turbulence remains the most challenging task of the three. Optimized

mixing condition (high turbulence) has in the later years been studied in more detail by using computers where computational fluid dynamics code (CFD) has been a helpful tool in predicting the flow conditions during the design of the combustion chamber.

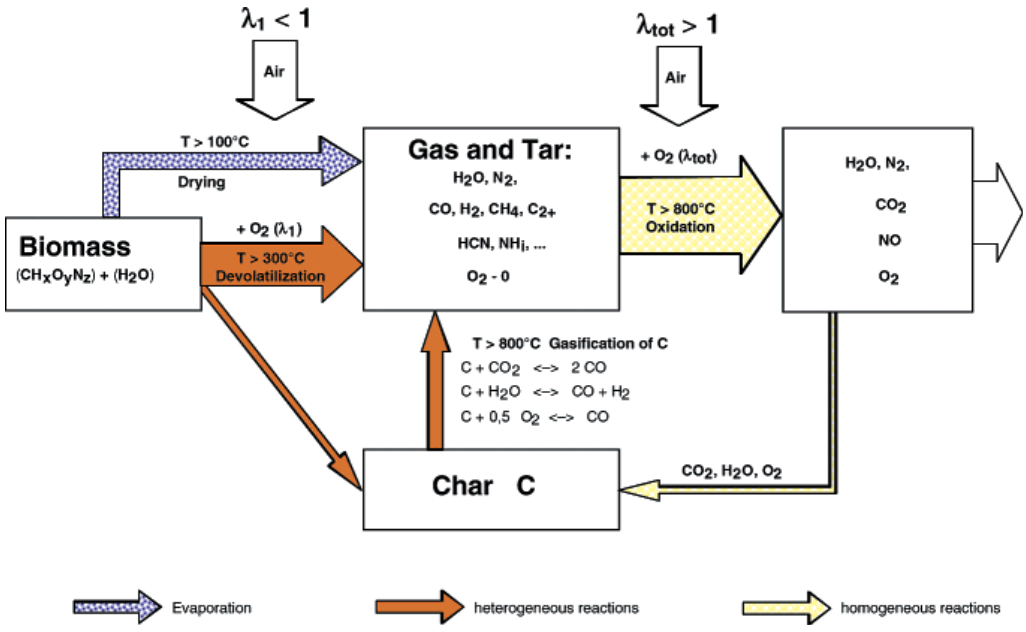

Figure 1-5: The different reactions in combustion of solid fuels [11]

The choice of technology for the combustion of solid fuels will depend mainly on the plant size and the fuel type. The main combustion technologies are underfeed stokers, grate combustion, bobbling fluidized bed (BFB) and circulating fluidized bed (CFB). Underfeed stokers are mostly suited for small scale systems with a maximum capacity of 6 MWth and for biomass types containing low levels of ash. Low ash levels are important because underfeed stokers usually have an inefficient ash removal system. The advantages and the drawback of the other three combustion technologies are shown in Table 1-2 below [12].

Table 1-2: The advantage and drawback of the different combustion technologies [12]

Grate combustion	
Advantage	Drawback
Low investment cost for plants < 10 MW_{th}	Problems during combustion of straw or straw/biomass co-combustion
Low operation costs	Effective measures for NO_x reduction require special technology
Low particle load in the flue gas	High air excess ratio reduces efficiency
Less slagging compared to bubbling and circulating fluidized bed	Combustion conditions are not homogenous compared to BFB and CFB
Good operation during partial load	
Good burn-out of fly ash particles	
Bubbling fluidized bed	
Advantage	Drawback
Low investments costs for plants > 10 MW_{th}	High operation costs
NO_x reduction under air staging works satisfactorily	High particle load in the flue gas compared to grate combustion
High fuel flexibility concerning particle size, moisture content and mixtures of biomass fuels	Good operation at partial load requires adjustment in form of special technology
No moving parts in the combustion chamber	Medium sensitivity due to ash slagging
Lower air excess ratio gives higher efficiency	Medium erosion in heat exchanger tube
Circulating fluidized bed	
Advantage	Drawback
No moving parts in the combustion chamber	High operation costs
NO_x reduction under air staging works satisfactorily	High investments costs, only interesting for plants > 30 MW_{th}.
High fuel flexibility concerning moisture content and mixtures of biomass fuels	Partial mode operation requires a second bed
Homogenous combustion if several fuel injections are used	Loss of bed material with the ash
High specific heat transfer due to high turbulence	Problems with ash slagging
Easy addition of additives	High particle load in the flue gas
Effective sulfur retention in the ash if enough calcium is available	Low flexibility concerning fuel particle size
	Medium problems with erosion of heat exchanger tubes

1.3 Biomass characteristics

Biomass is a biological material that originates from living organisms that includes both plant life and animal. The biomass diversity of origin makes it difficult to classify because of its varying properties. Physical and chemical properties of biomass make its conversion process to useful energy quite complex. Some characteristics, regarded important to thermal conversion are briefly explained below.

Heating value

The heating value can be defined as the higher heating value (HHV) which is based on the energy content in dry biomass or the lower heating value (LHV) which is basically the higher heating minus the condensation energy of the water vapor produced due to the hydrogen content in biomass. Another common term for the energy content in biomass is the effective heating value (EHV) which can be calculated from the LHV by subtracting the energy share used to evaporate the moisture in biomass. The elemental content in biomass has a great effect on the heating value; C and H tend to increase it while oxygen decreases it. The lignin content is also strongly correlated to the heating value where fuels with high lignin share are reported to have higher energy content than fuels with high cellulose and hemicellulose content.

Moisture content

Moisture content in biomass influences the volume of the flue gas in case of combustion and results in larger equipment for flue gas handling. It varies over a wide range from 10 – 70 %. Water content also influences the heating value of the fuel as it decreases with higher moisture values. Biofuels have normally a high moisture content which can cause ignition problems and reduce the combustion temperature. Consequently, the combustion of the reaction products is also affected which leads to higher fuel usage. During pyrolysis, the moisture content affects the physical properties and quality of the pyrolysis gases.

Volatile matter

Volatile matter during thermal degradation is released as gases consisting of light hydrocarbons, carbon monoxide, carbon dioxide, hydrogen, moisture, and tars. Biomass has a high volatile content which makes it easier to ignite even at low temperature. Since volatiles get released relatively fast during thermal degradation, its fraction in biomass becomes a decisive parameter in designing reactors. In combustion, one has to ensure enough residence time for the devolatilized products in order to ensure complete combustion and to ensure low pollutant emissions (CO and PAH). Biomass can lose up to 90% of its mass in its first stage of combustion. The amount of devolatilized products during the pyrolysis stage of combustion increases with increasing hydrogen to carbon ratio and, to some extent, with increasing oxygen to carbon ratio.

Ash content
Ash is the inorganic part of the fuel that is left after thermal conversion. It contains the bulk of the mineral fraction of the original biomass. The ash content in the biomass varies with different types and can vary from 1 % (wood) and up to 30 – 40 % (green house residues). The major ash elements found in biomass include Si, Al, Ti, Fe, Ca, Mg, Na, K, S, and P. The release of ash particles during thermal treatment can occur due to ash volatility or reaction with the organic fraction of biomass. Ash elements that become volatile at high temperatures are derivatives of some of the alkali and alkaline earth metals, most notably potassium and sodium. Other non volatile elements such as Ca and Mg can be released by convective transport during a fast devolatilization stage. The ash composition has a great effect on the ash melting point. Potassium and Si for instance yield lower ash melting point while Mg and Ca increase it. Certain fuels such as demolition wood contain heavy metals such as Cd, Cr, Cu, Pb, and Hg. Such elements are regarded hazardous for the environment and are normally found in the fly ash in combustion plants.

1.4 Biomass species used in this study

In this thesis several types of biomass fuels have been studied, some due to their fast growing abilities which will result in an efficient use of the available land. Others have been chosen because they are agricultural rest products that can become an important addition to the energy production. A brief description of the fuels is given below.

1.4.1 Short rotational energy crops

Energy grass
Energy grass (*Agropyron*) as the name indicates corresponds to the grass family which is also being considered for the purpose of producing energy in some European countries. These types of herbaceous crops are also valuable for vegetation because of their drought resistance and winter hardness. Pelletized form of the energy grass was used in our experimental study.

Poplar
Poplar Pannonia (*Populus×euramericana*) has a relatively high growth rate compared to other Poplar clones. In general, short rotation coppice cultivation with poplar rotations range from 2 – 5 years. The plantation density is also high (between 10 000 – 20 000 plants/ha) [13].

Tree of heaven

Tree of heaven (*Ailanthus Altisssima*) is native to China and was introduced to Europe in 1751. The tree of heaven is a very fast growing tree with hairy twigs and a flat-topped crown of stout branches. It is considered as being "invasive" because the female tree produces quantities of wind dispersed seeds that are capable of traveling great distances [14]. Nevertheless, Ailanthus in countries like Hungary can become an important source for the production of alternative energy.

1.4.2 Straw

Annual biomass such as straw is the most available agricultural residue both in Europe and North America with a yearly production of 800 million tons in 2002 [15]. In countries like Denmark, straw is available in surplus quantities and has been used as a fuel for larger heat and power plants for over a decade. Straw has been chosen in this study due to its higher sulfur content compared to other biomass types. Straw has been extensively studied in the literature due to its difficult behavior during thermal conversion. The high ash content generates problems such as corrosion because of the deposition of potentially corrosive elements such as K, Cl etc on the heat-transfer surface of the boiler. The high content of chlorine and sulfur will result in the release of acidic pollutants that will not only harm the environment but also create problems within the thermal conversion process.

Production of straw pellets

The samples were prepared at the Technical University of Denmark (DTU), Department of Mechanical Engineering, in a laboratory pellet mill used for testing and optimizing the pellets production of different solid fuels. The mill is equipped with a vertical ring type-die where solid fuels are pressed outward through cylindrical holes. The ring-die can be exchanged so that the dimension of the cylindrical holes and their number can be varied. This is useful because by varying these dimensions, the friction of the pellet pressing is changed. An optimal friction should produce enough force to compress the pellet without increasing the temperature of the contact surface above 90 ºC. Overheating this surface will lower the friction and causes burn marks on the pellet surface and thereby lowering its quality [16]. The ring-die that was used had 40 holes and a ratio of compression of 6.5. The ratio of compression is defined as the cylinder length (50 mm)/cylinder diameter (7.7 mm). Figure 1-6 shows the pellet mill and the blender that were used to produce the straw pellets.

Figure 1-6: Pellet mill (left), mixer (right).

The straw with its smooth and shiny surface was proved to be difficult to pelletize without the addition of a binding material. Suggestions of mixing 10 % CAP (Calcium phosphorus solution) with the straw were considered. However, for this study it was decided not to use CAP since further contamination of the elemental composition of the straw was not desired. Only 10 % of water was added along with the additives. The water would help cool down the die temperature as it evaporates while the pellets are being pressed. The straw was mixed with the additives 1 kg at a time in a Björn varimixer for 10 min. The correct amount of water was sprayed while the mixer was running in the first minutes of operation. CaO and $Ca(OH)_2$ were chosen as additives for the sulfur binding at the devolatilization stage. The added quantity was chosen to produce a molar ratio of Ca/S of 2 and 4. This is the ratio of the calcium added through the additive relative to the Sulfur found in the straw.

1.4.3 Hard and soft wood

Pine

Pine (*Pinus Silvestris*) is one of the most common wood species found in Norway. It is grown in a dense manner in order to encourage increasing both its length and the girth of the trunk. Grown crowded, pine can attain a length of 20 – 30 m and a diameter of 1 m. Pine is used extensively in the building industry and in the manufacturing of paper pulp, which makes it quite a demanded product. Tars produced from the root of pine trees has

been used for hundred of years to impregnate boats and houses [3]. In this work, char produced from pine has been used to study its gasification kinetics. Pine was chosen as a representative of a soft type wood.

Birch

Birch (*Betula Verrucosa*) is a robust tree that thrives in cold climate. Its adaptive nature makes it easy for it to grow on almost any type of soil; in addition birch can survive in extreme weather conditions. In Norway birch is spread across the whole country and is commonly used as a fire wood. Birch is easy to process which makes it an attractive material to work with for the manufacturing of furniture and other small household articles. Birch was chosen as a hard wood compound for the study performed in paper 4 [4].

1.4.4 Analysis of fuels used in this study

The proximate and ultimate analyses of all fuels used in this work are presented below.

Table 1-3: Proximate and ultimate analysis

Proximate analysis [Weight %]			
	Volatiles	**Fixed carbon**	**Ash**
Straw	76.47	18.07	5.46
Straw char	9.96	60.01	30.03
Pine	86.84	12.95	0.21
Pine char	20.38	78.57	1.05
Birch	87.87	11.82	0.31
Birch char	19.16	79.86	0.98
Energy grass	75.2	18.1	6.7
Poplar	83.0	15.6	1.4
Tree of heaven	82.2	16.0	1.8

Ultimate Analysis (Oxygen calculated by difference)						
	C	**H**	**N**	**O**	**S**	**Cl**
Straw	46.0	6.2	0.6	46.1	0.11	0.45
Straw char	67.4	1.7	0.9	21.6	0.13	0.68
Energy grass	46.5	6.3	1.0	46.2	0.08	-
Poplar	49.0	6.4	0.4	44.2	<0.02	-
Tree of heaven	51.1	6.8	0.7	41.5	0.04	-

1.5 Objective of this study

Most of the work performed in this study has concentrated on the thermal decomposition of biomass. This is because as much as 75 % or even more of the biomass is composed of volatile matter (see Table 1-3) that will start decomposing at lower temperatures. The characteristics of the devolatilized products during pyrolysis are reported in Paper I for

several fuels types that have been considered as sources for energy production due to their fast growing abilities. Paper I also reports results for the same biomass types in oxidative atmosphere. An oxidative atmosphere is also important from the gasification point of view because partial combustion is normally used in a gasification process in order to produce the necessary energy for the endothermic gasification reactions. For these studies and the rest of the pyrolysis experiments (papers II and III), the macro-TGA was used which allows the use of large biomass samples (80 g. for most of the experiments). The use of large samples has some advantages among these are the following:

- Reactions are limited by diffusion rates and the temperature gradients in the thermally thick samples which tend to replicate better situations found in fixed bed reactors and processes based on grate combustion.

- The generation of large amounts of gas products allows the use of more sophisticated gas analytical equipments such as FTIR and GC.

One of the main challenges of gasification of solid fuels is the increased process complexity and costs due to the gas cleaning step. Because the producer gas contains pollutants such as tars, nitrous and sulfuric compounds, it is important that such a process includes an efficient cleaning step in order to get a trouble free operation during the conversion. Since the producer gas usually has a relatively high temperature (800 ºC), gas cleaning becomes quite challenging. Of course one has the option of reducing the temperature prior to gas cleaning but only at the expense of lowering the process efficiency. Another goal of this study was to condition the devolatilized products in order to generate an upgraded gas product with reduced pollutants. Non-thermal plasma is a method that has a documented effect on the dissociation of tars, sulfuric and nitrous compounds and can operate at high temperature. Paper II gives a detailed study on the effect of non-thermal plasma on the devolatilized products from pyrolysis of straw pellets, while paper III concentrate on reducing the sulfuric compounds from the gas phase. These compounds will cause corrosion in turbine blades and lower the efficiency of solid oxide fuel cells (SOFC). Regardless on how the producer gas is to be utilized the sulfur fraction will most certainly end up as SO_2 after energy conversion and should be removed from the flue gas prior to release. Two different methods for reducing sulfur emission in pyrolysis of straw were looked upon. The first is an active method that involves hindering the sulfur release with the producer gas through chemical reactions in the char matrix. This was done

by introducing calcium based additives to the straw prior to pelletization. The second method was gas product treatment with non-thermal plasma.

Finally the gasification kinetics of two types of wood chars, pine and birch were reported in paper IV. This work was aimed at finding the reaction rates for these types of wood chars.

1.6 Organization of this thesis

All the work that has been performed for this study was published in four scientific papers that can be found in appendix A. The content prior to the scientific papers explains in more details the different aspects of topics treated in this study. Chapter 1 gives an introduction explaining the importance of biomass as an energy source in our modern society. It also gives a short theoretical explanation of the different thermochemical conversion processes. Important fuel characteristics of biomass are explained including the ones used in this study. Finally this chapter shows the motivation behind the different treaded subjects and how they are linked together.

Chapter 2 gives a comprehensive literature survey over three topics covered throughout the work on this thesis. The Sulfur release has been extensively studied in this thesis. Chapter 2.2 explains how the sulfur is incorporated in the straw, its release during thermal degradation and some possible routes for its retention in the ash. The role of calcium based additives in sulfur retention under pyrolysis is also explained along with the reactions mechanisms that are responsible for its capture. Non-thermal plasma was used in some of the experiments performed in the lab, where its effect on the major pyrolysis products and on sulfur reduction was reported. Chapter 2.3 gives a brief theoretical explanation of the different non-thermal plasma reactors that has been used in the literature for altering the chemical composition of the gases. It also mentions some of the topics that non-thermal plasma was proved useful among these are improvement in gas combustion, reduction in pollutants such as tars, nitrous- and sulfuric compounds. Reactions involved in the destruction of H_2S through non-thermal plasma are also explained. Finally chapter 2.4 gives details around char gasification reactivity where the different models used in the literature are explained along with biomass characteristics that can influence on the reaction rates.

Chapter 3 gives a description of the main reactors used in the experimental work, namely the micro-TGA, the macro-TGA and the non-thermal plasma.

Chapter 4 gives a summary over the published articles while chapter 5 gives an overall conclusion and recommendation of this work.

Appendix A includes all the publications that were produced.

Appendix B gives a description of the different analytical equipments and their principle of operation. Some preliminary work performed on the calibration of the advanced gas measuring equipments (FTIR and GC) is also explained. The literature warns of adsorption effects of sulfuric compounds due to improper use of materials. Some preliminary measures in order to eliminate such effects were performed. This includes cold runs for the investigation of the reliability of the gas cleaning equipment on the adsorption of H_2S and COS. Finally, some experiments were repeated at equal conditions in order to report the reproducibility.

2 Theoretical background

2.1 Introduction

This chapter gives a theoretical description of three topics covered throughout the work on this thesis. It includes details on sulfur incorporation in the straw, its release during thermal degradation and some possible routes for its retention in the ash. The role of calcium based additives in sulfur retention under pyrolysis is also explained along with the reactions mechanisms that are responsible for its capture. Details of the different non-thermal plasma (NTP) reactors used to study the alternation of the molecular structure of gases are also presented. NTP is used as a mean for the creation of gas radicals that improve combustion condition and is also useful at combating several types of harmful compounds. The chemical reactions involved in the destruction of H_2S through NTP are explained in a greater detail in this chapter. A literature survey on sulfur degradation in NTP is also presented here. Finally this chapter gives details around char gasification reactivity where the different models used in the literature are explained along with biomass characteristics that may influence the reaction rates.

2.2 Sulfur in straw

2.2.1 Sulfur incorporation in plants

Sulfur in the straw is usually assimilated by the roots as inorganic sulfate and transported to the leaves where a reduction process to sulfide occurs. The reduction reaction proceeds through several enzymatic catalyzed reduction steps. Sulfur can also be assimilated through sulfur containing gases such as H_2S. Sulfide is combined with organic molecules to form cysteine which is an amino acid from which proteins are formed [17]. On its way to the formation of cysteine, sulfur is transformed with the help of different mechanisms first to sulfite and later to sulfide. Figure 2-1 illustrates a proposed reaction route of sulfur transformation from its uptake through the plant roots and on to its way of forming cysteine [18].

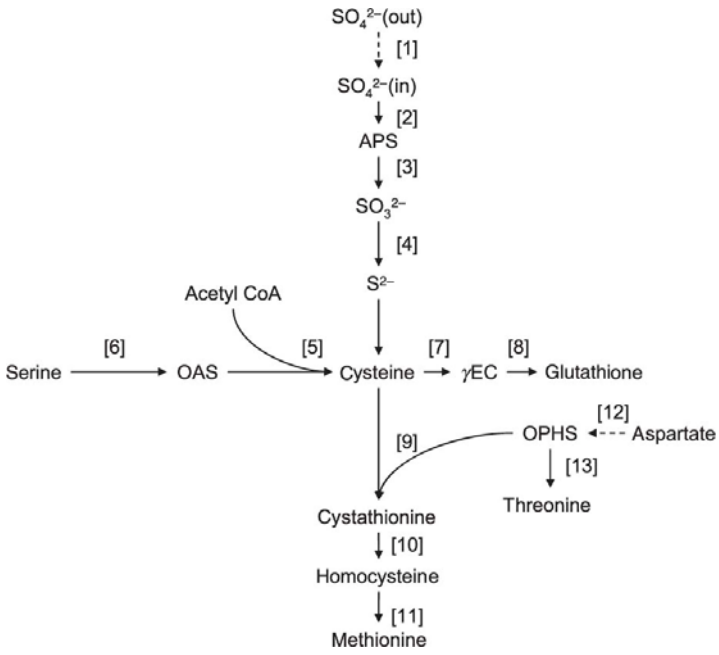

Figure 2-1: The sulfur pathways to cysteine, glutathione, and methionine biosyntheses.

Due to this complex steps of transformations, sulfur will be present in a variety of different compounds and may appear in oxidation stages from (-II) to (+VI). The sulfur uptake into the plant is necessary for the growth and development of the plant. Several other factors will influence the demand of sulfur among these is heavy metal exposure which seems to increase the demand of sulfur uptake. Sulfur distribution management in the plant is controlled by a gene family consisting of 14 members in *Arabidopsis*. There is clear evidence that this family gene is involved in the initial uptake at the soil-root interface, cell to cell transfer and vascular transportation [18]. The lack of sulfur availability will also change the distribution of sulfur and the way it is bound in the plant. For example, in case the supply of sulfur is greater than the demand, the excess sulfur can be present in the plant fluid as free sulfate esters. The sulfate esters are stored in the cell vacuole and accumulate during the growth period [19]. Alternatively, sulfur can also be emitted to the atmosphere as H_2S after a reduction step. As all these formations are continuously occurring in the plant, sulfur can have two forms, organically bound and inorganic sulfate. It is believed that the organically bound sulfur has a lower stability which will result in decomposition at low temperature (400 ºC) during the devolatilization period. The inorganic sulfates are more stable and will not be released during the devolatilization stage. The ratio of organic to inorganic sulfate, as well as the overall sulfur content depends on the growth conditions and the sulfur supply to the plant during the growth period. Due to the incorporation of the sulfur in the building structure of the plant, removing it in a pretreatment step like aqueous

leaching is more difficult compared to other compounds such as Chlorine (Cl) and Potassium (K) [20]. On the other hand, aqueous leaching will remove sulfates that are still not organically bound.

2.2.2 Sulfur release through thermal degradation

The reaction mechanism of sulfur release during the thermal decomposition depends on the different fractions of the trace elements that are found in the fuel. Potassium and calcium are the main elements that will influence the release of sulfur to the gas form, while chlorine has an indirect effect on the retention of sulfur during thermal decomposition. In addition, silicon (Si) presence in the fuel will greatly affect the pathways of several reactions among theses, the fate of sulfur. To better understand the behavior of the different elements during thermal degradation, it is important to have an idea on how they are incorporated into the straw. Potassium and chlorine remain usually in ionic form K^+ and Cl^- and are not metabolized by the plant. These compounds will therefore precipitate when the plant is dried and are easier to remove by aqueous leaching. Their main function in the plant is to maintain a neutral charge and pH value, as well as to regulate the osmotic pressure and stimulate enzyme activity [17]. Silicon is usually present in high quantities in annual biomass species. It is assimilated as monosilicic acid ($Si(OH)_4$) and it forms a silicate network structure in the cell walls. Silicon in straw is present as silicate on the external surface of the cell plant. It is responsible for giving the plant its structural strength and protection against microorganisms. Silicon may also be present in the plant as SiO_2 particles and clay minerals due to soil contamination. To better understand the sulfur behavior during both pyrolysis and combustion, the chemical equilibrium calculation performed by Knudsen et al. [15] is shown in Figure 2-2.

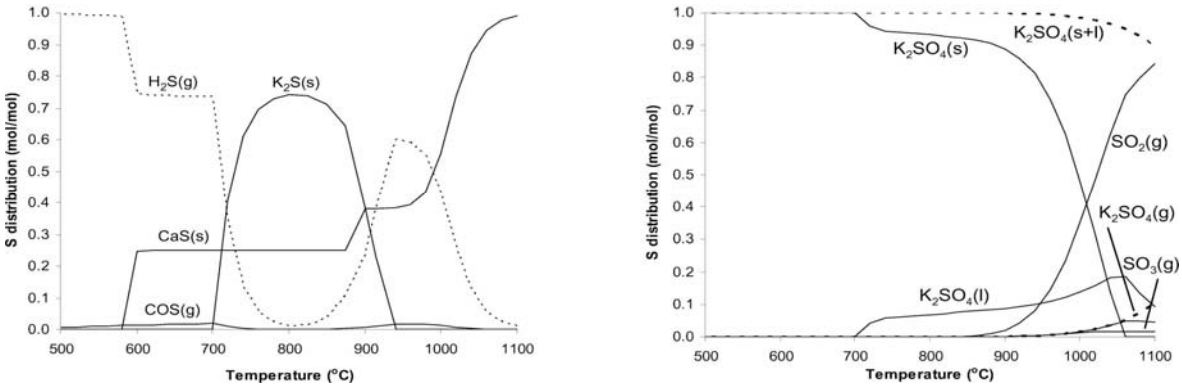

Figure 2-2: Equilibrium calculation of the distribution of S. Left side, straw pyrolysis case where Ca and K silicate are omitted ($\xi = 0$). Right side, straw combustion case ($\xi = 1.4$), dashed line represents S distribution where Ca and K silicates were omitted.

The equilibrium calculation is performed with FactSage version 5.1 and is based on Gibbs free energy minimization. It is important to point out that such programs reproduce results based on a global chemical equilibrium, a state that is never fulfilled during an experimental approach. Another limitation that is not taken into consideration is the reactions that occur between the gas-phase sulfur and the functional groups present in the char matrix that are capable of binding the sulfur. Nevertheless, such calculations might help to understand some chemical routes that are thermodynamically favored. Thermodynamic equilibrium helps also to understand the stability of the formed inorganic sulfur species. Results presented in Figure 2-2 describe the pyrolysis condition (left side) and combustion with an oxygen excess ratio of $\xi = 1.4$ (right side). During pyrolysis, we see that sulfur is present as H_2S at temperatures between 500 – 600 ºC. For temperatures above 600 ºC, the sulfur starts reacting with Ca and forms CaS. Between 700 ºC and 900 ºC the route to forming K_2S is favored, while for temperatures above 900 ºC Ca becomes active again. During combustion, we can see that K is an excellent element for sulfur retention as it is able to form potassium sulfate (K_2SO_4) which is thermally stable at temperatures up to 1000 ºC. At higher temperatures the sulfur is released as SO_2. In case where Ca and K silicate were omitted, the S is retained in the ash as K_2SO_4, even at higher temperatures (the dashed line in Figure 2-2, right side).

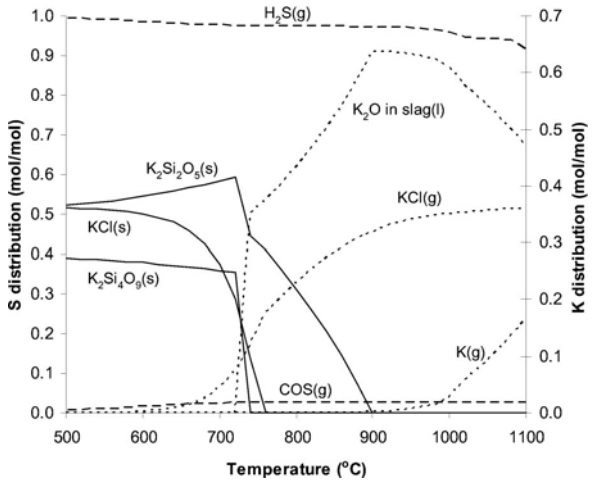

Figure 2-3: Equilibrium calculation of the distribution of S and K during pyrolysis. K silicate is included in the calculation.

In Figure 2-3, the equilibrium calculations during pyrolysis are reproduced by the same author [15] only this time silicon was included in the equilibrium calculation. As it mentioned before, silicon and chlorine play an indirect role on the sulfur reaction pathway.

As Figure 2-3 shows, sulfur is released as H_2S for all the pyrolysis temperature range. In the presence of high concentration of chlorine and silicon in the fuel, the potassium will be favorably released as potassium chloride (KCl) and potassium silicates. As it was clarified before, the calculations provided in Figure 2-2 and Figure 2-3 can not be reproduced in experiments due to reasons mentioned earlier. In case of silicon reactions, it is important also to point out the fact that silicon is mainly found at the outer structure of the plant and is not perfectly mixed in the fuel as it is assumed during the equilibrium calculations.

The presence of high concentrations of silicates in the fuel will lower the thermal stability of the formed calcium sulfate ($CaSO_4$) and potassium sulfate (K_2SO_4) under oxidative conditions as well. At temperatures above 700 – 800 ºC and for the silicate rich fuels, the captured sulfur is re-released to the gas phase as SO_3 by following the reaction routes (2-1) and (2-2) [21].

$$CaSO_4(s) + SiO_2(s) \leftrightarrow CaO \cdot SiO_2(s) + SO_3(g) \tag{2-1}$$

$$K_2SO_4(s) + SiO_2(s) \leftrightarrow K_2O \cdot SiO_2(s) + SO_3(g) \tag{2-2}$$

So far it has been shown by thermodynamic equilibrium that potassium has a high affinity for sulfur but because of elements such as chlorine and silicon, potassium might not be available for the reaction with sulfur. How does this translate in real experiments? Experiments performed by Knudsen et al. [15] have proved that during pyrolysis of straw up to a temperature of 700 ºC, no potassium silicates were found in the char rest fraction. While for temperatures above 700 ºC, significant amounts of potassium was retained by the silicon. This is contradictory to the equilibrium calculations presented in Figure 2-3 and can be explained by the fact that at low temperatures the structure of the cell walls was still intact while at higher temperatures it collapses. Only when the cell walls collapse, silicon and potassium will have a better mixing condition where chemical reaction between the two elements may take place. Silicon in coal however, might behave differently as it can have a beneficial effect on the sulfur retention at high temperature. In this case, silicon may physically enwrap sulfates of lower thermal stability and prevent the dissociation [15].

Chlorine is another compound that has a high affinity for potassium and will affect indirectly the release of sulfur. Knudsen et al. [17] reached the conclusion that K will be preferably released as KCl rather than retained in the ash as potassium silicate. The

volatility of chlorine during thermal decomposition of different biomass products has been investigated thoroughly by many [17, 21-25]. Studies done on alkali metal emission have shown that chlorine starts devolatilization at low temperatures and as much as 60 % of its initial amount will be released between 200 - 400 ºC [23]. The chlorine release during pyrolysis of straw proved to be dependent on the heating rate and on the sample size [23]. For small samples and fast heating rates (50 ºC/s) the chlorine was released in two steps, 60 % between 200 – 400 ºC and the rest was released between 700 – 900 ºC. For large samples (70 g) and slow heating rates (30 ºC/min) only 42 % of the chlorine was released at a temperature of 500 ºC. The later observation can prove that the organic char matrix is able to retain some of the chlorine and as a consequence, also influences the volatility of potassium. Not only chlorine can be retained in the organic matrix as Jensen et al. [23] stated; both sulfur and potassium are capable of forming intercalation compounds with carbon. Such compounds are stable up to a pyrolysis temperature of 830 ºC. It has also been shown the potassium is mainly released as KCl during the pyrolysis stage. During combustion, the released KCl can react with the SO_2 through the following reaction [15]:

$$SO_2(g) + \frac{1}{2}O_2(g) + H_2O(g) + 2KCl(g) \leftrightarrow K_2SO_4(g) + 2HCl(g) \qquad (2\text{-}3)$$

It is obvious that the different mechanisms that are involved in the chemical reactions of the inorganic elements are quite complex. The main findings of the behavior of the different inorganic elements during the thermal treatment of straw have been summed up in Figure 2-4.

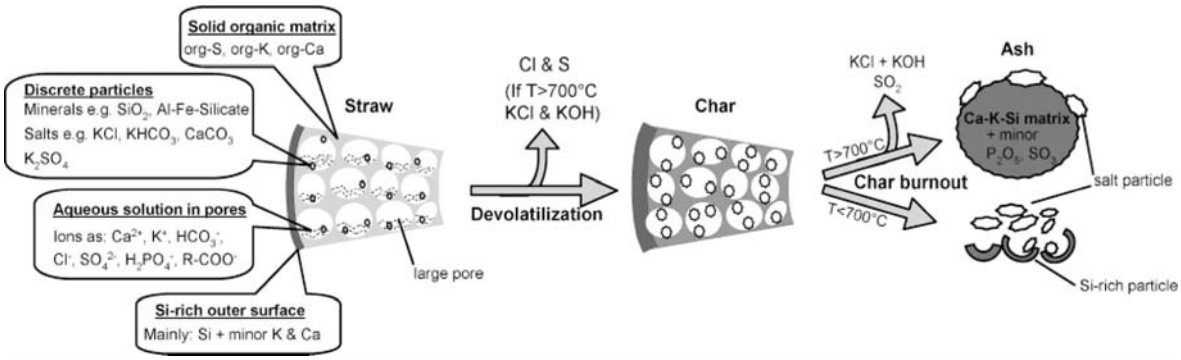

Figure 2-4: Illustration of the structural and inorganic transformation during the devolatilization and char burnout of annual biomass [17].

Figure 2-4 shows the structure and some of the elemental distribution of straw. During devolatilization the organic bound sulfur is released mostly as H_2S. Depending on the

pyrolysis temperature potassium is released mostly as KCl while chlorine is released at temperatures lower than 700 ºC. The outer surface which is rich in silicon is not deformed during the devolatilization stage. Due to separation of the silicon found at the outer surface from the calcium and potassium rich particles found inside the char matrix, the formation of potassium silicate is limited. During the burn off of the char, the outer silicon rich shell is disintegrated and reaction between silicon and potassium and calcium salts may occur. Depending on the combustion temperature, potassium may be retained in the ash as potassium silicate (up to temperature of 900 ºC). For higher combustion temperatures the potassium is released to gas phase. In cases of fuels rich in chlorine, potassium might be volatilized at lower temperatures. The release of sulfur during the combustion stage will depend on the presence of potassium and calcium elements that are not bound to silicon.

2.2.3 Role of additives in the chemical reaction of sulfur

For biomass, some investigation has been done on the retention of sulfur in the ash of some bio-fuel types such as straw [15, 21, 24 and 26]. It has been reported that the sulfur release during the devolatilization of straw comes from the organically bound sulfur at very low temperatures (200 – 400 ºC) and is difficult to retain [24]. Such conclusions were drawn while investigating calcium based additives on combustion of straw. Under these experiments the devolatilization temperature (1200 ºC) was well above the pyrolysis temperatures presented in this work (paper III) [8]. While retaining the sulfur in the ash under combustion has resulted in many investigations, little has been done on the retention of sulfur in biomass under pyrolysis conditions. As mentioned before, the retention of sulfur is usually possible in the presence of elements such as calcium and potassium that may be able to bind it under proper conditions. Equilibrium calculations have shown that potassium has a higher affinity for sulfur compared to calcium. Although this postulate is true, we have already seen that potassium might not be available for reactions with sulfur due to its affinity towards silicon and chlorine. The stability of the formed K_2SO_4 in the ash is also significantly lowered in the presence of silicate. Under such circumstances the - released sulfur has the opportunity to react with calcium under proper conditions and consequently, becomes retained in the ash. Investigation performed by Knudsen et al. [17] has shown that more than 60 % of the remaining sulfur in the ash was found as $CaSO_4$ at 1150 ºC, which proved that the dissociated sulfur from K_2SO_4 was retained in the calcium instead. The use of calcium based additives in coal combustion has already shown some promising results in improving their ash-binding ability [27-30]. So far the same has not

been done for biomass due to the relative lower concentration of sulfur compared to coal. During the pyrolysis it is expected that sulfur will be released as either H_2S or COS which even at low concentration can cause major problems. These compounds can be expected to bind with the calcium oxide and calcium hydroxide as follows:

$$CaO + H_2S \leftrightarrow CaS + H_2O \tag{2-4}$$

$$CaO + COS \leftrightarrow CaS + CO_2 \tag{2-5}$$

$$Ca(OH)_2 + H_2S \leftrightarrow CaS + 2H_2O \tag{2-6}$$

$$Ca(OH)_2 + COS \leftrightarrow CaS + CO_2 + H_2O \tag{2-7}$$

Reactions (2-4) and (2-6) are acid-base reactions that are thermodynamically favored at low and high temperatures [27]. As shown in the reaction scheme above, the sulfur will be retained as CaS in the ash. CaS in its pure form is stable up to 2400 ºC, nevertheless its presence in the ash is not so desired because it reacts with water at ambient temperature and releases the sulfur back to the atmosphere as H_2S [31]. Several publications have outlined a solution to this problem by transforming the CaS through reaction (2-8) [31-35].

$$CaS(s) + 2O_2(g) \leftrightarrow CaSO_4(s) \tag{2-8}$$

The oxidization in reaction (2-8) is controlled by product layer diffusion when a certain layer of $CaSO_4$ is formed. Reaction (2-8) might occur along with two other reactions (2-9) and (2-10).

$$CaS(s) + \frac{3}{2}O_2(g) \leftrightarrow CaO(s) + SO_2(g) \tag{2-9}$$

$$CaS(s) + 3CaSO_4(s) \leftrightarrow 4CaO(s) + 4SO_2(g) \tag{2-10}$$

Given (2-9) and (2-10), the sulfur will not be 100 % retained in the ash through (2-8). The optimum temperature for reaction (2-8) was found by Yrjas et al. [33] to be between 815 – 900 ºC. The solid to solid reaction (2-10) was studied by mixing CaS(s) and $CaSO_4$(s) and heating up the mixture. They showed that at 850 ºC no solid to solid reaction occurred while at 1050 ºC a 100 % conversion to CaO was achieved.

2.3 Chemical reactions under the influence of non-thermal plasma

Plasma is one of four matter phase that exists; the three others being solid, liquid and gas phase. Up to 99 % of the matter that could be found in the visible universe is plasma. In addition to neutral molecules and atoms, plasma is composed of free electrons and ions. There are two means of producing plasma from a gas phase; these are usually referred to as thermal- and non-thermal plasma (NTP). In thermal plasma, molecules are heated to extremely high temperatures which results in increased electron velocity in atoms and molecules up to a point where they leave their orbit and become unattached. Electrons and atoms are in thermal balance and have a typical temperature range of 5000 – 50000 K. In NTP, molecules and atoms are kept at ambient temperature while electron temperature can attain 10000 – 100000 K. Due to the strong electrical field in NTP, ions and electrons are produced with high average kinetic energy. These electrons target the atoms and produce not only free radicals and ions but also electrons through electron impact dissociation. The molecular dissociation of the different compounds does not only occur through the intermediate radicals but may also happen through direct collision with the migrated electrons.

Figure 2-5 shows different types of NTP reactors that are widely used in the literature. They differ in the plasma physical and electrical properties such as mean electron energy, mode of discharge, corona onset voltage, voltage-current characteristics and so on. Reactors in Figure 2-5 can be divided into 2 groups; the gas phase homogenous group ((a), (b) and (c)) and the gas-solid heterogeneous reactors ((d) and (e)). [36]

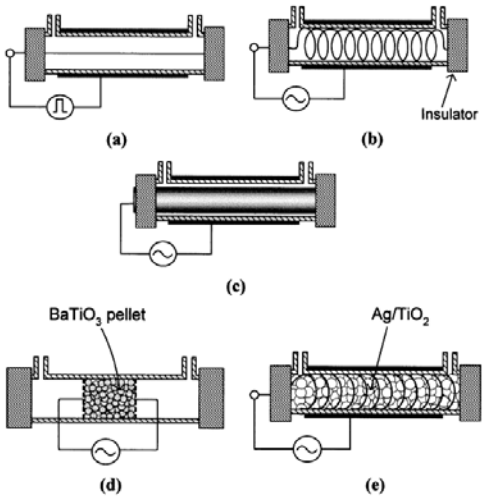

Figure 2-5: Schematic diagrams of NTP reactors. (a) Pulsed corona (b) Surface discharge (c) Dielectric barrier discharge (d) Packed bed (e) Plasma driven catalyst [36]

2.3.1 Plasma assisted combustion

Gas combustion enhancement can be achieved by applying NTP to the fuel, the oxidant or even both. Through the creation of active species and radicals, it becomes possible to dissociate the gaseous fuels into smaller and more easily combusted fragments. Whether the use of NTP for combustion enhancement will succeed in becoming a viable solution in a well established technological platform depends first on the energy cost and second on the complexity of such solutions. So far, the energy ratio of plasma power to flame duty has been in the range 0.01 – 0.03 which makes it promising from the energy consumption point of view [37-41]. NTP assisted combustion will result in an increased flame stability and reduced pollution due to the following improvements:

- The produced free radicals and active species will increase the flame propagation rate.
- The flammability limits are increased and leaner combustion conditions are possible. This has an indirect effect on NO_x emissions since lean combustion helps reduce peak temperatures in the combustion zone.
- NTP reduces ignition delays. Pancheshnyi et al. [42] was able to reduce the ignition delay of a premixed propane-air by an order of magnitude of 2.5.
- Soot reduction which in return will reduce high temperature peaks in the flame and result in NO_x reduction.

2.3.2 Plasma reactions in the destruction of pollutants

NTP treatment can operate at high temperatures and was proven successful in removing harmful compounds such as tars [43-48], sulfuric [49-55] and nitrous compounds [56-57]. The electron field which is generated by the NTP targets mainly the background gas, but also the rest of the compounds and produce free radicals and ions that in return activate chemical reactions. The molecular dissociation of the different compounds does not only occur through the intermediate radicals but may also occur through direct collision with the migrated electrons.

2.3.3 Sulfur decomposition

During gasification or pyrolysis of biomass, most of the sulfur that is found in the gaseous products is H_2S. The dissociation of H_2S through NTP could be a viable solution since the ionization potential of H_2S (10.4 eV) is considerably lower than many other gas

compounds found in the product gas. Other gas types that are known to promote chemical reactions in the presence of the plasma have also a higher ionization potential, He (24.6 eV), Ar (15.8 eV), H_2 (15.4 eV), N_2 (15.6 eV). However, higher applied voltage is required for the electrical breakdown of H_2S compared to other gases because H_2S is an electronegative gas with a high dielectric strength. When the balance gas of a NTP system is free from oxidants, the overall reaction of the decomposition of H_2S becomes as follows:

$$H_2S_{(g)} \rightarrow H_{2\,(g)} + S_{(s)} \qquad (2\text{-}11)$$

H_2S is a very weakly bound molecule where the theoretical energy required for its decomposition is 20.3 kJ/mol. Four reactions pathways that lead to the dissociation of H_2S with a NTP were proposed by Zhao et al. [53].

1. Direct ionization of H_2S followed by dissociative neutralization

$$e + H_2S \rightarrow H_2S^+ + 2e \qquad (2\text{-}12)$$

$$H_2S^+ + e \rightarrow HS + H \qquad (2\text{-}13)$$

2. Ionization of the balance gas, leading to charge transfer reaction and subsequent dissociative neutralization

$$e + M \rightarrow M^+ + 2e \qquad (2\text{-}14)$$

$$M^+ + H_2S \rightarrow H_2S^+ + M \qquad (2\text{-}15)$$

$$H_2S^+ + e \rightarrow HS + H \qquad (2\text{-}16)$$

3. Dissociation through direct electron collision with H_2S

$$e + H_2S \rightarrow HS + H + e \qquad (2\text{-}17)$$

4. Electron collision with the balance gas, which produce active species that contribute to the dissociation of H_2S. In this case the active species can be either dissociated radicals or molecules in exited state

$$e + M \rightarrow M^* + e \qquad (2\text{-}18)$$

$$M^* + H_2S \rightarrow H + HS + M \qquad (2\text{-}19)$$

In all of the proposed pathways, the outcome of the H_2S dissociation is the radicals H and HS that react with each other and with other H_2S molecules to form H_2 and pure sulfur. Experiments performed with different balance gases resulted in the rejection of 1 and 2 ((2-20) to (2-21)) as possible pathways for H_2S dissociation. Furthermore for experiments performed in paper III [8], the pathway 4 is more likely to occur due to the lower concentration of H_2S in the produced gas. To obtain an inert atmosphere for the experiments performed in this study, N_2 was used. N_2 can therefore be considered as being the balance gas in the NTP reactor and the main compound responsible for the dissociation of H_2S through reactions (2-18) and (2-19) of pathway (4). In case of N_2, dissociative reactions can occur through either the first exited state of N_2, ($N_2(A)$) or the radical N through equation (2-22) and (2-23).

$$e + N_2 \rightarrow N + N + e \quad (2\text{-}22)$$

$$e + N_2 \rightarrow N_2(A) + e \quad (2\text{-}23)$$

It has been shown that the rate of reaction (2-23) is 7 orders of magnitude higher than (2-22) and will more likely be the responsible reaction in this study [58]. It is important to point out that the processed gas in this study is quite complex and the produced radicals might favor reactions with other compounds than H_2S. On the other hand, the dissociation of H_2S might occur through radicals produced from other sources than the balance gas, for example H radicals produced from the dissociation of H_2.

When using NTP with other types of background gases than the ones mentioned earlier, other radical species will be generated, which in turn will influence the conversion pathway of H_2S. For instance, air with low concentration of H_2S is generated due to anaerobic bacterial action in manure storage facilities. Processing this type of gas in a NTP reactor will most likely produce Ozone (O_3) because of the presence of oxygen. Nitrogen radicals produced through (2-22) and (2-23) can also react with oxygen to form nitrous oxide through reactions (2-24) to (2-27).

$$N + O_2 \rightarrow NO + O \quad (2\text{-}24)$$

$$N + NO \rightarrow N_2 + O \quad (2\text{-}25)$$

$$N_2(A) + O_2 \rightarrow N_2O + O \quad (2\text{-}26)$$

$N_2(A) + O_2 \rightarrow N_2 + 2O$ (2-27)

If water is present in the treated gas, OH radicals can be produced through reactions with oxygen radicals or through dissociation by electron collision. A possible reaction for the dissociation of H_2S is by reaction with O_3 to produce SO_2 and H_2O (2-28).

$H_2S + O_3 \rightarrow H_2O + SO_2$ (2-28)

Finally SO_2 can react further to produce acids such as HSO_3 and H_2SO_4 through the following reactions ((2-29) to (2-31)).

$OH + SO_2 \rightarrow HSO_3$ (2-29)

$OH + HSO_3 \rightarrow H_2SO_4$ (2-30)

$2NH_3 + H_2SO_4 \rightarrow 2(NH_4)_2SO_4$ (2-31)

Reaction (2-31) will only occur in case of the presence of ammonia. In anaerobic processes such as bacterial degradation of manure, ammonia is produced along with H_2S.

2.3.4 Work on sulfur decomposition in NTP

Helfritch et al. [51] experimented on the removal efficiency of H_2S in a pulsed corona discharge reactor. H_2S was diluted in H_2 at different concentrations (0.125 % – 2 %). In their work H_2S concentration, reactor energy consumption, reactor diameter and gas velocity through the reactor were varied. 75 % removal efficiency was achieved at 10 J/std cc. Better efficiencies were reported at increased energy consumption levels. The removal efficiency decreased with increasing H_2S concentration. Decreasing the reactor diameter has also increased the removal efficiency. Zhao et al. [53] also employed a corona discharge reactor for their study of H_2S dissociation in different background gases (Ar, He, H_2 and N_2). The breakdown voltage was reported for the pure compounds as a function of gas pressure. Gases at normal temperatures and pressures contain very low concentrations of current carriers (free electrons and ions) and therefore behave as insulators. In an electric field, any electrons or ions present are accelerated over a distance corresponding to their mean free path between collisions. If they gain enough kinetic energy to ionize gas molecules, they create new current carriers which in turn ionize more molecules. This avalanche-like process forms channels of conducting plasma called streamers. The electrical resistance of the gas between the electrodes becomes nearly zero. This transition

of a gas between the insulating and conducting states is known as breakdown. The voltage at which it occurs is called the breakdown voltage. For the experiments performed by Zhao et al. [53], the breakdown voltage was plotted at increased H_2S concentration for all the background gases. It is important to point out that the breakdown voltage depends on the specific reactor configuration. Their main findings were that it was not possible to ionize pure H_2S in their particular reactor setup. H_2S conversion was more efficient in atomic balance gases (Ar and He) than diatomic gases (H_2 and N_2). Conversion efficiency decreased with increased H_2S concentration for all balance gases. H_2S concentration was varied between 5 % and 25 %, and the highest conversion of 30 % was obtained at 5 % H_2S in the balance gas He. Energy consumption seemed to have a minimum value at a H_2S concentration of 15 %. The lowest energy consumption was obtained with Ar and He as balance gases followed by N_2 and then H_2. Ma et al. [49] have worked on the removal of the odorous NH_3 and H_2S in silent plasma discharge using air as a balance gas. Experiments where performed on low concentrations in the range of 3 – 30 ppm. For their reactor configuration the removal efficiency was close to 100 % for H_2S and 75 % for NH_3 at the low concentration range. The efficiency decreased for both compounds when the concentration was increased. For H_2S at a concentration of 14 ppm, the removal efficiency dropped down to 40 % while for NH_3 at a concentration of 16 ppm, the removal efficiency dropped to 20 %. The removal efficiency was enhanced by injecting a small concentration of ozone. The effect of increased NH_3 concentration on the removal of H_2S was also tested. It was shown that NH_3 level had no effect on the removal efficiency of H_2S. Finally, it was shown that H_2O concentration plays an important role on enhancing the removal efficiency due to the generation of OH radicals through the dissociation of water. Dalaine et al. [54, 55] employed a gliding arc reactor for their study on the destruction of H_2S balanced in dry air. The H_2S concentration was varied between 2 and 60 ppm. The only transformation product was found to be SO_2. Two power supplies at different frequencies were tested, 50 and 25000 Hz. Up to 75 % conversion efficiency was possible with the 50 Hz power supply while for the other (25 kHz) the removal efficiency was lower. The energy consumption for the 25 kHz power supply was close to 500 eV/destroyed molecules while for the 50 Hz power supply, energy consumption varied between 500 and 1500 eV.

2.4 Gasification reactivity

Heterogeneous reactions play an important role in many applications and especially in chemical-industrial activities such as gasification and combustion of solid fuels, catalytic processes, and processes based on chemical vapor deposition as in the semiconductor industry [59]. Whether gas-solid interactions are of physical or chemical nature, a kinetic analysis helps enhancing such processes through the identification of the reaction rates. In case of gasification, suitable models that are able to predict reaction rates can be transferred to practical applications such as reactor design and optimizing operational parameters. In order to determine the gas-solid reaction rates, the weight loss of the reacting solid has to be measured preferably in short time increments. Two methods have been extensively used in the literature, thermogravimetric and spectrometric techniques. In thermogravimetry, one measures the weight variation of the sample with a balance placed inside a temperature controlled furnace. With the spectrometric techniques, one measures the concentration of the gasified products from which the sample weight loss can be derived. While a thermogravimetric analyzer is quite accurate in terms of measuring the weight loss, its limitations lies in problems related to heat and mass transfer issues because the sample is enclosed in a crucible inside the furnace. On the other hand, heat-transfer limitations are avoided in spectrometric techniques by using drop tube reactor types, while the draw back being a less accurate reaction rate calculation. Recently, Di Blasi [60] has given an excellent literature review of developed combustion and gasification models for lingocellulosic chars. In the following, a short review of kinetic models will be given.

2.4.1 Kinetic models

The main reactions responsible for the gasification of solid carbon are the Boudouard reaction and the water gas reaction presented in (2-32) and (2-33).

$$C(s) + CO_2 \rightarrow 2CO \tag{2-32}$$

$$C(s) + H_2O \rightarrow CO + H_2 \tag{2-33}$$

Both reactions are quite slow and are considered to be insignificant at temperatures below 800 ºC. In order to be able to predict the reaction rate in the Boudouard reaction (2-32) several models have been developed. The common goal for all models is to find a suitable function that will predict the gasification rate of a carbon particle through its conversion to gaseous products.

Global reaction rate

The simplest model for the prediction of a global reaction rate is the n^{th} order intrinsic rate equation expressed in (2-34).

$$r = k \cdot p_{CO_2}^n \tag{2-34}$$

Where

r is the intrinsic reaction rate.

P_{CO_2} is the partial pressure of the gasification agent CO_2.

n is the true reaction order.

k is the intrinsic rate coefficient which is related to temperature through the Arrhenius expression:

$$k = Ae^{-E/RT} \tag{2-35}$$

Here

A is a pre-exponential factor.

E is the global activation energy.

R is the gas constant.

T is the temperature.

The Langmuir-Hinshelwood kinetic equation

More complex expressions have been derived based on the active site theory with the postulation that chemical reactions occur at favored active sites on the surface of the solid particle. The most widely used model is based on the adsorption of CO_2 on the surface, followed by CO desorption (equations (2-36) and (2-37)).

$$C_f + CO_2 \underset{k_2}{\overset{k_1}{\leftrightarrow}} C(O) + CO \tag{2-36}$$

$$C(O) \xrightarrow{k_3} CO + C_f \tag{2-37}$$

Where

C_f represents an active carbon site.

$C(O)$ is a carbon-oxygen complex.

By assuming a pseudo-steady-state for the C(O) complex $\left(dC(O)/dt = 0\right)$, the Langmuir-Hinshelwood kinetic equation can be derived (2-38).

$$r = \frac{k_1 C_t p_{CO_2}}{1 + \left(k_2/k_3\right) p_{CO} + \left(k_1/k_3\right) p_{CO_2}} \tag{2-38}$$

Here C_t is the total number of active carbon sites.

The Langmuir-Hinshelwood differs from the nth order equation in three important areas [61]:

1. The intrinsic reactivity is a non-linear function of the CO_2 partial pressure. The equation (2-38) does depend on an uncertain pressure order n but will reduce to the nth order equation in the case where p_{CO} is close to zero.

2. It is based on an adsorbtion-desorption 2-step reaction and therefore has a mechanistic basis.

3. The inhibition effect of CO is taken into account which is clearly demonstrated in (2-38). Increasing the partial pressure of CO reduce the intrinsic reactivity.

In order to be able to calculate the pre-exponential factors and the activation energies of all the rate coefficients in equation (2-38), many thermogravimetric experiments are needed. A step by step explanation of the calculation procedure can be found in [62]. The intrinsic reaction rate of equation (2-38) depends on the number of active carbon sites C_t, a variable that is likely to change with the conversion rate of the particle. The number of active carbon sites is quite difficult to measure and attempts to relate it to other carbon char properties have been developed [63].

2.4.2 Reactivity related to changes in the char particle structure

Relating reactivity to changes in the physical properties of the char particle has resulted in the development of many models. Two types of models are quite common to find in the literature, structural types and volumetric models [64]. With structural type models, the internal solid matrix (grain) or the internal pore structure is mathematically described as a function of the conversion rate. The structural model types usually require a larger number of experimental data compared to other models. For the volumetric models, the changes in porosity are linked to the conversion rate of a carbon particle. Three models that have been widely used in the literature are presented next.

The random pore model

The structural evolution of a particle undergoes two competing effects during the course of conversion. In the initial stage the char particle undergoes growth of the internal pores followed by a gradual collapse of the pore structure due to the coalescence of neighboring pores [65]. Consequently, the internal surface area will exhibit an increase at an early gasification stage followed by a decrease at a later stage. One of the widely used models that relates the free carbon site to the internal distribution of the particle pores is the random pore model (RPM). This model which was developed by Bhatia and Perlmutter [66] represents the variation of pore structure within the solid as conversion progresses using only one dimensionless parameter ψ. The RPM takes into consideration the effects of pore growth and coalescence [67], but it is assumed that no new pores are formed during the gasification reaction [68]. The pore surface area within a solid is described in the following equation.

$$S = S_0\sqrt{1-\psi \ln(1-X)} \tag{2-39}$$

Where

S_0 is the initial pore surface area of the randomly overlapping pores with a size distribution $V_0(r)$

X is the carbon conversion which can be written as:

$$X = \frac{w_0 - w}{w_0 - w_a} \tag{2-40}$$

w_0 is the initial sample weight

w_a is the weight of the ash

w is the weight of the char at a certain time during the conversion

$$\psi = \frac{4\pi L_0 (1-\varepsilon_0)}{S_0^2} \tag{2-41}$$

ε_0 is the porosity which can be calculated from the initial total volume of the randomly overlapping pores with a size distribution $V_0(r)$

L_0 is the initial length volume of the randomly overlapping pores with a size distribution

The reaction rate based on the random pore model can be written as follows:

$$\frac{dX}{dt} = \frac{k_s C^n S_0}{1-\varepsilon_0}(1-X)\sqrt{1-\psi \ln(1-X)} \tag{2-42}$$

Where

k_s is the intrinsic rate constant

C is the concentration of the gasifying agent.

The RPM is able to predict the conversion rate of char up to 70 % conversion (X = 0.7) after which it becomes inaccurate and predicts a systematic drop of reaction rate to zero [67,69].

Homogenous model or volume reaction model (VRM)

This model assumes the solid-gas reaction occur on active sites that are uniformly distributed through the whole particles. Gas diffuses also uniformly through the entire particle. The volume of the particle remains constant as reactions progress while the density decreases. The reaction kinetic is derived applying a mass balance for the first-order reaction in a single particle which results in the following kinetic expression [70-71]:

$$\frac{dX}{dt} = k(1-X) \tag{2-43}$$

Another more complex version of the VRM, the modified VRM assumes that the apparent rate constant (k) changes with conversion. k is then integrated to obtain an average rate constant.

Shrinking core or changing grain size model (CGSM)
The gaseous reactants in the CGSM diffuse through a gas film and then through an ash layer after which they react on the core surface. The core, which is usually assumed to be spherical, shrinks as a function of the conversion. As conversion progresses, the reaction rate varies with relation to the core particle.

The reaction rate expression is as follows:

$$\frac{dX}{dt} = \left(3/\tau\right)(1-X)^{\frac{2}{3}} \tag{2-44}$$

Where τ is a model related parameter which is compromised of some solid characteristics, the constant rate and the concentration of the gasification agent.

2.4.3 Parameters that influence reaction rates

In reality, the reactivity of heterogeneous reactions is quite complex and difficult to predict accurately in one model. This is because reaction rates are easily influenced by the physical and chemical properties of both the gas and the solid phase. Parameters that will have an effect on the reaction rates are described below.

Inhibition effect of different gas species
It is quite obvious that the gasification agent in commercial size reactor will not consist of pure CO_2 but a mixture of other compounds such as CO, H_2O and H_2 that will certainly influence reaction rates in one direction or the other. It has already been shown how the Langmuir-Hinshelwood kinetic equation takes into account the inhibition effect of CO. Similar equations can be derived to take into account the inhibition effect of other compounds such as H_2. The inhibition effect of H_2 on CO_2 gasification reactivity has been addressed in [72] while Barrio et al. [73] studied H_2 inhibition in steam gasification. Barrio et al. studied also the inhibition of CO on CO_2 gasification [74].

Effect of the internal particle structure
The effect of the internal surface area on reaction rates has been discussed in section 2.4.2. In these models the evolution of the internal surface area during the course of conversion is related to the reaction rate. The size of the internal particle area might be also linked

indirectly to the reaction rate because of the effect of chemisorption. It was mentioned earlier that through the gasification process oxygen atoms are adsorbed on active carbon sites. In some other models it is postulated that CO_2 can also be adsorbed entirely on a carbon site ($C(CO_2)$). Measuring the weight loss rate with a TGA might be disturbed by chemisorbed complexes on the reactive carbon surface. This is because the observed rate of weight of change is actually the difference between the rates of chemisorption and desorption. In the work of Feng et al. [75], a surface area of 312 m^2/g was found to be critical for the steady state assumption. It was concluded the internal surface area that were above this limit should be corrected for the chemisorption effect.

Diffusion limited reactions

The dependency of the intrinsic rate constant on temperature is clearly seen in the Arrhenius expression. It can also be seen from all the derived reaction rates that the partial pressure of the gasification agent influences the conversion velocity. In fact, common sense alone should dictate that by increasing gasification temperature and pressure, one should expect an increase in reaction rate. At a certain level, the chemical reactions are so fast that the limiting factor becomes the transport of the gasification agent to the solid surface. This diffusion limitation is illustrated in Figure 2-6 where reactant concentration profile is drawn for increasing intrinsic reactivity [76]. Curve I represents no diffusion limitations due to slow reactivity, hence the uniform reactant concentration. As reactivity increases, it becomes more difficult to transport the reactant inside the particle (curves a and II). For higher reaction rates, the concentration starts to decrease at the boundary layer. Curve IV shows the case where reactants are not able to penetrate inside the particle and for curve III reactants are consumed at the boundary layer.

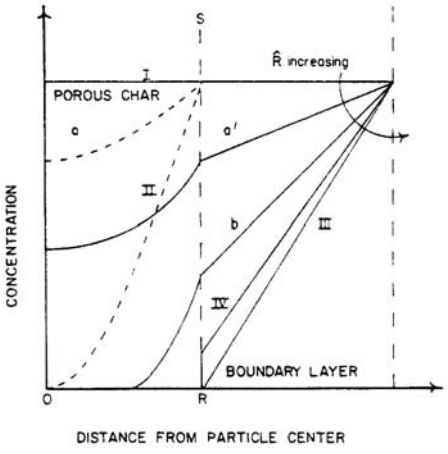

Figure 2-6: Concentration profile of reactant inside a particle (<R) and outside (>R) [76]

The mass transfer limitations are often related to intrinsic reaction rates with a factor of effectiveness as shown in Figure 2-7. The zones in Figure 2-7 correspond to the same numbered curves in Figure 2-6. In zone I, the logarithmic value reaction rate increases linearly with increasing temperature, a fact that is often demonstrated in the kinetic literature. This linear dependency fails when the transport of reactant becomes the limiting factor.

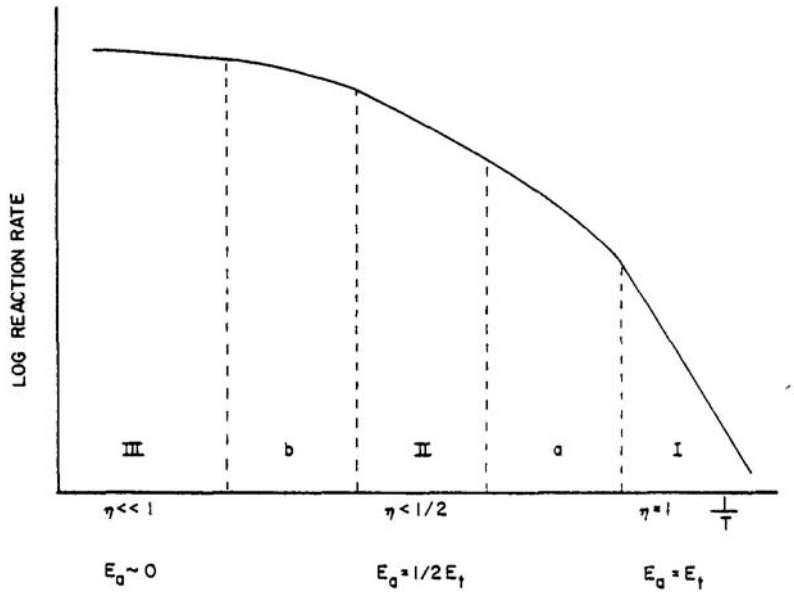

Figure 2-7: Change of reaction rate as a function of temperature. [76]

The effectiveness factor (η) has been calculated from the CO_2 partial pressure gradients along the particle radius and the molecular diffusivities of CO_2 and CO in the internal pores of the solid particle [61, 64, and 77]. Usually it is normal to use an effective diffusivity which is the sum of the contribution of the diffusivity for macro-, meso-, and micro-pores. The apparent reaction rate can than be written as follows:

$$R_{app} = \eta R_{in} S \tag{2-45}$$

Mineral content in char

Inorganic impurities in the surface area of the carbon matrix can have a catalytic effect on the gas solid reactions which will result in an increase of the reactivity. This catalytic effect has been studied for both coal char and other derived chars. Sun et al. found that reactivity of Shenmu maceral chars decreased after demineralization [78]. They also demonstrated increased reactivity after catalyst loading, where better result was obtained by ultrasonic

loading of the catalyst. In another study, cottonwood was sorbed with ferrous and ferric sulfates $FeSO_4$ and $Fe_2(SO_4)_3$ and pyrolysed [79]. The rest char was used later in thermo gravimetric experiments to examine the catalytic effect of the treated wood on gasification reactivity. Ferric sulfate was found to have good catalytic properties for CO_2 gasification. The impregnation of char coal with metal species and its influence on char reactivity was also studied by Struis et al. [80]. It was found that heavy metals decrease reactivity by 15 % throughout all the conversion range. The authors got better results when earth-alkali metals where added which resulted in high reactivity at an early conversion stage, but flawed rapidly thereafter.

2.4.4 Model used in this work

The motivation behind our study is to try and identify differences in reaction rates between two types of woods, a hard wood type (birch) and a soft wood (pine). Prepared char from those two types might differ due to their internal structure which might influence the reactivity. The differences in the wood types are not only reduced to the internal surface area and pore-size distribution but also to the ash content and the way the different metals are dispersed in the char matrix [78]. Metal oxides are known to enhance char reactivity because of their catalytic activities.

The chemical reactions were modeled using three parallel reactions where 2 describe the devolatilization stage using first-order kinetics that are independent of gas concentration. Theses reactions are described in equations (2-46).

$$dX_j/dt = A_j \exp(-E_j/RT)\,(1-X_j)\,(_j = 1, 2) \qquad (2\text{-}46)$$

The gasification reaction kinetics is described in a third equation according to:

$$dX/dt = A \exp(-E/RT)\, f(X)\, C_{CO2}{}^{v} \qquad (2\text{-}47)$$

Where $f(X) = \text{normfactor} * (X+Z)^a\,(1-X)^n$

a, Z and n are adjustable parameters and normfactor is a normalizing factor ensuring that max f(X) = 1.

f(X) is basically an empirical function that can mimic a wide variety of shapes in order to take into account the changing pore structure of the char matrix during gasification.

The unknown parameters of the model are determined from a series of experiments by the method of least-squares. The following sum is minimized:

$$S = \sum_{k=1}^{N_{exp}} \sum_{i=1}^{N_k} \left[\left(\frac{dm}{dt} \right)_k^{obs} (t_i) - \left(\frac{dm}{dt} \right)_k^{calc} (t_i) \right]^2 / N_k / h_k^{\,2} \qquad (2\text{-}48)$$

Where

Subscript k indicates the experiments differing in CO_2 partial pressure and/or heating program.

N_{exp} is the number of experiments evaluated simultaneously.

t_i denotes the time values in which the digitized $(dm/dt)_{obs}$ values were taken.

N_k is the number of the t_i points in a given experiment.

h_k denotes the heights of the evaluated curves that strongly depend upon the experimental conditions.

The division by $(h_k)^2$ serves for normalization.

3 Experimental approach

3.1 Introduction

Most of the work performed in this thesis relies on the use of experimental and analytical equipments that needs a great deal of care in order to generate reliable results. For the gasification kinetic studies, a micro-TGA was used to record the weight loss. Work on large samples required the use of a more complicated system consisting of a macro-TGA, gas cleaning equipment, a gas conditioning reactor (non-thermal plasma) and several analyzers for the measurement of gas concentration. Chapter 3 gives a description of the different equipments and their principle of operation. Prior to the experimental work some preliminary work was done on the calibration of the gas analytical equipments (FTIR and GC) which is also explained in this chapter. Cold runs where performed in order to study the reliability of the gas cleaning equipment on the adsorption of some critical minor gas species (H_2S and COS), which are also reported in this chapter. Finally, some control experiments are presented in order to report the reproducibility of experiments.

3.2 Micro-TGA

The micro-TGA used in this work is a SDT 2960 Simultaneous Thermogravimetric Analyzer –Differential Thermal Analyzer (TGA-DTA) from TA Instruments (Figure 3-1). It consists of a dual beam horizontal balance where each arm holds one cup placed above a thermocouple. The thermocouples are of platinum/platinum-rhodium type contained inside the ceramic arms. During an experimental run, one cup holds the sample while the other is left empty and used as a reference to generate the DTA (ΔT) and for temperature correction. The weight change is measured by a taut-band meter movement located at the rear of each of the ceramic arms. An optical activated servo loop maintains the balance arm in the horizontal reference position by regulating the amount of current flowing through the transducer coil. An infrared LED light source and a pair of photosensitive diodes detect movement of the arm. A flag at the end of the balance arm controls the amount of light reaching the respective photo sensor. During a mass change, the beam becomes unbalanced causing unequal light to strike the photodiodes. This imbalance is compensated to retain the null position by a restoring current which is translated directly to weight change. The balance has a sensitivity of 0.1 μg and a maximum weight capacity of 200 mg. The balance is placed inside of an electrical furnace which provides a uniform temperature distribution up to 1500 ºC. The heating rate can be varied from 0.1 – 100 ºC/min and up to a

temperature of 1000 ºC using ambient temperature purge gas. To attain the maximum temperature of 1500 ºC the heating rate is limited to 25 ºC/min.

Figure 3-1: The STD 2960 micro TGA

3.3 Macro-TGA

The reactor is made off 4 different parts, the purge gas inlet at the bottom, the heater, the reactor core and the top section for the diversion of the gas to a ventilation system. The heater which is placed vertically under the main reactor is composed of a ceramic core with an inner diameter of 100 mm. A heating element with a maximum duty of 6 kW and a maximum temperature of 1200 ºC is placed in the middle of the heater. Two thermocouples are placed within the heater; one in the middle close to the heating element and is used as a safety measure to prevent over heating. The other is placed close to the outlet and is used for the control of the gas temperature. The main reactor is composed of a ceramic oven with an inner diameter of 125 mm and a corresponding outer diameter of 225 mm. The oven is placed in water cooled, double mantled stainless steel cylinder. The oven is composed of five heating elements which can be regulated separately. The two bottom elements are identical with a length of 35 mm each and with an electrical duty of 500 W. The other three have each a 2 kW electrical duty and are 300 mm in length. The main reactor wall is a cylinder composed mainly of aluminum oxide (Al_2O_3) and can

withstand temperatures up to 1500 ºC. This cylinder has a total length of 1000 mm, an inner diameter of 100 mm and is placed inside the ceramic oven. Several thermocouples are installed along the inner wall. These are divided into 6 levels where on each level there are two thermocouples facing each other. Theses elements are glued to the wall so that only the wall temperature is measured. Five levels of thermocouples are placed, each in the middle of a heating zone. The average temperature of each section is used to control the duty level of the heating elements. The 6th thermocouple level is placed in the middle of the reactor and is used as an external safety measure to prevent overheating. The reactor is shown in Figure 3-2.

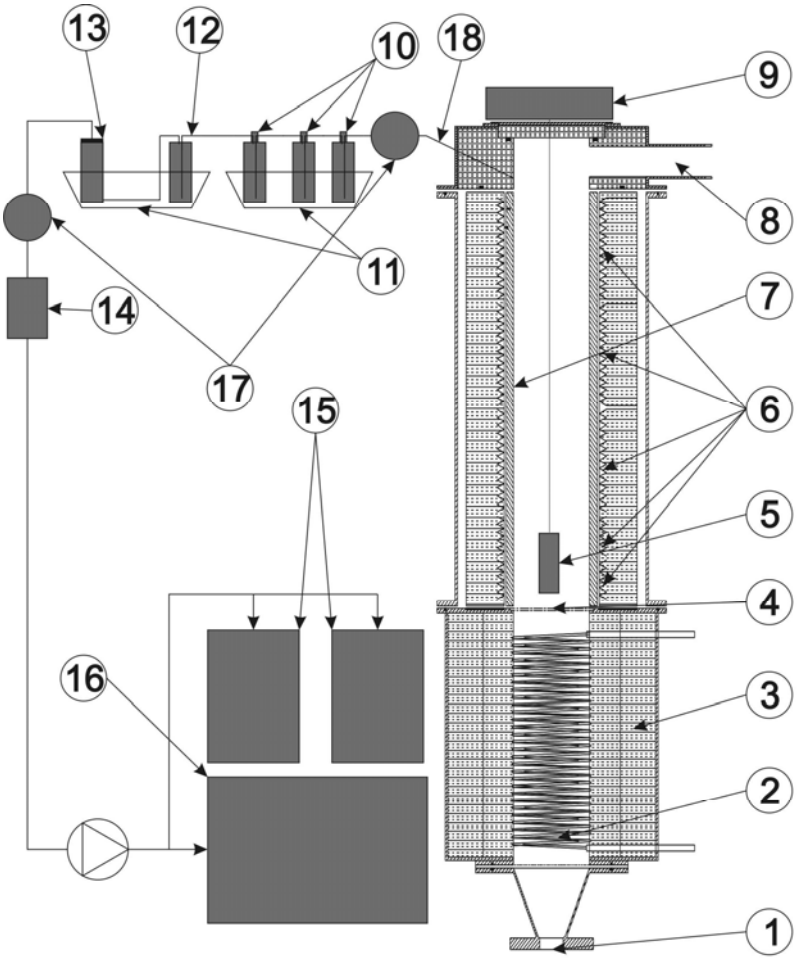

1-Gas inlet; 2-Pre-Heater; 3-Insulation; 4-Distribution plate; 5-Sample basket; 6-Five zones with heating elements; 7-Al_2O_3 Cylinder; 8-Gas outlet; 9-Balance; 10-Glass bottles filled with glass wool; 11-Ice bath; 12-Steel condenser; 13-Glass wool cylinder with paper filter on top; 14-Heated particle filter; 15-GC; 16-FTIR; 17-Positions of NTP; 18-Sampling outlet

Figure 3-2: A schematic drawing of the macro-TGA along with the condensation train and the gas measuring instruments.

During the experiment the sample is weighted continuously with a “Sartorius CP 153” scale type. The scale has a maximum weighting range of 150 g and a precision of 1 mg. The scale lies inside a pressure tight chamber attached to a pneumatic lift. The chamber has a hole in the bottom part through which the scale can be accessed. A Chrome-Alumina wire is used to attach the sample basket to the scale. When the top-lock along with the scale closes, the bottom of the sample basket lies approximately at the start of the first heating zone of the reactor. The scale chamber is set on a slight overpressure by letting a small flow of nitrogen purge through it. This helps protecting the scale by preventing hot gases from entering the chamber. The sample basket has the shape of a cylinder with an outer diameter of 65 mm and a length 120 mm. It is made of two stainless steel rings that are kept together by netted wires of metal, which makes up the wall of the cylinder. A perforated plate is welded to the bottom ring and makes up the base of the basket were the solid sample can be placed. The plate is perforated to allow the interaction of the hot gases with the sample. The weight of the sample basket is approximately 80 g.

Input and output signals are handled by a PC through a signal processing system “field-point”. Software was developed locally with Microsoft’s Visual Basic to control and register the different parameters. This includes a programmed PI-regulator for the temperature control of the different heating zones and of the pre-heater. The software controls also several flow-controllers that are used for purging the reactor with a combination of gas mixture. All signals are written to a text file at a predefined interval. Signals that are logged are; the sample weight, all the installed thermocouples, the power of the different heating elements and the mass-flow through the flow controllers. As a safety measure the software is able to cut all the electrical power to the heating elements in case of a temperature overheat or in case of a thermocouple malfunction. This is done by placing thermocouples close to all the heating elements inside the reactor and the pre-heater. One external signal processor is also installed and is programmed to cut power to the reactor in the following cases:

- The module is linked to one thermocouple close to a heating element in the middle of the reactor and will stop the power in case of a temperature over-heat.
- The module also receives a voltage signal from the software at a one second interval. In case of a program crash this module will cut all electrical power to the reactor.

3.4 Nonthermal plasma reactor

The nonthermal plasma reactor is a coaxial dielectric barrier discharge (DBD) type reactor. A Powertron 1000S was used to supply an alternating current (AC) to a transformer where both the main voltage and the frequency could be varied. The main voltage can be set at a range of 20 – 80 volts, while the frequency could be modified depending on the chosen set point of the main voltage. A transformer was used to increase the voltage by 100 times on its secondary output. The inner electrode of the DBD is made of a brass tube with an outer diameter of 9 mm and a length of 400 mm and was attached to the secondary output voltage of the transformer. The high voltage electrode was mounted inside a quartz tube with an inner diameter of 14.6 mm and a thickness of 1.5 mm. The sample gas flows through the annular gap between the inner electrode and the quartz tube. The residence time of the producer gas in the plasma region was calculated to 0.12 s at standard conditions. The discharges take place in this gap and only over the length of the outer electrode. The outer electrode was coated on the outer wall of the quartz reactor with a fluid containing silver. The length of the outer electrode was 100 mm. The primary voltage/input (RMS) voltage was determined through the high-voltage source while for the secondary/output voltage a Tektronix P6015A probe (1:1000) was used. From the outer electrode, a BNC cable was used for the measurement of electric discharges. Both signals were connected to a Tektronix TDS 684A oscilloscope and were used for the calculation of the electrical power. The frequency for all the experiments was set to 1500 Hz. The electrical power deposited through the plasma varied between 100 and 150 Watts. Figure 3-3 shows the NTP reactor placed upstream to the liquid condensation train shown in the right side of the picture. The outer electrode shown in Figure 3-3 was from initial tests that are not included in this work.

Figure 3-3: The nonthermal plasma reactor, the outlet from the macro-TGA (left) and the inlet to the condensation bottles (right).

4 Summary of papers

4.1 Conclusions Paper I – Thermal analysis of energy crops Part I: The applicability of a macro-thermobalance for biomass studies

In this work, the thermal characteristics of three biomass species have been studied. The experimental work was performed on thermally thick samples in both oxidative and inert atmosphere. A slow heating rate was chosen and both the weight loss and the evolved gaseous products were monitored as a function of time and temperature. The results confirm that the macro-TGA is suitable for the study of the pyrolysis and combustion of large samples. Due to differences in the density of the samples and in the elemental composition of the fuels, the weight loss under the pyrolysis experiments starts first with the poplar sample followed by tree of heaven and then the energy grass sample. The reported gas concentration profile under pyrolysis was similar for all the samples. The decomposition of all species starts with the evolution of CO and CO_2 first, followed by methane and the C_2 compounds and later hydrogen is released. The methane profile for the energy grass pellet differs in having a less pronounced first peak. This is probably due to charring reaction that might be more favored for the grass sample because of its larger amount of inorganic ions, which catalyze charring reactions. Experiments performed in oxidative atmosphere also confirm that the woody and herbaceous species exhibit significant differences under combustion. The second peak that is clearly visible in the pyrolysis experiments has disappeared due to oxidation. The CO profile for the grass sample is higher and flatter than that of the poplar sample. This could be due to the fact that for the grass pellet, the solid residues after the devolatilization stage contain a higher amount of carbon. This char is slowly attacked by oxygen and produces CO under combustion.

The performance of the macro-thermobalance instrument coupled with gas analysis should be compared with the results of traditional thermogravimetric studies, and the factors influencing the thermal decomposition processes should be determined. Further experiments are needed to answer the above questions.

4.2 Conclusions Paper II – Straw Pellets Pyrolysis: Effect of Nonthermal Plasma on the Devolatilized Products

Experiments on pyrolysis of straw pellets have been performed in a macro-TGA. The experiments were performed at isothermal conditions in the temperature range from 400 to 800 ºC. A detailed analysis of the main gas products has been presented along with the

effect of a NTP reactor on the gaseous product distribution. The NTP reactor was used for treating a flow of 5 nL/min taken from the macro-TGA for the quantification of the gaseous products. The NTP treatment was performed in three different modes while keeping all the geometric and electric properties of the dielectric barrier discharge (DBD) constant. The main findings are:

- The use of NTP in general influences the total gas production as well as the product distribution and higher heating value of the pyrolysis gases.

- The total gas production at a pyrolysis temperature of 400 ºC was increased by 14 % when the NTP reactor was placed upstream relative to liquid condensation. For temperatures above 400 ºC the total gas amount decreased due to carbon deposits in the NTP reactor and an increase of the liquid fraction.

- For a pyrolysis temperature of 400 ºC, placing the NTP upstream to the condensation unit has shown to have a positive effect on increasing the production of all the measured gaseous compounds. This also holds true at 500 ºC for CO and H_2.

- The difference in changing the background gas in the NTP by purging the macro-TGA with CO_2/N_2 instead of pure N_2 has shown to produce significant differences in the distribution of the gaseous products. The addition of CO_2 increased significantly the total amount of CO and decreased the hydrogen content. Ethane was also slightly increased compared to NTP treatment with pure nitrogen.

- The higher heating value of the produced gas increased with the use of NTP. This can be explained by the dissociation of some of the CO_2 present in the devolatilized products. At a pyrolysis temperature of 400 ºC the increase is also due to the conversion of some of the heavier hydrocarbons to combustible gaseous products.

4.3 Conclusions Paper III – Sulfur Abatement in Pyrolysis of Straw Pellets

Danish straw has been mixed with the calcium based additives CaO and $Ca(OH)_2$ at different Ca/S ratios. The mixed straw was pelletized and pyrolized at different temperatures in a macro-TGA reactor in order to study the sulfur retention in the ash. A detailed analysis of the sulfur species in the gas products has been presented along with the

effect of a NTP on the abatement of sulfur release. The NTP reactor was used for treating a flow of 5 nL/min taken from the macro-TGA for the quantification of the sulfur products. The NTP treatment was performed in three different modes while keeping all of the geometric and electric properties of the DBD constant. The main findings are:

- The sulfur release with the devolatilized products increased with increasing temperatures. The effect of the additives could not be determined accurately by solely studying the composition of the evolved gases. By performing an elemental analysis of the straw pellets and the solid residues after pyrolysis at 600 ºC, some tendencies towards increased sulfur retention could be observed, although this effect appeared to be marginal. Data from literature reporting the influence of the same type of additives on the pyrolysis of coal was more noticeable. This is most probably due to the higher content of sulfur in coal compared to straw. Another major difference between coal and straw is the higher ash content of the later fuel combined with an already high calcium content.

- Increasing the pyrolysis temperature has resulted in an increased release of H_2S with the devolatilized products. COS formation decreased with increasing pyrolysis temperature.

- The NTP reactor was proved to have a high H_2S removal efficiency. In pure N_2 and at a concentration of 42 ppm, the maximum removal efficiency was close to 95%. Increasing the H_2S concentration to 165 ppm has resulted in improved removal efficiency.

- The removal efficiency of H_2S in the pyrolysis experiments was highest when the NTP reactor was placed downstream liquid removal and at a pyrolysis temperature of 400 ºC. At this configuration 86 % of H_2S was removed from the devolatilized products. Best plasma reactor placement was proved to be downstream liquid removal for both H_2S and COS. Increasing the CO_2 amount in the carrier gas has improved the removal efficiency of H_2S at the cost of increased COS formation.

4.4 Conclusions Paper IV – CO_2 Gasification of Biomass Chars. A Kinetic Study

The gasification kinetics of two charcoals were determined using TGA experiments with linear and stepwise T(t) programs. The method of least squares was used. Contrary to the

isothermal studies when one has to wait for the stabilization of the experimental conditions, we studied the whole gasification process. A particular care was given to ensure a true kinetic control by employing much lower sample masses than it is usual in the TGA studies on the gasification of biomass chars. The results were justified by the fit between the experimental and calculated data in series of 7 and 14 experiments.

The devolatilization of the charcoal was described by the way proposed earlier by Branca and Di Blasi18 [81] for charcoal combustion. The dependence of the gasification on the conversion was examined by a versatile, 3-parameter empirical f(α) formula. The results were identical or close to the power law (nth order) kinetics.

Despite the differences between the feedstock, ash composition and pore structure of the two chars, their decomposition kinetics revealed considerable similarities. This made possible to describe all the 14 experiments on the two samples together assuming common activation energies and common reaction order of the CO_2 concentration on both charcoals. In this model the dependence of the reaction rate on the conversion was approximated by power law kinetics. Altogether 18 adjustable parameters were determined from 14 TGA experiments. The reactivity differences between the two charcoals were expressed by different preexponential factors while the structural differences were described by different reaction orders with respect to the conversion.

The activation energy of the gasification step, E3, proved to be a well defined quantity: all evaluations and test calculations in the present study resulted in values 262 – 263 kJ/mol.

5 Recommendation for future work

Experiments with the macro-TGA have shown to give valuable information concerning the study of product release during the thermal treatment of solid fuels. The thermally thick samples provided in this manner additional information in the form of a detailed gas mapping of the fuels that were tested. In comparison to similar tested performed at the micro-scale levels, such experiments include the gas diffusion limitation, a condition that is more realistic in real processes. At the same time one is able to have more controlled operating condition compared to real processes. The use of calcium based additives for the retention of sulfur has shown to give limited effectiveness during the pyrolysis of straw pellets. The work on additive incorporation to the pellets for future work should concentrate on combustion experiments where such additives are believed to be more effective. Adding calcium to biomass would also change the characteristics of the produced ash which could be an important aspect to investigate.

Work on the non-thermal plasma was proven successful on the removal of sulfuric compounds in the pyrolysis products. Future experiments should focus on enhancing the plasma efficiency and the possibility to run the plasma reactor at higher gas temperatures. Gas cleaning at high temperatures is a major challenge where plasma discharge could prove to be successful at the removal of harmful compounds and the upgrade of the producer gas. This is thought off in relation to gasification products where non-thermal plasma treatment could render the gaseous products more suitable for further utilization in gas turbines, engines and solid oxide fuel cells. The possibility of using such a technology should be investigated in terms of both the economical costs and the removal efficiency. Later experiments with non-thermal plasma should therefore concentrate on the direct treatment of gasification products. These products differ from the devolatilized products tested in paper II and III in two quite important areas; the different chemical composition of the tar products and the water content in the producer gas.

The work on gasification kinetics gave important reaction rate data of two types of chars generated from soft and hard wood. A mathematical gasification model suitable for different heating rates was developed. Such models can be used directly in modeling the gasification stage of these fuels. Further work should concentrate on defining char characteristics that have a significant influence on the gasification reaction rates.

Incorporating such characteristics in a mathematical model would render the model more useful for different type of wood chars.

6 References

[1] Berg L. N., Jørgensen P. F., Heyerdahl P. H., Wilhelmsen G. *"Bioenergiressurser i Norge"* Norges vassdrags- og energidirektorat (2003).

[2] van Loo S., Koppejan J. *"The handbook of biomass combustion & Co-firing"* ISBN: 978-1-84407-249-1 (2008).

[3] Grønli M. G. *"A theoretical and experimental study of the thermal degradation of biomass"* Ph.D. thesis, Norwegian University of Science and Technology (1996).

[4] Khalil R. A., Várhegyi G., Jäschke S., Grønli M. G., Hustad J. E. *"CO2 Gasification of Biomass Chars: A Kinetic Study"* Energy & Fuels 23 (2009) 94-100.

[5] Khalil R. A., Mészáros E., Grønli M. G., Várhegyi G., Mohai I., Marosvolgyi B., Hustad J. E. *"Thermal analysis of energy crops Part I: The applicability of a macro-thermobalance for biomass studies"* Journal of Analytical and Applied Pyrolysis 81 (2008) 52-59.

[6] Khalil R. A., Seljeskog M., Hustad J. E. *"Straw Pellets Pyrolysis: Effect of Nonthermal Plasma on the Devolatilized Products"* Energy & Fuels 22 (2008) 686-692.

[7] Becidan M., Skreiberg Ø., Hustad J. E. *"NOx and N2O precursors (NH3 and HCN) in pyrolysis of biomass residues"* Energy & Fuels 21 (2007) 1173-1180.

[8] Khalil R. A., Seljeskog M., Hustad J. E. *"Sulfur Abatement in Pyrolysis of Straw Pellets"* Energy & Fuels 22 (2008) 2789-2795.

[9] Knoef H. *"Handbook Biomass Gasification"* ISBN: 90-810068-1-9 (2005).

[10] Stanghelle D., Slundgaard T., Sønju O. K. *"Granular bed filtration of high temperature biomass gasification gas"* Journal of Hazardous Materials 144 (2007) 668-672.

[11] Nussbaumer T. *"Combustion and Co-combustion of biomass: Fundamentals, technologies, and primary measures for emission reduction"* Energy & Fuels 17 (2003) 1510- 1521.

[12] Obernberger I. *"Decentralized biomass combustion: state of the art and future development"* Biomass and Bioenergy 14 (1998) 33-56.

[13] Klasnja B., Kopitovic S., Orlovic S. *"Wood and bark of some poplar and willow clones as fuelwood "* Biomass and Bioenergy 23 (2002) 427-432.

[14] Almeida M. T., Mouga T., Barracosa P. *"The weathering ability of higher plants. The case of Ailanthus altissima (Miller) Swingle"* International Biodeterioration & Biodegradation 33 (1994) 333-343.

[15] Knudsen J. N., Jensen P. A., Lin W., Frandsen F. J., Dam-Johansen K. *"Sulfur Transformations during Thermal Conversion of herbaceous biomass"* Energy & Fuels 18 (2004) 810-819.

[16] Holm J. K., Henriksen U. B., Hustad J. E., Sørensen L. H. *"Toward an Understanding of Controlling Parameters in Softwood and Hardwood Pellets Production"* Energy & Fuels 20 (2006) 2686-2694.

[17] Knudsen J. N., Jensen P. A., Dam-Johansen K. *"Transformation and Release to the Gas Phase of Cl K and S during Combustion of Annual Biomass"* Energy & Fuels 18 (2004) 1385-1399.

[18] Hawkesford M. J., De Kok L. J. *"Managing sulphur metabolism in plants"* Plant, Cell and Environment 29 (2006) 382-395.

[19] Ernst W. H. O. *"Sulfur metabolism in higher plants: potential for phytoremediation"* Biodegradation 9 (1998) 311-318.

[20] Dayton D. C., Jenkins B. M., Turn S. Q., Bakker R. R., Williams R. B., Belle-Oudry D., Hill L. M. *"Release of Inorganic Constituents from Leached Biomass during Thermal Conversion"* Energy & Fuels 13 (1999) 860-870.

[21] Wolf K. J., Smeda A., Muller M., Hilpert K. *"Investigations on the Influence of Additives for SO2 Reduction during High Alkaline Biomass Combustion"* Energy & Fuels 19 (2005) 820-824.

[22] Björkman E., Strömberg B. *"Release of Chlorine from Biomass at Pyrolysis and Gasification Conditions"* Energy & Fuels 11 (1997) 1026-1032.

[23] Jensen P. A., Frandsen F. J., Dam-Johansen K., Sander B. *"Experimental Investigation of the Transformation and Release to Gas Phase of Potassium and Chlorine during Straw Pyrolysis"* Energy & Fuels 14 (2000) 1280-1285.

[24] Knudsen J. N., Jensen P. A., Lin W., Dam-Johansen K. *"Secondary Capture of Chlorine and Sulfur during Thermal Conversion of Biomass"* Energy & Fuels 19 (2005) 606-617.

[25] Kuramochi H., Wu W., Kawamoto K. *"Prediction of the behaviors of H2S and HCl during gasification of selected residual biomass fuels by equilibrium calculation"* Fuel 84 (2005) 377-387.

[26] Nordin A. *"Optimization of Sulfur retention in ash when combusting high sulfur fuels and biomass fuels in a small pilot scale fluidized bed"* Fuel 74 (1995) 615-622.

[27] Guan R., Li W., Li B. *"Effects of Ca-based additives on desulfurization during coal pyrolysis"* Fuel 82 (2003) 1961-1966.

[28] Cheng J., Zhou J., Liu J., Cao X., Zhou Z., Huang Z., Zhao X., Cen K. *"Physicochemical properties of Chinese pulverized coal ash in relation to sulfur retention"* Powder Technology 146 (2004) 169-175.

[29] Folgueras M. B., Diaz R. M., Xiberta J. *"Sulphur retention during co-combustion of coal and sewage sludge"* Fuel 83 (2004) 1315-1322.

[30] Cheng J., Zhou J., Liu J., Zhou Z., Huang Z., Cao X., Zhao X., Cen K. *"Sulfur removal at high temperature during coal combustion in furnaces: a review"* Progress in Energy and Combustion Science 29 (2003) 381-405.

[31] Qiu K., Lindqvist O., Mattisson T. *"Regeneration of Calcium Sulfide under Alternating Oxidizing and Inert Conditions Kinetics and Mechanism"* Industrial and Engineering Chemistry Research 37 (1998) 923-928.

[32] Hansen P. F. B., Dam-Johansen K., Østergaard K. *"High-temperature reaction between sulphur dioxide and limestone-V. The effect of periodically changing oxidizing and reducing conditions"* Chemical Engineering Science 48 (1992) 1325-1341.

[33] Yrjas P., Hupa M., Iisa K. *"Pressurized Stabilization of Desulfurization Residues from Gasification Processes"* Energy Fuels 10 (1996) 1189-1195.

[34] Mattison T., Lyngfelt A. *"The reaction between limestone and SO2 under periodically changing oxidizing and reducing conditions – effect of temperature and limestone type"* Thermochimica Acta 325 (1999) 59-67.

[35] Qiu K., Mattisson T., Steenari B-M., Lindqvist O. *"Thermogravimetric combined with mass spectrometric studies on the oxidation of calcium sulfide"* Thermochimica Acta 298 (1996) 87-93.

[36] Kim H. H., Kobara H., Ogata A., Futamura S. *"Comparative Assessment of Different Nonthermal Plasma Reactors on Energy Efficiency and Aerosol Formation From the Decomposition of Gas-Phase Benzene"* IEEE Trans. Ind. Applicat. 41 (2005) 206-214.

[37] Lee S. M., Park C. S., Cha M. S., Chung S. H. *"Effect of Electric Fields on the Liftoff of Nonpremixed Turbulent Jet Flames"* IEEE Trans. Plasma Sci. 33 (2005) 1703-1709.

[38] Stange S., Kim Y., Ferreri V., Rosocha A. L., Coates M. D. *"Flame Images Indicating Combustion Enhancement by Dielectric Barrier Discharges"* IEEE Trans. Plasma Sci. 33 (2005) 316-317.

[39] Criner K., Cessou A., Louiche J., Vervisch P. *"Stabilization of turbulent lifted jet flames assisted by pulsed high voltage discharge"* Combustion and Flame 144 (2006) 422-425.

[40] Pilla G., Galley D., Lacoste A. D., Lacas F., Veynante D., Laux O. C. *"Stabilization of a Turbulent Premixed Flame Using a Nanosecond Repetitively Pulsed Plasma"* IEEE Trans. Plasma Sci. 34 (2006) 2471-2477.

[41] Vincent-Randonnier A., Larigaldie S., Magre P., Sabel'nikov V. *"Plasma assisted combustion: effect of a coaxial DBD on a methane diffusion flame"* Plasma Sources Sci. Technol. 16 (2007) 149-160.

[42] Pancheshnyi S. V., Lacoste D. A., Bourdon A., Laux C. O. *"Ignition of Propane–Air Mixtures by a Repetitively Pulsed Nanosecond Discharge"* IEEE Trans. Plasma Sci. 34 (2006) 2478-2487.

[43] Jiang C., Mohamed A. H., Stark R. H., Yuan J. H., Schoenbach K. H. *"Removal of Volatile Organic Compounds in Atmospheric Pressure Air by Means of Direct Current Glow Discharges"* IEEE Trans. Plasma Sci. 33 (2005) 1416-1425.

[44] Nair S. A., Yan K., Pemen A. J. M., Winands G. J. J., Gompel F. M., Leuken H. E. M., Heesch E. J. M., Ptasinski K. J., Drinkenburg A. A. H. *"A high-temperature pulsed corona plasma system for fuel gas cleaning"* Journal of Electrostatics 61 (2004) 117-127.

[45] Nair S. A., Pemen A. J. M., Yan K., van Heesch E. J. M., Ptasinski K. J., Drinkenburg A. A. H. *"Chemical Processes in Tar Removal from Biomass Derived Fuel Gas by Pulsed Corona Discharges"* Plasma Chem. Plasma Process. 23 (2003) 665-680.

[46] Mok Y. S., Nam C. M., Cho M. H. *"Decomposition of Volatile Organic Compounds and Nitric Oxide by Nonthermal Plasma Discharge Processes"* IEEE Trans. Plasma Sci. 30 (2002) 408-416.

[47] Pemen A. J. M., Nair S. A., Yan K., van Heesch E. J. M., Ptasinski K. J., Drinkenburg A. A. H. *"Pulsed Corona Discharges for Tar Removal from Biomass Derived Fuel Gas"* Plasma Polymers 8 (2003) 209-224.

[48] van Heesch E. J. M., Pemen A. J. M., Yan K., van Pasen V. B., Ptasinski K. J., Huijbrechts A. H. J. *"Pulsed Corona Tar Cracker"* IEEE Trans. Plasma Sci. 28 (2000) 1571-1575.

[49] Ma H., Chen P., Ruan R. *"H2S and NH3 Removal by Silent Discharge Plasma and Ozone Combo-System"* Plasma Chem. Plasma Process. 21 (2001) 611-624.

[50] Yankelevich Y., Pokryvailo A. *"High-Power Short-Pulsed Corona: Investigation of Electrical Performance SO2 Removal and Ozone Generation"* IEEE Trans. Plasma Sci. 30 (2002) 1975-1981.

[51] Helfritch D. J. *"Pulsed Corona Discharge for Hydrogen Sulfide Decomposition"* IEEE Trans. Ind. Applicat. 29 (1993) 882-886.

[52] Kim H. H., Wu C., Kinoshita Y., Takashima K., Katsura S., Mizuno A. *"The Influence of Reaction Conditions on SO2 Oxidation in a Discharge Plasma Reactor"* IEEE Trans. Ind. Applicat. 37 (2001) 480-487.

[53] Zhao G. -B., John S., Zhang J., Hamann J. C., Muknahallipatana S. S., Legowski S., Ackerman J. F., Argyle M. D. *"Production of hydrogen and sulfur from hydrogen sulfide in a nonthermal-plasma pulsed corona discharge reactor"* Chemical Engineering Science 62 (2007) 2216-2227.

[54] Dalaine V., Cormier J. M., Lefaucheux P. *"A gliding discharge applied to H2S destruction"* Journal of Applied Physics 83 (1998) 2435-2441.

[55] Dalaine V., Cormier J. M., Pellerin S., Lefaucheux P. *"H2S destruction in 50 Hz and 25 kHz gliding arc reactors"* Journal of Applied Physics 84 (1998) 1215-1221.

[56] Okubo M., Inoue M., Kuroki T., Yamamoto T. *"NOx Reduction Aftertreatment System Using Nitrogen Nonthermal Plasma Desorption"* IEEE Trans. Ind. Applicat. 41 (2005) 891-899.

[57] Shang K., Wu Y., Li J., Li G., Li D. *"Enhancement of NOx abatement by advancing initiation of C3H6 oxidation chemistry with a corona radical shower"* Plasma Sources Sci. Technol. 16 (2007) 104-109.

[58] Zhao G. -B., Garikipati S. V. B. J., Hu X., Argyle M. D., Radosz M. *"The effect of gas pressure on NO conversion energy efficiency in nonthermal nitrogen plasma"* Chemical Engineering Science 60 (2005) 1927-1937.

[59] kapteijn F., Meijer R., Moulijn J. A. *"Transient kinetic techniques for detailed insight in gas-solid reactions"* Energy & Fuels 6 (1992) 494-497.

[60] Di Blasi C. *"Combustion and gasification rates of lignocellulosic chars"* Progress in Energy and Combustion Science 35 (2009) 121-140.

[61] Liu G., Tate A. G., Bryant G. W., Wall T. F. *"Mathematical modeling of coal char reactivity with CO2 at high pressures and temperatures"* Fuel 79 (2000) 1145-1154.

[62] Ollero P., Serrera A., Arjona R., Alcantarilla S. *"The CO2 gasification kinetics of olive residue"* Biomass and Bioenergy 24 (2003) 151-161.

[63] Scott S. A., Davidson J. F., Dennis J. S., Fennell P. S., Hayhurst A. N. *"The rate of gasification by CO2 of chars from waste"* proceedings of the Combustion Institute 30 (2005) 2151-2159.

[64] Gómez-Barea A., Ollero P., Arjona R. *"Reaction-diffusion model of TGA gasification experiments for estimating diffusional effects"* Fuel 84 (2005) 1695-1704.

[65] Ochoa J., Cassanello M. C., Bonelli P. R., Cukierman A. L. *"CO2 gasification of Argentinean coal chars: a kinetic characterization"* Fuel Processing Technology 74 (2001) 161-176.

[66] Bahatia S. K., Perlmutter D. D. *"A random pore model for fluid-solid reactions: I. isothermal, kinetic control"* AIChE Journal 26 (1980) 379-386.

[67] Struis R. P. W. J., von Scala C., Stucki S, Prins R. *"Gasification reactivity of charcoal with CO2. Part I: Conversion and structural phenomena"* Chemical Engineering Science 57 (2002) 3581-3592.

[68] Morimoto T., Ochiai T., Wasaka S., Oda H. *"Modeling on pore variation of coal chars during CO2 gasification associated with their submicropores and closed pores"* Energy & Fuels 20 (2006) 353-358.

[69] Lui H., Kaneko M., Kato S., Kojima T. *"Gasification of seven coals in carbon dioxide at elevated temperatures and high heating rates: Unification approach of reactivity"* Journal of Chemical Engineering of Japan 36 (2003) 751-758.

[70] Murillo R., Navarro M. V., Lopez J. M., Aylon E., Callen M. S., Garcia T., Mastral A. M. *"kinetic model comparison for waste tire char reaction with CO2"* Ind. Eng. Chem. Res. 43 (2004) 7768-7773.

[71] Ye D. P., Agnew J. B., Zhang D. K. *"Gasification of a South Australian low-rank coal with carbon dioxide and steam: kinetics and reactivity studies"* Fuel 77 (1998) 1209-1219.

[72] Biederman D. L., Miles A. J., Vastola F. J., Walker P. L. *"Carbon-carbon dioxide reaction: Kinetics at low pressures and hydrogen inhibition"* Carbon 14 (1976) 351-356.

[73] Barrio M., Gøbel B., Risnes H., Henriksen U., Hustad J. E., Sørensen L. H. *"Steam gasification of wood char and the effect of hydrogen inhibition on the chemical kinetics"* Progress in Thermochemical Biomass Conversion Volume 1 (2001) 32-46.

[74] Barrio M., Hustad J. E. *"CO2 gasification of birch char and the effect of CO inhibition on the calculation of chemical kinetics"* Progress in Thermochemical Biomass Conversion Volume 1 (2001) 47-60.

[75] Feng B., Bhatia S. K. *"On the validity of thermogravimetric determination of carbon gasification kinetics"* Chemical Engineering Science 57 (2002) 2907-2920.

[76] Laurendeau N. M. *"Heterogeneous kinetics of coal char gasification and combustion"* Prog. Energy Combust. Sci. 4 (1978) 221-270.

[77] Ollero P., Serrera A., Arjona R., Alcantarilla S. *"Diffusional effects in TGA gasification experiments for kinetic determination"* Fuel 81 (2002) 1989-2000.

[78] Iniesta E., Sánchez F., García A. N., Marcilla A. *"Yields and CO2 reactivity of chars from almond shells obtained by a two heating step carbonisation process. Effect of different chemical pre-treatments and ash content"* Journal of Analytical and Applied Pyrolysis 58-59 (2001) 983-994.

[79] Ponder G. R., Richards G. N. *"Oxygen and CO2 gasification of chars from wood treated with iron (II) and iron (III) sulfates"* Energy & Fuels 8 (1994) 705-713.

[80] Struis R. P. W. J., von Scala C., Stucki S, Prins R. *"Gasification reactivity of charcoal with CO2. Part II: Metal catalysis as a function of conversion"* Chemical Engineering Science 57 (2002) 3593-3602.

[81] Branca C., Di Blasi C. *"Global Kinetics of Wood Char devolatilization and combustion"* Energy & Fuels 17 (2003) 1609-1615.

[82] *http://student.britannica.com/eb/art-17906/The-Michelson-interferometer-consists-of-a-half-transparent-mirror-oriented (2008).*

[83] *http://www.varianinc.com/cgi-bin/nav?products/chrom/gc/microgc/ionfilter&cid=KHKILKKMFIH (2008).*

[84] Mitomo A., Sato T., Kobayashi N., Hatano S., Itaya Y., Mori S. *"Adsorption Removal of Hydrogen Sulfide by Activated Coke Produced from Wood Pellet in the Recycle System of Biomass"* Journal of Chemical Engineering of Japan 36 (2003) 1050-1056.

[85] Robbie S. S., McC. Paterson N. P. *"Gas sampling from a hot, dirty gas stream"* Fuel 60 (1981) 1096-1098.

[86] Lindgren E. R., Klrchgessner D. A., Drehmel D. C. *"Fuel rich sulfur capture in a combustion environment"* Environ. Sci. Technol. 26 (1992) 1427-1433.

[87] Ståhlberg R., Lappi M., Kurkela E., Simell P., Oesch P., Nieminen M. *"Sampling of contaminants from product gases of biomass gasifiers"* Technical research center of Finland (1998).

Appendix A (papers)

Paper I

Thermal analysis of energy crops Part I: The applicability of a macro-thermobalance for biomass studies

Khalil R. A., Mészáros E., Grønli M. G., Várhegyi G., Mohai I., Marosvolgyi B., Hustad J. E.

Journal of Analytical and Applied Pyrolysis. Vol. 81, 52-59 (2008)

Available online at www.sciencedirect.com
ScienceDirect
J. Anal. Appl. Pyrolysis 81 (2008) 52–59
JOURNAL of ANALYTICAL and APPLIED PYROLYSIS
www.elsevier.com/locate/jaap

Thermal analysis of energy crops Part I: The applicability of a macro-thermobalance for biomass studies

R.A. Khalil [a,*], E. Mészáros [b], M.G. Grønli [a], G. Várhegyi [b], I. Mohai [b], B. Marosvölgyi [c], J.E. Hustad [a]

[a] *Norwegian University of Science and Technology, NO-7491 Trondheim, Norway*
[b] *Institute of Materials and Environmental Chemistry, Chemical Research Center, Hungarian Academy of Sciences, H-1525 Budapest, P.O. Box 17, Hungary*
[c] *Institute of Energetics, University of West Hungary, Sopron, Hungary*

Received 14 December 2006; accepted 31 August 2007
Available online 14 September 2007

Abstract

In this work young shoots of poplar (*Populus euramericana*), tree of heaven (*Ailanthus altissima*) and pellets of a type of energy grass (*Agropyron*) were studied in order to get information about the applicability of these biomass materials for energy production by direct combustion. During the combustion of plant materials three main processes take place: (i) formation of volatiles, (ii) burning of volatiles and (iii) burn-off of the produced char. The thermal behavior of the samples was studied with the help of a macro-thermobalance built at the Norwegian University of Science and Technology. Pyrolysis experiments have been performed in inert atmosphere to get a deeper insight into the formation of volatile products, whereas measurements in oxidative atmosphere have provided information about the burn-off of the samples, as well. In addition to monitoring the weight loss of the samples, the analysis of the evolved gases was carried out with gas chromatography (GC).

The TG and DTG curves and the profiles of the evolved gases obtained in the pyrolysis experiments are similar in the case of the poplar and the tree of heaven samples implying that the thermal behavior of these crops is alike, whereas those of the energy grass sample show significant differences. The decomposition of poplar occurs at a lower temperature in the presence of oxygen than that of energy grass. The evolution curves of the monitored products also exhibit differences. The results will be interpreted in terms of the chemical composition of the samples determined by proximate and ultimate analysis.

Keywords: *Agropyron* pellet; *Ailanthus altissima*; Biomass; Combustion; *Populus euramericana*; Pyrolysis; Thermogravimetry

1. Introduction

The public awareness to environmental problems that we are facing as well as the political motivation towards a cleaner environment has led the research community to focus more on alternative fuels. It is believed that such energy sources will leave less impact on the environment in the future. Due to the depletion of fossil fuel reserves and a future energy economy that is affected by a political factor, it is believed that alternative energy sources will become major contributors to the global energy needs. Biomass as a fuel source already makes a big contribution to the energy balance in some countries and the potential for an increased production to attain the goals that are set is quite high. Countries in the EU have already set a target to increase energy production from alternative energy sources. For the whole EU this target is set at 21% of electricity and 12% of total energy by the year 2010 [1]. The electrical production from renewable energy sources in the EU in 1997 was at a level of 12.9%.

While the fossil energy sources have a well-defined composition and uniformity, the same cannot be said about biomass. This means that in order to reach a commercial status that can compete with other more traditional energy sources, detailed studies should be made on new promising bio-fuels.

* Corresponding author.
E-mail address: roger.a.khalil@sintef.no (R.A. Khalil).

0165-2370/$ – see front matter © 2007 Elsevier B.V. All rights reserved.
doi:10.1016/j.jaap.2007.08.004

Previously, several types of biomass species have been studied using different techniques on both the micro- and the macro-scale. Experiments on the micro-scale level are usually conducted with samples in the ''mg'' range. Samples are also sieved to a low and uniform particle size [2–10]. As a result of the small sample size the reaction mechanisms are not limited by the mass and heat diffusion, which in return allow a good prediction of the chemical reaction kinetics.

Single particle experiments [11,12] are usually carried out with the purpose of finding the limiting effect of heat and mass transfer in a solid particle. Such data can be used to implement improvements to mathematical models aiming at simulating the thermal treatment of solid fuels.

Another method of conducting experiments is by varying the density of ''a bed of particles''. This is normally done by changing the particle size of the bed. In this way, one can study different types of transport mechanisms that can influence the global reaction rate [11]. The sample weight used under such conditions varies a lot, usually between 0.1 and 20 g, and depends on the particle size under investigation [13–17].

Finally macro-scale experiments [18–20] (also referred to as ''thermally thick'') tend to be more complex and time consuming, especially, if the evolved gases are being measured. This is due to the relatively large sample size (20–500 g) that is usually used. These types of experiments are not suitable for kinetic studies, but they give some information about how solid fuels might behave differently in commercial plants due to limitations in heat and mass transfer.

The thermal decomposition and the composition of a great number of species have been studied with the help of the above methods. Lately, special fast growing species grown on energy plantations [3,21–24] have been in the focus of interest in addition to wastes of plant origin [24–26]. Among the energy plantation products, one can find wood species and herbaceous crops, as well. Hybrid poplars are the most widespread woody crops in Hungary since the climate is rather favorable for this species [27]. However, a number of other plant species also seem to be suitable for production in energy plantations.

The aim of our work was to get information about the thermal behavior of novel energy plants in a macro-scale thermobalance. Two wood samples and a herbaceous crop have been selected for the study. The thermal behavior of these species has already been investigated using small sample sizes [3,28,29]. Nevertheless, the results obtained from such experiments only give some implications about the chemical composition and thermal decomposition with no limitations in heat and mass transfer. As these processes cannot be avoided in reactors using large sample sizes, the macro-scale thermobalance may provide a good means for investigating the performance of the selected species in commercial plant installments [30]. In addition to the characterization of the thermal behavior of the samples, proximate and ultimate analyses were also performed. The heating value and the ash composition were also determined.

2. Experimental

2.1. Samples

Poplar Pannonia (*Populus* × *euramericana cv. Pannonia*), a poplar hybrid developed in Hungary and tree of heaven (*Ailanthus altissima*) were cut to small pieces of 2–4 cm during harvesting, while energy grass (*Agropyron*) was pelletized. These samples are grown on Hungarian experimental energy plantation fields. All samples were studied with the macro-thermobalance (macro-TG) as received without any pretreatment, while for proximate and ultimate analysis and calorimetric experiments the samples were milled and dried. The moisture content of the milled biomass was determined according to the ASTM E871 standard method.

The proximate analysis of the samples was performed according to ASTM E872 (volatile matter) and ASTM D1102 (ash content) standards. The ultimate analysis of the samples was performed on a Carlo Erba Instruments, type EA1108. The higher heating value of the samples was measured using an IKA Labortechnik C5000 control type bomb calorimeter. All the above characteristics of the samples are listed in Table 1.

Table 1
Proximate and ultimate analysis, higher heating value and calorific value of the tested fuels

	Energy grass pellets	Poplar Pannonia	Tree of heaven
Proximate analysis			
Volatiles (%)	75.2	83.0	82.2
Fixed carbon (%)	18.1	15.6	16.0
Ash (%)	6.7	1.4	1.8
Ultimate analysis			
C (%)	46.5	49.0	51.1
H (%)	6.3	6.4	6.8
N (%)	1.0	0.4	0.7
O (%)[a]	46.1	44.2	41.4
S (%)	0.08	<0.02	0.04
$HHV_{calculated}$ (MJ/kg) (based on proximate analysis) [31]	18.1	18.4	18.5
$HHV_{calculated}$ (MJ/kg) (based on ultimate analysis) [32]	18.5	19.4	20.2
$HHV_{measured}$ (MJ/kg)	18.3	19.5	20.6
Calorific value (db) (MJ/kg)	16.8	18.0	19.0

[a] Determined by difference.

Table 2
Ash composition determined by ICP-OES experiments

	Energy grass	Poplar	Tree of heaven
Amount of elements (w/w%)			
Ca	3.1	19.5	22.1
K	13.5	9.0	14.8
Mg	1.5	4.9	6.1
P	1.1	3.0	2.0
Na	5.1	2.4	3.8
Amount of elements (ppm)			
Al	3195	<0.1	1659
Zn	125	1175	613
Fe	3315	2890	3586
Mn	473	982	524
Cu	202	93	413

The data given in this table are the average of two parallel experiments.

2.2. Determination of ash composition

The composition of the ash was determined using a Thermo-Jarell Ash Atomscan 25 ICP-OES apparatus. Prior to analysis the ash samples were digested using an Anton Parr MW 3000 microwave digestion system. Forty to sixty milligrams ash was treated with 3 ml 30% H_2O_2, 8 ml HNO_3 and 1 ml 40% HF, and heated to 190 °C in 15 min. This temperature was kept for 20 min. Following the decomposition with the acid mixture, the samples were additionally treated with 10 ml 4% H_3BO_3 solution and heated again to 150 °C for 15 min to allow complexation of the rest fluoride. Subsequently, the samples were diluted to 50 ml and analyzed. The results of the ICP analysis are listed in Table 2.

2.3. Macro-TG apparatus

All three samples were tested in a multi-fuel reactor designed with the purpose of testing large samples simulating combustion or pyrolysis by changing the type of purge gas that runs through the reactor. The description of the reactor has already been described in an earlier publication [30]. A schematic diagram of the reactor and the gas sampling line is shown in Fig. 1. The experiments were performed using 39–60 g samples. The samples were heated in the pyrolysis experiments at a rate of 10 °C min^{-1} to 900 °C in nitrogen atmosphere. Combustion experiments were performed in air with a heating rate of 10 °C min^{-1}, the final temperature was 650 °C. The reactor was purged with the desired gas for at least 1 h prior to the start of the experiment. During pyrolysis experiments, an online oxygen analyzer was used to make sure that the reactor was free from oxygen. During the experiment the sample is heated according to a given temperature program and is weighted continuously with a "Sartorius CP 153" balance. The experiment is stopped after approximately one and a half hours (the time needed for the reactor to reach 250 °C (25 min) is not included.

2.3.1. Gas analysis by gas chromatography

All the gas compounds from the experiments are identified and quantified using a Varian CP-4900 micro-GC equipped with two injectors each connected to a separate column. The first column is a 10 m Pora-plot type with an internal diameter of 0.25 mm and uses Helium with 6.0 quality as a carrier. This column is used for the separation of CO_2, CH_4, $C_2H_2 + C_2H_4$, and C_2H_6. The second column is a 20 m long Molsieve with an inner diameter of 0.25 mm and uses Argon of 5.5 quality as a carrier gas. Argon was used instead of Helium in order to be able to detect Hydrogen. This column is able to separate O_2, N_2, CH_4 and CO. The properties of both columns along with the retention time of all compounds are presented in Table 3.

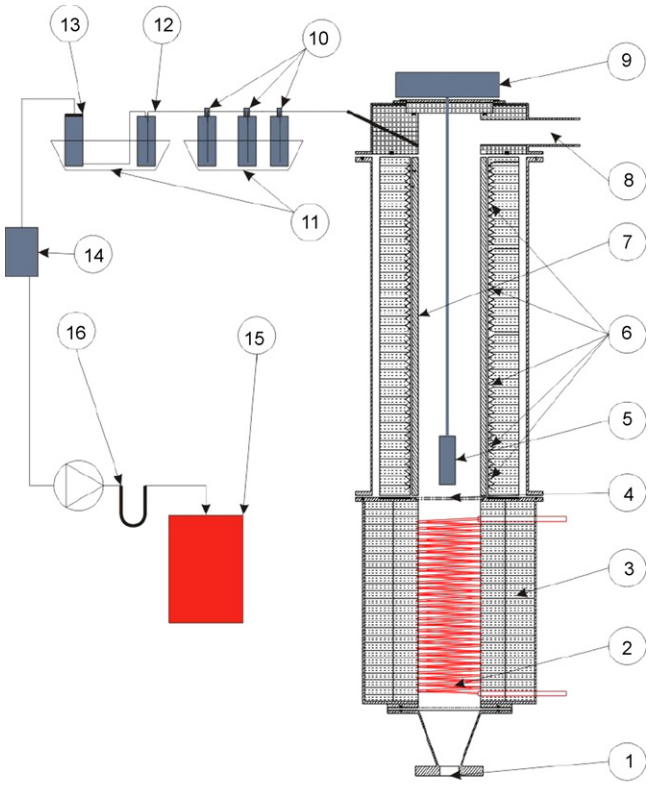

1-Gas inlet; 2-Pre-Heater; 3-Insulation; 4-Distribution plate; 5-Sample basket; 6-5 zones with heating elements; 7-Al_2O_3 Cylinder; 8-Gas outlet; 9-Balance; 10-Glass bottles filled with glass wool; 11-Ice bath; 12-Steel condenser; 13-Glass wool cylinder with paper filter on top; 14-Heated particle filter; 15-Gas Chromatographer; 16-Silicagel

Fig. 1. Schematic diagram of the reactor and the gas sampling line.

3. Results and discussion

The analytical data listed in Table 1 suggest that the composition of poplar and tree of heaven are similar and quite comparable to other wood species [33]. Energy grass however, has higher ash and fixed carbon content compared to the other two bio-fuels. The results of ultimate analysis show that energy grass has the highest nitrogen and sulfur content. This is in agreement with the fact that herbaceous species usually contain a significant amount of proteins [34–35]. The calculated and the measured higher heating values are in good agreement. As it was expected, energy grass possesses a slightly lower heating value than the wood species. The calculated calorific values show the same tendency as the higher heating values.

Table 3
Method used for the micro-GC and the retention times for the gas compounds

	Pora-plot	Molsieve
Column temperature (°C)	60	155
Injector temperature (°C)	50	100
Injection time (ms)	100	100
Initial pressure (KPa)	150	310
Run time (s)	100	100

Retention times for the different compounds (s)

	Pora-plot		Molsieve
CH_4	25	H_2	55
CO_2	28	O_2	65
$C_2H_2 + C_2H_4$	35	N_2	71
C_2H_6	40	CH_4	92
		CO	95

In addition to the characteristics of the samples listed in Table 1, the composition of the ash also plays a significant role in determining whether a certain bio-fuel is suitable for energy production. The quantification of the ash composition is, therefore, important in order to be able to predict the behavior of the fuel in a combustion furnace. Ash sintering and fouling problems may occur in cases where the melting point of the ash is low. The melting point of the ash can be directly related to the ash's elemental composition. Among the inorganic elements of biomass, potassium causes the largest problems since their high concentration in the bio-fuel causes the ash melting temperature to decrease significantly [36]. The composition of the ash has been determined with ICP-OES technique. Note that the ash was obtained after heating the sample to 600 °C as described in the Section 2 (ASTM E872 and ASTM D1102 standard method). At this temperature, it is possible that the elements are present not only in the form of oxides, but also carbonates and sulphates, etc. might be formed as well. Thus, the oxygen content was not included in the table. The silica content of the samples was not measured. As a result, only the amounts of some of the most important inorganic elements have been determined. As it is shown in Table 2, the main element in the ash of poplar is calcium, whereas in the case of the other two samples a considerable amount of potassium is also present. The amounts of potassium and calcium are comparable in the ash of the tree of heaven sample. From the ICP results it can be concluded that poplar is the best fuel among the studied samples. Ash sintering problems may arise mostly in the case of the other two samples. However, if one takes into account that the ash content of the tree of heaven sample is significantly lower than that of the energy grass, the former sample can be considered as having favorable properties.

Fig. 2 shows the normalized weight loss, in addition to the total amount of released gases in the pyrolysis experiments. The third set of series, indicated as liquid, is calculated by taking the difference between the weight loss and the amount of produced gases. Note that the start time in all the figures presented in this paper is related to the temperature of the reactor as it attains 250 °C. This starting point is also used for the start of the integration in the calculation of the total gas release. The tars are not measured online because it is not possible to trap these compounds and at the same time measure their weight continuously. From Fig. 2 we can also see that the devolatization of poplar occurs first followed by that of the tree of heaven and then the energy grass pellets. One can also notice that the amount of residues formed from the energy grass is higher than from the wood samples. This is most likely due to the higher amount of ash in the grass. This higher inorganic content adds to the carbonaceous residue, and it also influences the decomposition pathways by favoring charring reactions.

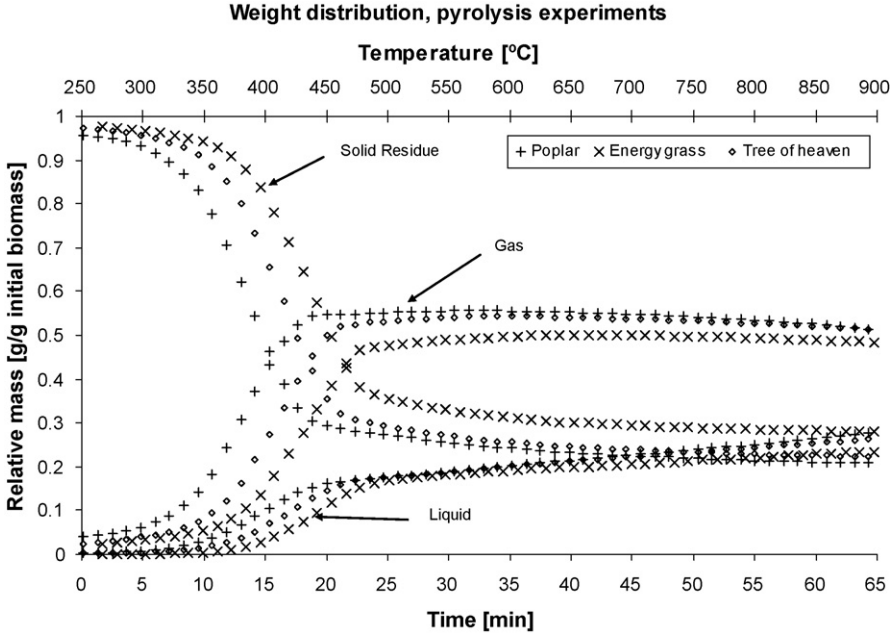

Fig. 2. The solid fuel conversion to gas and tar products as a function of time and temperature. (Data above 65 min are omitted.)

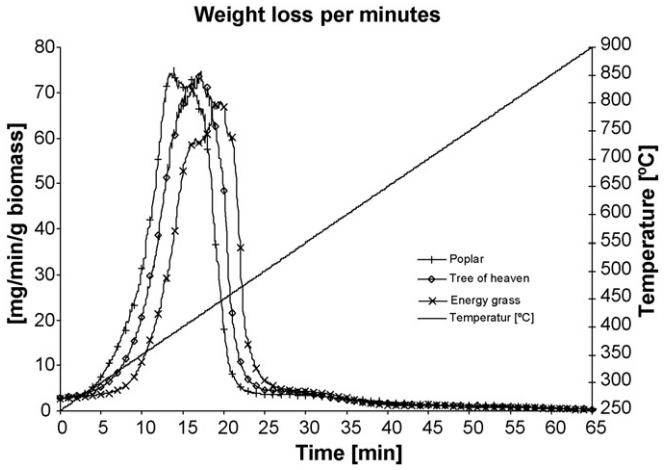

Fig. 3. DTG curves; weight loss per minute normalized to the initial dry sample mass. (Pyrolysis experiments.)

Fig. 3 shows the DTG curves of the bio-fuels in inert atmosphere. The decomposition of the two wood species shows some similarities as suggested by the similar DTG curves. The energy grass, on the other hand, has a different peak shape implying that the thermal decomposition is considerably different from that of the wood samples.

The evolution profiles of the most important gaseous products for the pyrolysis experiments are presented in Fig. 4. This figure shows the formation of carbon dioxide (CO_2), carbon monoxide (CO), hydrogen (H_2), methane (CH_4) and the sum of the light hydrocarbons acetylene (C_2H_2), ethylene (C_2H_4) and ethane (C_2H_6), indicated in the figures as C_2. The concentration is presented as a weight fraction of the original dry sample per minute. The evolution profiles of the different products are similar for all the studied fuel types, and show that the relatively simple DTG peak occurs as a result of different overlapping processes. The decomposition of all species starts with the evolution of CO and CO_2. At a somewhat higher temperature (at approximately 350 °C for poplar and tree of heaven; at 450 °C for the energy grass pellet) methane and C_2 compounds are also released. The evolution curves of these compounds show multiple peaks implying that these gases are formed in different decomposition processes. In the last stages of decomposition hydrogen (at about 550 °C for all the test fuels) is formed accompanied by minor amounts of carbon dioxide.

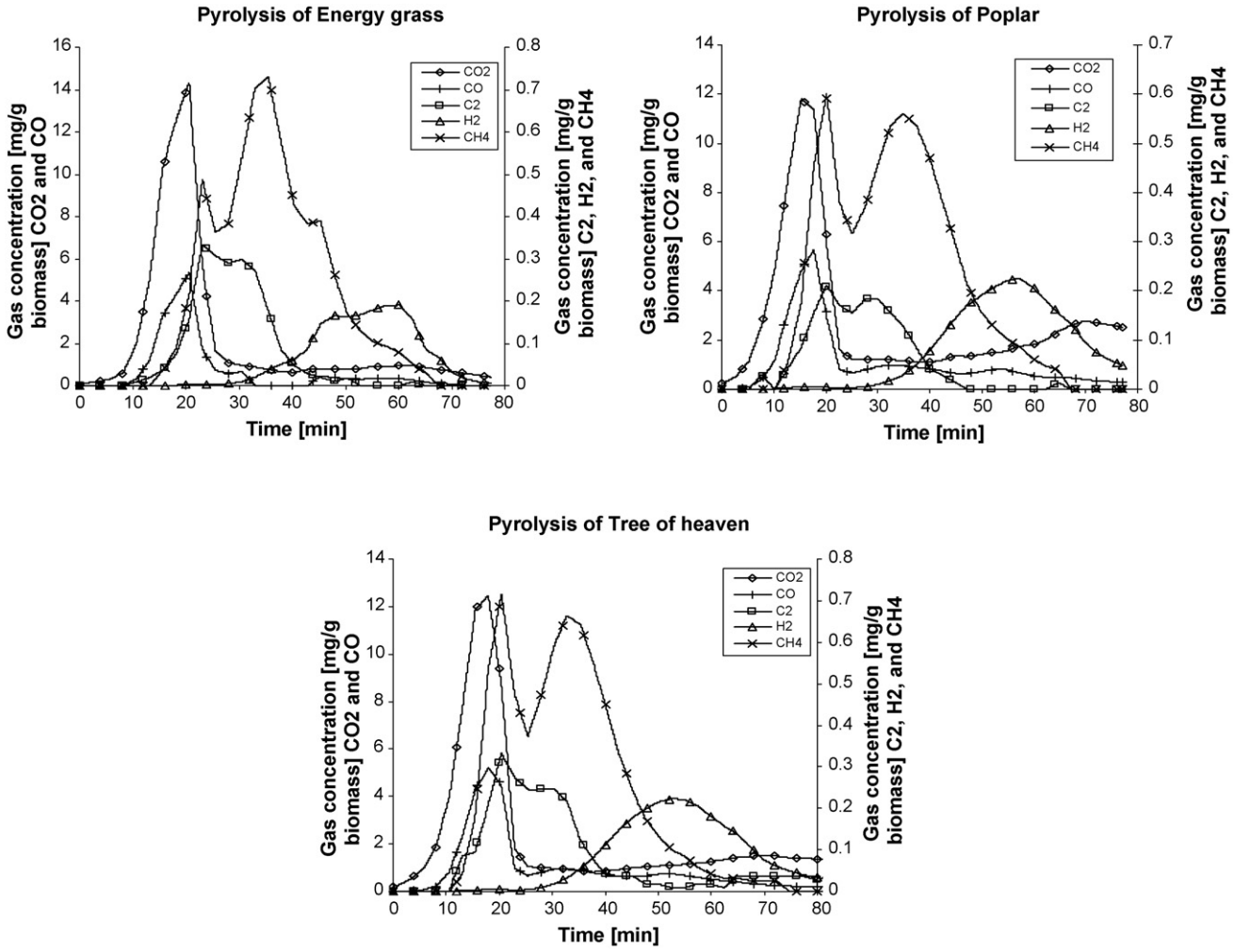

Fig. 4. Gas concentration from the pyrolysis of the different solid fuels.

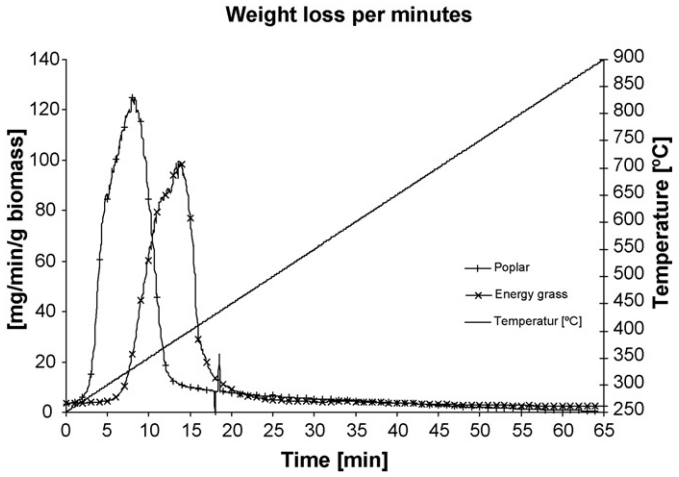

Fig. 5. DTG curves; weight loss per minute normalized to the initial dry sample mass. (Combustion experiments.)

The evolution curves of the various gaseous compounds of the studied wood species are similar, whereas those of energy grass show some differences. These differences are the most conspicuous in the formation of methane and hydrogen. In the case of the energy grass the second peak of methane formation occurring at about 36 min (610 °C) is more pronounced, while the first peak is lower. The peak at 610 °C can be attributed to methane released during the charring processes [24]. Hence, the charring reactions play a more significant role in the pyrolysis of grass than in the pyrolysis of the wood species. This is in accordance with the fact that a larger amount of inorganic ions, which catalyze charring reactions [37], can be found in the herbaceous sample (Table 1).

As the thermal behavior of the two wood samples was similar in inert atmosphere, only one of them has been studied in oxidative atmosphere (Figs. 5 and 6). The DTG curves for the combustion experiments are shown in Fig. 5. Similarly to the inert experiments, the DTG curve of the energy grass is lower than that of poplar. The shapes of the DTG curves are rather similar as opposed to the results of pyrolysis experiments. For poplar the peak occurs at 8.5 min (335 °C), while for the grass pellets the peak is at 14 min (390 °C). The formation of gaseous compounds has been monitored, and the curves corresponding to the various products are shown in Fig. 6. The evolution of gaseous products ends after about 20 min for the poplar and about 40 min for the grass pellets. In the case of poplar all compounds evolve in the same temperature range giving one sharp peak. The formation of carbon dioxide, however, proceeds at higher temperatures. In the combustion of energy grass CO_2 evolves at the beginning of decomposition. The

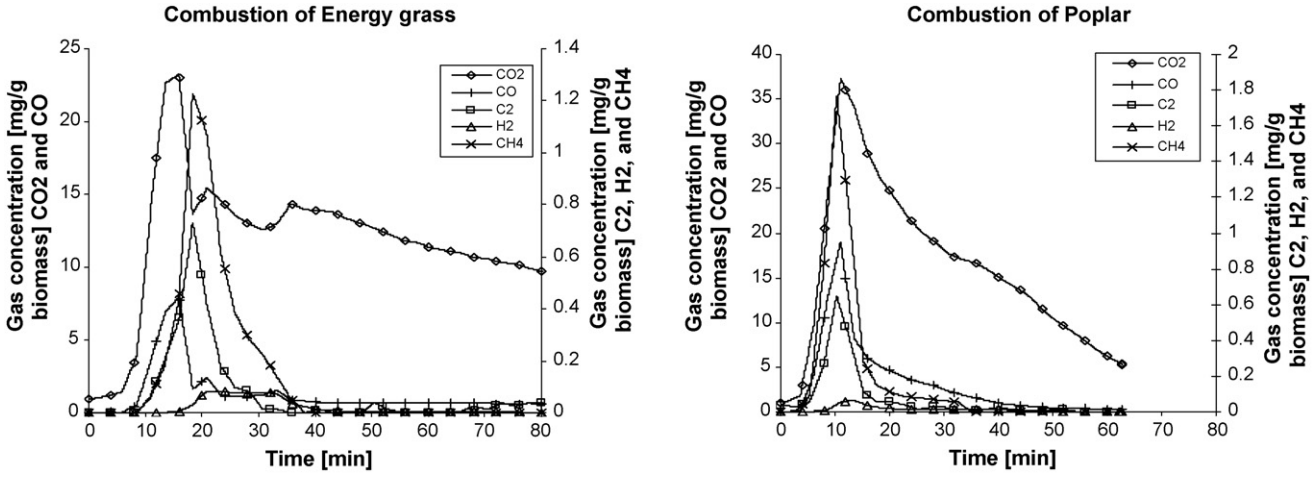

Fig. 6. Gas concentration from the combustion of the different solid fuels.

Table 4
Weight distribution of the different products from the pyrolysis and combustion experiments

Fuel	CH_4 (wt.%)	CO_2 (wt.%)	C_2 (wt.%)	H_2 (wt.%)	CO (wt.%)	Liquid	Solid residue	HHV (MJ/NM^3)
Pyrolysis experiments								
Energy grass	1.5	16.3	0.5	0.4	5.2	47.4	28.6	15.8
Poplar	1.6	21.1	0.4	0.6	8.3	46.5	21.5	14.6
Tree of heaven	1.7	20.0	0.7	0.7	7.9	46.4	22.6	16.2
Combustion experiments								
Energy grass	1.2	95.0	0.6	0.2	10.5	N.A.	12.5	N.A.
Poplar	1.1	101.6	0.5	0.1	20.1	N.A.	0.6	N.A.

Liquid calculated by difference.

formation of other gaseous products starts at a somewhat higher temperature (approximately 350 °C). The curves of these compounds have shoulders suggesting that these gases evolve in different decomposition processes. The second zone of decomposition (approximately 500 °C), observed in the pyrolysis experiments, is absent probably due to the fact that by that time the temperature becomes too high for such gases to stay un-oxidized. The second zone has, therefore, been replaced by the burning of the char, which happens at a much slower rate.

In Table 4 the total amounts of the different products are presented. The gas products are split into the major compounds measured by the GC. These values are integrated from the gaseous profiles showed earlier. Data are presented in terms of weight percent relative to the initial weight of the raw sample. The higher heating value for these gas products is also calculated and presented in the last column. The liquid yield in the pyrolysis experiment is calculated by difference. Also in the case of the total devolatilized products under pyrolysis the yields are comparable with the exception of the grass sample which exhibits some differences in the total yields of CO and CO_2.

4. Conclusions

In this work, the thermal characteristics of three biomass species have been studied. The experimental work was performed on thermally thick samples in both oxidative and inert atmosphere. A slow heating rate was chosen and both the weight loss and the evolved gaseous products were monitored as a function of time and temperature. The results confirm that the macro-TGA is suitable for the study of the pyrolysis and combustion of large samples. Due to differences in the density of the samples and in the elemental composition of the fuels, the weight loss under the pyrolysis experiments starts first with the poplar sample followed by tree of heaven and then the energy grass sample. The reported gas concentration profile under pyrolysis was similar for all the samples. The decomposition of all species starts with the evolution of CO and CO_2 first, followed by methane and the C_2 compounds and later hydrogen is released. The methane profile for the energy grass pellet differs in having a less pronounced first peak. This is probably due to charring reaction that might be more favored for the grass sample because of its larger amount of inorganic ions, which catalyze charring reactions. Experiments performed in oxidative atmosphere also confirm that the woody and herbaceous species exhibit significant differences under combustion. The second peak that is clearly visible in the pyrolysis experiments has disappeared due to oxidation. The CO profile for the grass sample is higher and flatter than that of the poplar sample. This could be due to the fact that for the grass pellet, the solid residues after the devolatization stage contain a higher amount of carbon. This char is slowly attacked by oxygen and produces CO under combustion.

The performance of the macro-thermobalance instrument coupled with gas analysis should be compared with the results of traditional thermogravimetric studies, and the factors influencing the thermal decomposition processes should be determined. Further experiments are needed to answer the above questions.

Acknowledgements

The work was supported by The Research Council of Norway through the program ‘‘Energi For Fremtiden’’, The 6th Framework Programme of the European Commission and its support to ENGAS (Contract no. RITA-CT-2003-506502) and by the Hungarian National Research Fund (grants T37705 and K61504). The authors are grateful to Zsuzsanna Laczkó for her valuable help in the ICP measurements.

References

[1] Renewable Energy Policy Network for the 21st Century, http://www.ren21.net/default.asp, Global Status Report, 2005.
[2] J.A. Caballero, R.F.A. Marcilla, J. Anal. Appl. Pyrol. 36 (1996) 159.
[3] E. Mészáros, E. Jakab, G. Várhegyi, P. Szepesvary, B. Marosvölgyi, J. Anal. Appl. Pyrol. 72 (2004) 317.
[4] Å. Ingemarsson, U. Nilsson, M. Nilsson, J.R. Pederen, J.O. Olsson, Chemosphere 36 (1998) 2879.
[5] W. De Jong, A. Pirone, M.A. Wojtowicz, Fuel 82 (2003) 1139.
[6] R. Bassilakis, R.M. Carangelo, M.A. Wójtowicz, Fuel 80 (2001) 1765.
[7] M. Müller-Hagedorn, H. Bockhorn, L. Krebs, U. Müller, J. Anal. Appl. Pyrol. 68/69 (2003) 231.
[8] M.G. Grønli, G. Várhegyi, C. Di Blasi, Ind. Eng. Chem. Res. 41 (2002) 4201.
[9] S. Şenzös, Bioresour. Technol. 89 (2003) 307.
[10] J.J.M. Órfão, J.L. Figueiredo, Thermochim. Acta 380 (2001) 67.
[11] R. Bilbao, J. Arauzo, M.B. Murillo, M.L. Salvador, J. Anal. Appl. Pyrol. 43 (1997) 27.
[12] K.O. Davidsson, M. Hagstroem, B. Stojkova, P.U. Andersson, B. Lonn, The Pyrolysis Kinetics of Large Biomass Particles, Report, 2002, pp. 24.
[13] J.M. Encinar, J.F. González, J. Gonzalez, Fuel Proc. Technol. 68 (2000) 209.
[14] J.F. González, J.M. Encinar, J.L. Canito, E. Sabio, M. Chacon, J. Anal. Appl. Pyrol. 67 (2003) 165.
[15] C. Acikgoz, O. Onay, O.M. Kockar, J. Anal. Appl. Pyrol. 71 (2003) 417.
[16] C. Di Blasi, G. Signorelli, C. Di Russo, G. Rea, Ind. Eng. Chem. Res. 38 (1999) 2216.
[17] J.L. Figueiredo, C. Valenzuela, A. Bernalte, J.M. Encinar, Fuel 68 (1989) 1012.
[18] A. Chong Lua, F. Yow Lau, J. Guo, J. Anal. Appl. Pyrol. 76 (2006) 96.
[19] J. Leppalahti, Fuel 74 (1995) 1363.
[20] G. Chen, J. Andries, Z. Luo, H. Spliethoff, Energy Convers. Mgmt. 44 (2003) 1875.
[21] Å. Ingemarsson, M. Nilsson, J.R. Pederson, J.O. Olsson, Chemosphere 39 (1999) 103.
[22] K. Senelwa, R.E.H. Sims, Biomass Bioenergy 17 (1999) 127.
[23] I. Laureysens, W. Deraedt, T. Indeherberge, R. Ceulemans, Biomass Bioenergy 24 (2003) 81.
[24] C.J. Gómez, E. Mészáros, E. Jakab, E. Velo, L. Puigjaner, J. Anal. Appl. Pyrolysis 80 (2007) 416.
[25] G. Skodras, O.P. Grammelis, P. Balinas, E. Karakas, G. Sakellaropoulos, Ind. Eng. Chem. Res. 45 (2006) 3791.
[26] G. Várhegyi, E. Jakab, F. Till, T. Székely, Energy Fuels 3 (1989) 755.
[27] B. Marosvölgyi, L. Halupa, I. Wesztergom, Biomass Bioenergy 16 (1999) 245.
[28] E. Mészáros, G. Várhegyi, E. Jakab, B. Marosvölgyi, Energy Fuels 18 (2004) 497.
[29] E. Mészáros, E. Jakab, G. Várhegyi, P. Tóvári, J. Therm. Anal. Calor. 88 (2007) 477.
[30] M. Becidan, Ø. Skreiberg, J.E. Hustad, J. Anal. Appl. Pyrol. 78 (2007) 207.

[31] J. Parikh, S.A. Channiwala, G.K. Ghosal, Fuel 84 (2004) 487.
[32] A. Demirbaş, A.H. Demirbaş, Energy Explor. Exploit. 22 (2004) 135.
[33] A. Demirbaş, Energy Convers. Mgmt. 39 (1998) 685.
[34] S.E. Florine, K.J. Moore, S.L. Fales, T.A. White, C. Lee Burras, Biomass Bioenergy 30 (2006) 522.
[35] B.S. Dien, H.J.G. Jung, K.P. Vogel, M.D. Casler, J.F.S. Lamb, L. Iten, R.B. Mitchell, G. Sarath, Biomass Bioenergy 30 (2006) 880.
[36] L.L. Baxter, T.R. Miles, B.M. Jenkins, T. Milne, D. Dayton, Fuel Proc. Technol. 54 (1998) 47.
[37] W.F. DeGroot, F. Shafizadeh, J. Anal. Appl. Pyrol. 6 (1984) 217.

Paper II

Straw Pellets Pyrolysis: Effect of Nonthermal Plasma on the Devolatilized Products

Khalil R. A., Seljeskog M., Hustad J. E.

Energy & Fuels Vol. 22 686-692 (2008)

Is not included due to copyright

Paper III

Sulfur Abatement in Pyrolysis of Straw Pellets

Khalil R. A., Seljeskog M., Hustad J. E.

Energy & Fuels Vol. 22 2789-2795 (2008)

Is not included due to copyright

Paper IV

CO_2 Gasification of Biomass Chars. A Kinetic Study

Khalil R. A., Várhegyi G., Jäschke S., Grønli M. G., Hustad J. E.

Energy & Fuels Vol. 23 94-100 (2009)

Is not included due to copyright

Appendix B (Gas analysis)

Gas analysis

Sampling train

The sample for gas analysis is taken through a hole on the side of the top-lock that is drilled with an angle of 30º from a horizontal line. A quartz tube with an outside diameter of 6 mm and an inside diameter of 1 mm is used for the gas sampling. The tube is placed approximately 10 mm inside the reactor wall and at the top of it. The sample gas passes first through an ice cooled trap made of three glass bottles. The first bottle is filled with glass balls so that heat transfer is increased; the second bottle is left empty while the third one is filled with glass wool so that the produced tar is trapped. The sample gas is then led to another ice trap made of one steel condenser and another container filled with glass wool with a paper filter on the top. The stream is then split where the first one is directed to 2 micro-GCs and the second one passes to a heated filter prior to its entry to the FTIR. A schematic drawing of the gas cleaning module is shown in Figure 3-2.

FTIR

Measuring principle

Fourier transform infrared (FTIR) measurement principal is based on the interaction of light and matter. The light source emits photons within a defined spectral range (IR wave length in a range 2.5 to 15 μm). Since most molecules vibrate at a characteristic frequency, they are able to absorb the energy from the IR light that corresponds to this particular frequency. The absorbed intensity is correlated to the change of the dipole moment due to the vibration and the concentration of molecules. By measuring the absorbed intensity for the different frequencies, it is possible to both identify and quantify most gas compounds. Almost all molecules can be identified with the exception of symmetrical molecules (O_2, N_2, H_2, etc) and inert gases (Ar, He, etc) the dipole moment in such molecules can not be changed.

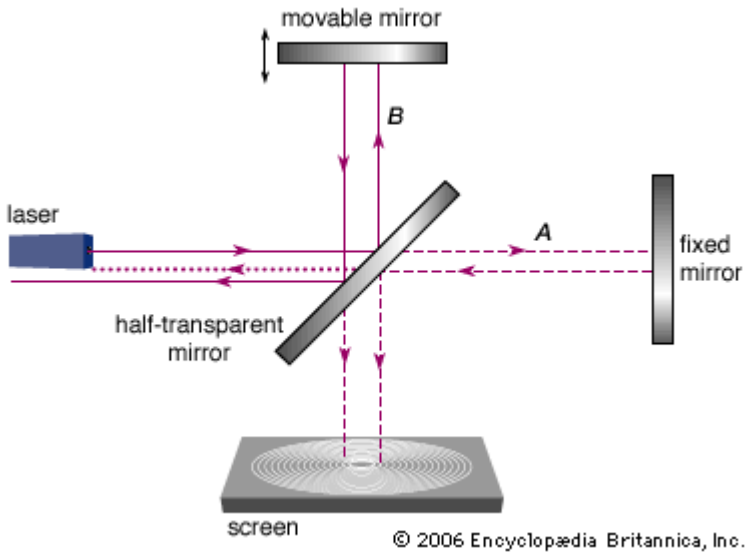

Figure B-1: The Michelson interferometer [82]

In the heart of all FTIR instruments we find a Michelson interferometer (Figure B-1) where its main purpose is to reduce the IR frequency so that it could be picked up by a detector. The Michelson interferometer produces a new signal at a much lower frequency which contains the same information as the original IR signal. The interferometer splits the IR light in two half, where the first half is reflected to a stationary mirror and then back to the splitter. The other half passes through the splitter and is reflected back by a movable mirror. The two reflected beams recombine at the splitter with a slight interference due to the difference in the traveled path of the two sources. Finally when the source light is read by the detector, the intensity which is now plotted as a function of time is transformed back to a single spectrum where it is plotted as function of wave number. The transformation is implemented through a mathematical process known as the Fourier transformation.

FTIR used in this work

The Bomem 9100 analyzer was used to quantify CO_2, CO, CH_4, C_2H_2, C_2H_4, CH_3OH and SO_2. This analyzer was kept at a constant temperature of 176 ºC with a help of several parts composed of heated pipes, a preheated oven and the FTIR cell, all controlled through a controller that is integrated in the instrument. The cell that was used has an inner volume of 5 liters and an optical path length of 6.4 meter. The instrument is equipped with two detectors where the choice between the two could be made by flipping a side port that reflects the laser light from one detector to the other. Only the deuterated triglycine sulfate (DTGS) detector with the maximum instrument resolution of 1 cm^{-1} was used in this work. For accuracy purposes, the average of 12 scans was chosen for the generation of the

spectra which gave a sampling interval of 1 min/sample. Due to the complex gas composition and the wide range of concentration variation, it was decided to manually treat the generated spectra. This is a tedious work that requires a lot of time and careful operation. Usually it is common to use special software for the calibration of FTIR where the concentration is predicted through advanced mathematical techniques that take into account the effect of interfering compounds. In this work it was decided not to use such a step because of the complexity of the gas composition and its variation over a wide concentration range. Unfortunately, the software that was bundled with the FTIR was not up to a good standard when the gas complexity increased. Instead, it was decided to fetch a single peak in the IR spectral range for each compound of interest that was not disturbed by any other compounds present in the sample gas. Figure B-2 shows an example of a calibration curve generated for CO both a high and low concentration. The figure shows the gas concentration as a function of the absorbed laser intensity at a specific wave number. The calibration parameters for both the micro-GC and the FTIR are summarized in Table B-2.

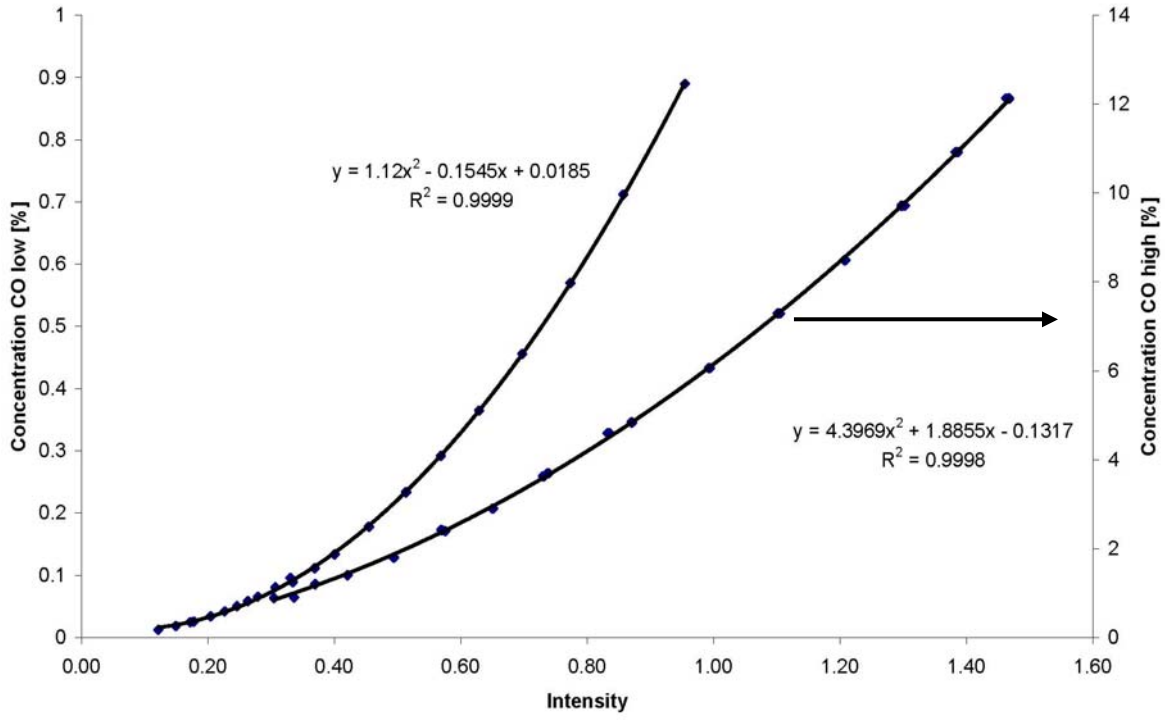

Figure B-2: Concentration of CO as a function of absorbed intensity.

Most of the spectra that were used for the instrument calibration were performed in our laboratory. In addition, we had access to a library of spectra generated by the same type of

instrument at Chalmers University of Technology in Sweden. The calibration of the different compounds was performed by mixing two gas streams delivered through gas cylinders, pure N_2 for diluting purposes and a cylinder containing a mixture of N_2 and the calibration gas. This was done in order to obtain several concentrations of the same compound. The flow of gas from the two cylinders was controlled with two identical flow controllers with digital signal processing for increase of accuracy. The gases were mixed in a special container prior to feeding the FTIR. The volume flow of the mixture to the FTIR was kept constant at 5 nL/min. In order to maintain good mixture accuracy, the lowest used range of the flow controller was never under the 10 % of maximum range. With this mixing method, it was possible to dilute the gas by a factor of 10 and obtain 10 different concentrations where the highest one belonged to the concentration in the calibration cylinder. In most cases 2 different gas cylinders were used for each gas compound, one for a low concentration range and another for the high concentration range.

Finding the proper wave number at which no interference occurs was a challenging task. This was done for all gas compounds except for SO_2, where more advanced techniques were employed in order to be able to predict the concentration. However, since SO_2 has proven to be under the detection limit for all the experiments, no detailed information on the quantification procedure will be given.

An example on choosing a proper wave number for the prediction of low concentration CH_4 is given in Figure B-3. To the upper left side of the figure, clean CH_4 spectra at different concentrations are overlaid. At the right side, the spectra from straw pyrolysis at 400 ºC are presented for the exact wave number range as in the left side figure. Only spectra with the relevant concentration range are chosen for graphical presentation. It can be clearly seen that almost the entire range is disturbed by other compounds present in the pyrolysis products with the exception of a small part at the left hand side. The chosen peak for the concentration prediction is shown in the bottom part of the figure both for the clean CH_4 compounds (left side) and the spectra from the same experiment (right side). The left side peak is base corrected and the height of the peak is measured relative to this baseline correction. We can see that the shape of this peak is preserved for the pyrolysis experiment which proves that no disturbances are present at this particular wave length range.

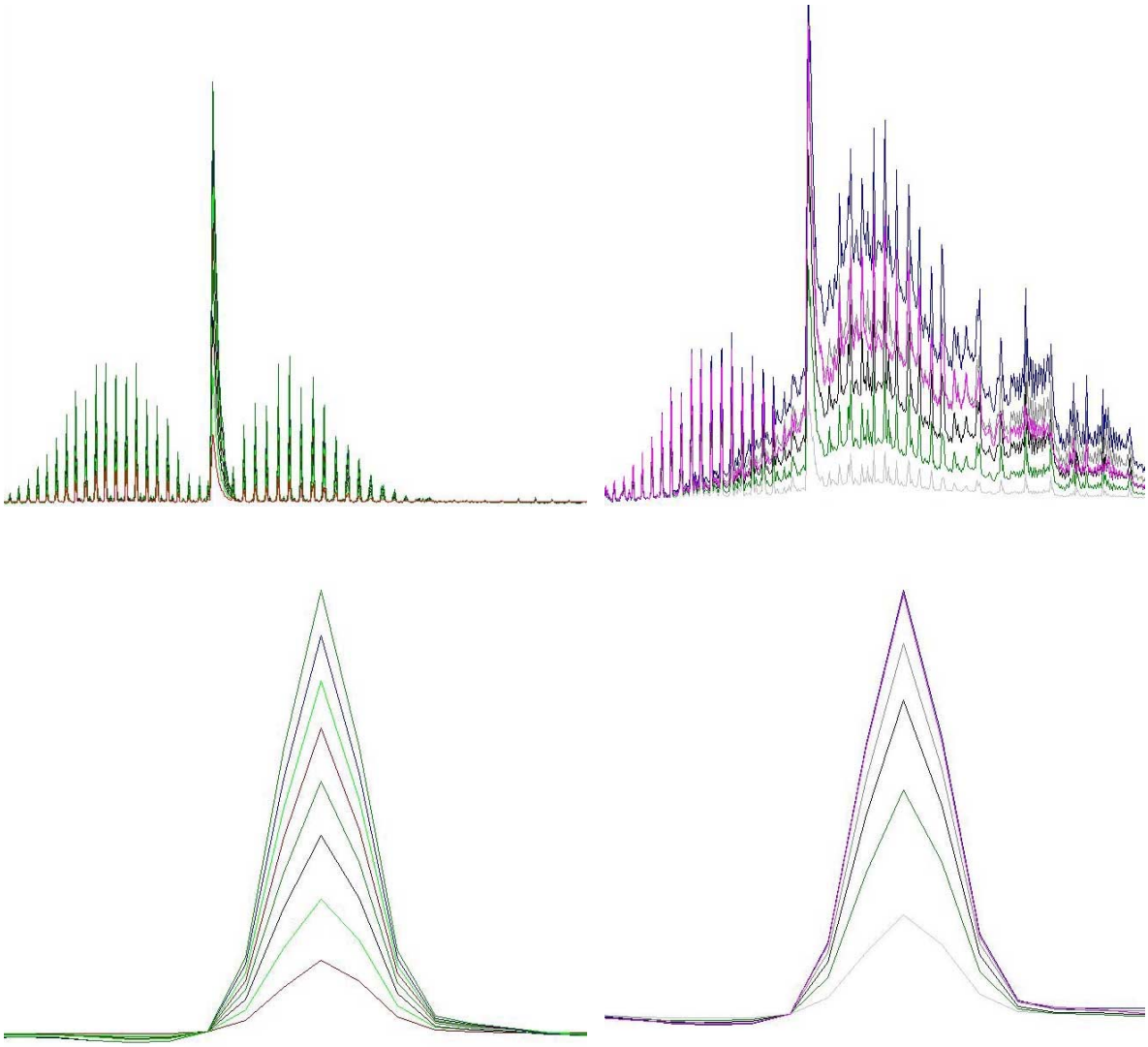

Figure B-3: FTIR overlaid spectra of CH_4. Clean CH_4 spectra used for low concentration calibration (left side). Spectra of the same region taken from a straw pyrolysis experiment at 400 ºC (right side).

Gas chromatography

Measuring principal

The major parts of most gas chromatographic system are the injector, the column and the detector. The system is based on separating all the gas compounds that are present in the sample and then measuring their concentration, one component at a time. The system relies on the differences in the affinity of a moving phase (the sampling gas) towards a stationary phase. The stationary phase is usually a tube (column) where its inner wall has been coated or bonded. An inert high purity gas (carrier gas) goes through the column continuously usually in two separate but identical column systems; one is used as a reference and the other for measuring the gas compounds. The sample is introduced into the injector usually

with a syringe or an exterior sampling device. The compounds in the sample travel through the column at different rates, as a result of different forces between each molecular type and the stationary phase. The fastest moving compound exits the column first followed by the remaining compounds in a corresponding order. As the different compounds leave the column, they enter the detector where the concentration is determined. The GC system can be equipped with many types of detectors which will use a specific gas property for the prediction process. For example a thermal conductivity detector (TCD) uses the thermal property of the gas in order to quantify its concentration. This detector is basically composed of a filament where its temperature is closely monitored by a thermo couple. It is kept at a constant temperature by letting an electrical current run through it. When the separated gas compounds flow through, the filament is cooled and the voltage is increased to keep the temperature at a constant level. This voltage signal is recorded by a data system and is plotted against elapsed time to produce a chromatogram. The different gas concentration will show up in the chromatogram as separated peaks where the time for the peak to appear in the chromatogram is called the retention time. The type of gas is identified by its retention time while its concentration is related to the area of the peak. The identity of a compound cannot be determined solely by its retention time. A known amount of an authentic, pure sample of the compound has to be analyzed and its retention time and peak size determined. When compounds are not perfectly separated, they appear in the chromatogram as overlapping peaks. Several parameters are possible to change in order to optimize the separation of the different compounds. The main influencing parameters are the column temperature, injection time and column pressure. More complicated GC system are composed of several columns that are linked together with a system automated valves in order to obtain perfect separation and are usually used for identification of complex gas samples.

Micro GC used for main compounds

The Varian CP-4900 micro-GC was used for the quantification of most of the major compounds released during pyrolysis. This micro-GC was a necessity since it is capable of quantifying O_2, H_2 and N_2 all of which are not detectable with the FTIR. This micro-GC composed of two systems each equipped with its own column, injector, detector and pump. The first column is a 10 m PoraPlot Q type with an internal diameter of 0.25 mm, 10 μm film thickness and uses Helium as a carrier. This column is used for the separation of CO_2, CH_4, C_2H_2 + C_2H_4 (not separated), and C_2H_6. The second column is a 20 m MolSieve 5 Å

PLOT with an inner diameter of 0.25 mm, 30 µm film thickness and uses argon as a carrier gas. Argon was used in order to be able to detect hydrogen. This column is able to quantify H_2, O_2, N_2, CH_4 and CO. Both columns use a thermal conductivity detector (TCD) for the quantification of the gas compounds.

Micro GC used for sulfur compounds

This GC is also a Varian CP-4900 model that is equipped with a special detector which allows it to quantify trace elements of sulfur compounds. The micro-GC has only one column of type PoraBond, length 10 m and internal diameter 0.25 mm. The column is linked to two detectors placed in series upstream to the column. The first detector is a TCD detector similar to the ones installed in the other GC while the second is a differential mobility detector (DMD). The DMD is a tunable ion filter that selectively allows specific ion species to pass through the filter. This is done by ionizing the molecules while the carrier gas leads the sample through the detector. Molecules are than subject to a high-frequency electric field with oscillating field strength that induces oscillatory lateral motion, as shown in Figure B-4. The amplitude of the motion as well as its lateral symmetry is dependent on the differential mobility characteristics of each ion. In case the imposed lateral motion is asymmetric with respect to the alternating field strength, the affected ions will drift toward the wall of the transport tube, collide, and become neutralized. Only charged ions with differential mobility in a range to which the detector has been tuned will maintain a non collision path through the transport tube. These ions will be detected during the transfer of their charge to the electrometers.

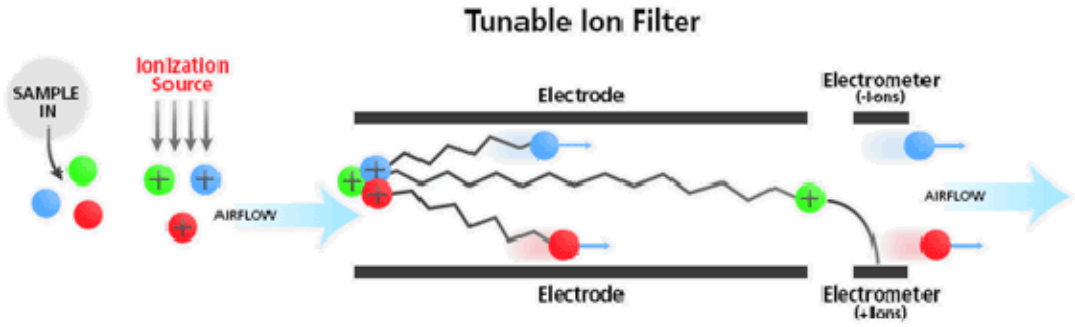

Figure B-4: A schematic drawing of the principal behind the DMD detector [83]

The DMD is extremely selective and to detect specific ions while eliminating the rest of the sample. The electrometers at the end of the drift tube are sensitive, both positive and negative ions can be detected simultaneously. Because of the selectivity property of the

DMD, it is not dependent on a complete sample separation. Its selectivity allows it to make trace analysis possible when co-eluting with bulk components. Its detection limit for the sulfur compounds is 10 ppb.

1.1 Comments on measuring the minor species H_2S and COS

Polar inorganic compounds like H_2S are difficult to quantify. Such compounds are particularly sensitive to reactions with the surface of the sampling line or with other impurities that are caught in the filter such as water and tar compounds. Reactive SH group in H_2S are adsorbed on glass and metal surfaces and can cause problems when quantifying low H_2S concentrations. With the use of inert materials like ceramics and different PTFE tubes, this problem can be avoided. However, since inert materials can not be used in hot parts (close to the reactor), some sort of a compromise had to be made. The biggest challenge comes in avoiding the problems of condensable matters such as tars and water. Carbonaceous dust has also shown a tendency to adsorb H_2S [84, 85]. A heated sampling line to avoid condensable matter was not a viable solution in our setup, mainly for two reasons. First, by using a heated line the complexity of detecting the different compounds with the FTIR would increase significantly. Already high concentrations of CO_2 and hydrocarbons such as CH_4 and C_2H_4 cause a serious challenge in identifying the different components in the gas stream. Adding water and higher hydrocarbon compounds would result in interference over a large frequency band in the final spectra. Second, one should avoid taking any risk in letting tars condense on the mirror walls inside the FTIR cell since doing so would render the system less accurate and at worth unusable. The tars and water are also harmful for the GC and especially to the molecular sieve column which has a very low tolerance to such compounds. As it was mentioned earlier, the sampling line is composed of two sets of ice traps for the condensation of water and heavy tar compounds. The gas stream passes then through a heated particle filter and a heated Teflon tube prior to its entry to the different measuring instruments. The 15 meter Teflon tube has an inner diameter of 4 mm which compared to the volume flow that passes through (5 nL/min) is enough to minimize H_2S adsorption [86]. The effect of adsorption of H_2S by the clean sampling line was studied prior to the experiments. Calibration gas of different concentrations of H_2S was passed through the sampling line and the area of the H_2S peak was compared the chromatogram with the initial calibration. The initial calibration was done with special tubes recommended by the GC producer as being resistive to H_2S adsorption. The inner surface of these tubes was carefully treated so that a smooth surface

was produced. The different pieces of the sampling line were added one at a time in an attempt to single out the parts to cause adsorption problems. Surprisingly, no particular part in the sampling line was more conspicuous than the other. However, this experiment proved that each new element introduced to the sampling line caused an augmentation of the adsorption problem. During that testing period, it was also discovered that the GC used for the quantification of the sulfur compounds was unstable and needed calibration on a daily basis. Once calibrated, it would stay reliable through the entire day. Since it was not also sure how much a dirty line would affect our concentration prediction, it was decided to calibrate the instrument by passing the calibration gas through the sampling line before and after each experiment. For H_2S the calibration was performed with the concentrations between 3 – 100 ppm, while COS was only calibrated for a single concentration (3 ppm). The results for all the calibration points that were performed are shown in Figure B-5.

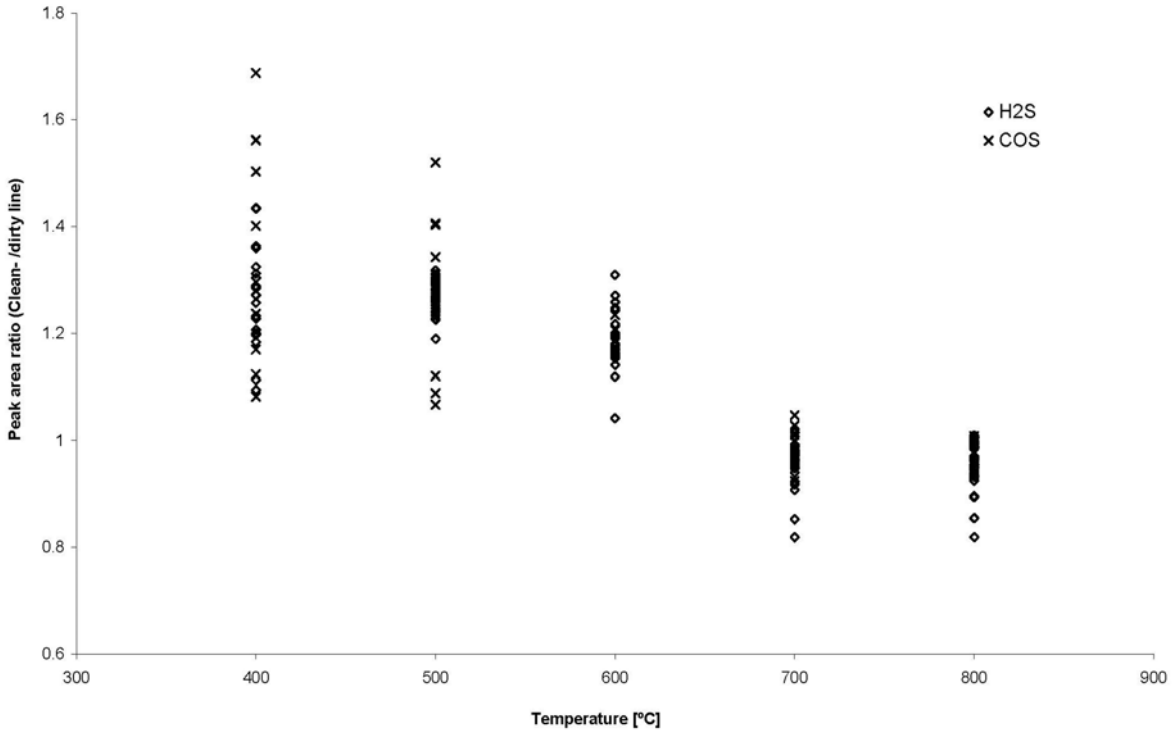

Figure B-5: Peak area ratio of H_2S and COS. Clean line/dirty line.

The x-axis represents the pyrolysis temperature used during the experiments, which in return affects the chemical composition and the amount of tar products trapped in the sampling line. It is well known that low pyrolysis temperature will result in a larger liquid fraction. The y-axis is the peak area ratio of the gas concentration run with a clean line to the one run with a dirty line. From Figure B-5 we can see that for the lower temperature

(400 – 600 ºC) the area ratio fluctuates between 1 and 1.7 with most of the data points falling close to a ratio of 1.2. The high amounts of liquid products formed at such low temperature certainly play a role in absorbing the sulfur compounds, which in return result in a lower sulfur concentration in the devolatilized products. At low pyrolysis temperature the sulfur compounds are released in moderate quantities compared to high temperature pyrolysis which in return renders the retention of sulfur in the filter more effective. At lower temperatures the COS area ratios are more scattered than H_2S ratios. This could be due to the extreme low level of concentration for the COS calibration. At higher temperatures (700 and 800 ºC), the ratio is close to unity, resulting in a less sulfur adsorption. At high temperatures the sulfur compounds are saturating the sampling line due to two reasons, a relatively higher sulfur concentration in the product gas and a lower liquid fraction in the sampling line. The information available in the literature concerning the effect of condensable matters on the concentration of sulfuric compounds is quite contradictory [87]. Results presented in Figure B-5 might shed a light on why this is so since it shows a varying tendency of the effect of adsorption that is dependent on the pyrolysis temperature. The sulfur concentration in all the experiments where compensated for this effect.

1.2 Reproducibility during the integration of a dynamic profile

For all the macro-TGA experiments, the data were used to calculate the mass balance of the different elements in the biomass sample. Since the concentration profiles vary with time, some uncertainties are introduced due to the limited amount of data points describing the profile. During the integration of the concentration profile a linear interpolation between the measured points was assumed. This is because the instruments are unable to report the concentration in a continuous mode. For the FTIR the sampling time is one minute while for the GC two minutes are needed. The problem is illustrated in Figure B-6 where a normal second degree curve is redrawn twice with fewer points and with linear interpolation.

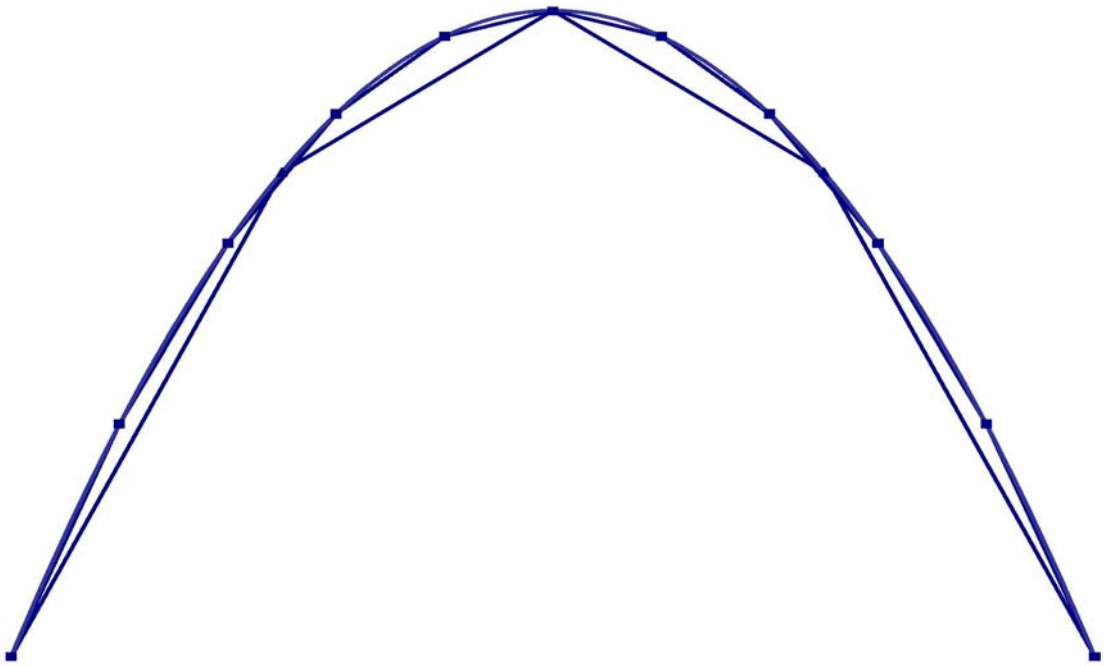

Figure B-6: Schematic drawing explaining the loss of integration accuracy due to low resolution.

This type of uncertainty is quite hard to estimate since the actual concentration profile is not known. Uncertainties could increase due to two reasons:

1. Increase in the pyrolysis temperature which in return makes the profile quite dynamic with respect to the time. The concentration profile becomes more difficult to describe with a limited set of data points

2. Increase of the sampling time which would basically result in the same problem as in 1.

Assuming that the concentrations of the different gaseous compounds have a similar profile as the weight loss curve, the later profile can be used to estimate the uncertainty caused by the lower resolution. The logging interval for the weight loss signal is set to five seconds which should be enough to generate an integrated value that is very close to the true weight loss of the sample. This value is then compared to the value obtained from the integration with the same profile but with limited sampling points. In order to quantify a standard deviation of the "true" total weight loss, the same procedure is executed with data points that are shifted in time five seconds compared to the previous set. This step is

repeated until the new data set coincides with the first chosen set. This is similar to what happens during the experiment since it is quite difficult to control the time from the moment the sample is lowered inside the reactor and the time the instruments are started. The integration is performed for all the generated data sets by assuming a linear fit between the data points. Finally a standard deviation is calculated for all the experiments that have been performed and for the sampling resolution of 1, 1.5, 2 and 2.5 minutes. The results for the relative standard deviation are plotted as a function of temperature and sampling resolution in Figure B-7.

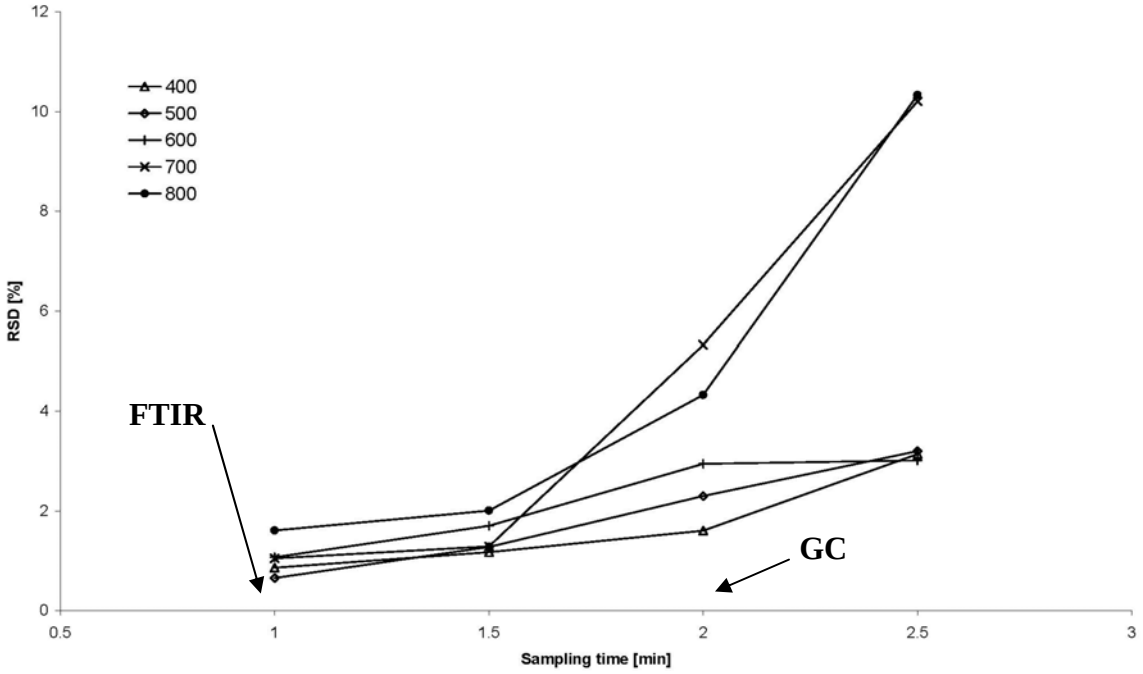

Figure B-7: The relative standard deviation for the weight integration as a function of pyrolysis temperature and sampling time resolution.

For a sampling time of one minute (FTIR) the deviation is kept under 2 % while for the GC (2 min) the deviation more scattered and close to three times the error of the FTIR for temperatures higher than 600 ºC.

The reproducibility was also tested for a pyrolysis temperature of 500 ºC and for the experiments with straw pellets. As such experiments are time consuming; only three repetitions were made where the purpose was to have an idea on the variation range. The relative standard deviation (RSD) is presented in Table B-1 for the integrated values of the different gas products. It can be seen that the relative standard deviation for the gas products measured with the FTIR (CH_4, CO_2, and CO) have a lower deviation than the

products measured with the micro GC. This is due to the better sampling resolution of the FTIR which was explained earlier. The deviation values are caused by the sum of several sources of uncertainties but it is believed that the biggest contribution comes from the effect of the sampling time has on the integration. The reproducibility for the minor compounds, H_2S and COS is much larger because lower concentrations at ppm range are measured. Another reason might be the adsorption that such compounds exhibit while passing through the filter line.

Table B-1: The relative standard deviation of the gas products, performed at 500 ºC

	CH_4	CO_2	C_2H_2+C_2H_4	C_2H_6	H_2	CO	H_2S	COS
Repetition 1	11.9	177.6	2.9	4.5	1.3	69.3	73.0	5.0
Repetition 2	11.0	173.6	2.8	4.2	1.1	67.3	74.9	3.2
Repetition 3	11.2	176.5	3.1	3.9	1.2	67.8	52.4	3.0
RSD	4.2 %	1.2 %	5.9 %	7.7 %	7.2 %	1.5 %	18.7 %	28.8 %

Table B-2: Calibration data for the FTIR and the micro-GC

Calibration data used for the detection of species with the FTIR					
Specie	Cal. Range	I. range	Wave nr. [cm^{-1}]	Calibration Formula	R^2 value
CO(low)	125 – 8900 ppm	0.121 – 0.955	2113.34 – 2109.49	$1.12x^2 – 0.1545x + 0.0185$	0.9999
CO(high)	0.89 – 9.71 Vol %	0.305 – 1.468	2039.57 – 2035.23	$4.397x^2 + 1.886x – 0.1317$	0.9998
CO_2(low)	0.26 – 0.85 Vol %	0.035 – 1.207	2278.26 – 2276.32	$0.0353x^2 + 0.468x + 0.239$	0.9999
CO_2(high)	0.9 – 9 Vol %	0.032 – 0.219	5020.00 – 4977.43	$65.79x^2 + 26.70x – 0.0196$	1
CH_4(low)	194 – 5900 ppm	0.024 – 0.624	3159.17 – 3156.28	$1.221x^2 + 0.158x + 0.0163$	1
CH_4(high)	0.49 – 5.94 Vol %	0.104 – 0.710	2744.50 – 2740.15	$5.8671x^2 + 4.291x – 0.017$	0.9994
C_2H_2(low)	19 – 142 ppm	0.005 – 0.024	3229.57 – 3227.15	$–8456x^2 + 8647.1x – 20.24$	0.9993
C_2H_2(high)	152 – 6406 ppm	0.025 – 0.681	3229.57 – 3227.15	$10264x^2 + 2097.6x + 114.5$	0.9994
C_2H_4(low)	5 – 680 ppm	0.023 – 1.357	953.729 – 946.979	$0.0111x^2 + 0.03x – 0.0002$	0.9999
C_2H_4(high)	0.068 – 1.1 Vol %	0.111 – 0.854	1890.10 – 1886.24	$1.205x^2 + 0.2395x + 0.023$	0.9998
Calibration data used for the detection of species with the GC					
Specie	Cal. Range	Column & detector	Curve fit type		R^2 value
CO_2	0.86 – 97.98 Vol %	PPQ/TCD	Linear forced through zero		0.9992
CH_4	0.086 – 3 Vol %	PPQ/TCD	Linear forced through zero		0.9998
C_2H_2+C_2H_4	0.071 – 2.47 Vol %	PPQ/TCD	Linear forced through zero		0.9994
C_2H_6	0.043 – 1.51 Vol %	PPQ/TCD	Linear forced through zero		0.9993
H_2	0.171 – 5.95 Vol %	MolSeive/TCD	Linear forced through zero		0.9983
O_2	0.162 – 5.66 Vol %	MolSeive/TCD	Linear forced through zero		0.9552
N_2	1.93 – 98.44 Vol %	MolSeive/TCD	Linear forced through zero		0.9972
H_2S	0 – 90 ppm	PPB/DMD	Point to point		n. a.
COS	0 – 3 ppm	PPB/DMD	Point to point		n. a.